# Towards climate-smart sustainable management of agricultural soils

## SCALE

Managing Sediment Connectivity in Agricultural Landscapes for reducing water Erosion impacts

## Deliverable WP4-D1

# Guidelines on uncertainty and optimized parametrization strategies depending on scale and modelling approach

Due date of deliverable: 31 Oct 2022
Actual submission date: 28.05.2024

# GENERAL DATA

Grant Agreement: 862695
Project acronym: SCALE
Project title: Managing Sediment Connectivity in Agricultural Landscapes for reducing water Erosion impacts
Project website: [www.scale-ejpsoil.eu](http://www.scale-ejpsoil.eu)

Start date of the project: February 1st, 2021
Project duration: 42 months
Project coordinator: Elmar M. Schmaltz (BAW)

Funding source: H2020-SFS-2018-2020 / H2020-SFS-2019-1
Type of action: European Joint Project COFUND

| | |
|---|---|
| DELIVERABLE NUMBER: | WP4-D1 |
| DELIVERABLE TITLE: | Guidelines on uncertainty and optimized parametrization strategies depending on scale and modelling approach |
| DELIVERABLE TYPE: | Report |
| WORK PACKAGE N: | WP4 |
| WORK PACKAGE TITLE: | Modelling approaches across scales, and incorporation of erosion control measures and connectivity elements in mitigation scenarios |
| DELIVERABLE LEADER: | Rosario Napoli (CREA) |
| AUTHORS: | Timo A. Räsänen, Mika Tähtikarhu, Jaana Uusi-Kämppä (LUKE), Frédéric Darboux, Roger Moussa (INRAE), Rosario Napoli, Sergio Pellegrini, Chiara Piccini, Filippo Rocchi (CREA), Julien Fouché (SupAgro), Seth Callewaert, Petra Deproost (VPO), Peter Kastelic (AIS), Sacha Gobeyn (Fluves) |

This project has received funding from the European Union's Horizon 2020 research and innovation programme under grant agreement N° 862695

## ABSTRACT

This deliverable presents the activities of task one within work package four (WP4-T1) of the SCALE project under EJP SOIL programme (https://ejpsoil.eu/soil-research/scale). The task evaluates commonly used models in terms of uncertainty and incorporation of sediment connectivity features. Its objective is to provide guidelines on uncertainty and optimized parameterization strategies depending on scale and modeling approach.

Various models for estimating soil erosion and their relationships with connectivity elements were analyzed. These models were run in different pilot areas at plot/field and catchment scales, with varying levels of geographic detail in the input parameters. Both physically based and empirical models were tested and evaluated in relation to prediction uncertainty and sediment connectivity features. Additionally, an existing sediment connectivity approach was implemented and assessed.

The empirical models tested included the Revised Universal Soil Loss Equation (RUSLE) for Finland, the Water and Tillage Erosion/Sediment Delivery (WaTEM/SEDEM) model for Flanders, and the RUSLE-USPED (Unit Stream Power–based Erosion Deposition) model for the Italian pilot areas. The physically based WEPP model was also applied and evaluated at the plot scale for Italian experimental fields. Finally, some other examples and suggestions about possible options for parametrization are reported from previous studies, also for those partially or not implemented in the case studies.

# Table of Contents



This project has received funding from the European Union’s Horizon 2020 research and innovation programme under grant agreement N° 862695 

# 1. Introduction

This deliverable reports the activity of task one of work package four (WP4-T1) of the SCALE project of EJP SOIL (https://ejpsoil.eu/soil-research/scale). The task assesses frequently used erosion models in terms of uncertainty and incorporation of sediment connectivity features and aims to provide some useful guidelines on uncertainty and optimized parametrization strategies depending on scale and modelling approach.

Soil erosion by water has negative impacts on agricultural productivity and surface waters. The erosion causes harmful structural changes in the soil and loss of fertile topsoil (Pimentel et al., 1995), and in surface waters it increases turbidity, sedimentation, and eutrophication (Ulén et al., 2012). The former impacts are commonly referred to as on-site impacts, and the latter as off-site impacts, and their relative significance varies by region.

Computational models are widely used tools for studying and evaluating the erosion process (Batista et al., 2019; Borrelli et al., 2021) and they are often used to support decision making as well (Johannsen et al., 2022). For example, models can be used to produce erosion maps at varying spatial scales, for the identification of high erosion areas, and planning of erosion mitigation measures. The model types vary from empirical models, with simplified description of the erosion process, to process-based models that describe different aspects of erosive processes. The empirical models are often more easily implemented over larger spatial scales due to more modest requirements for data, parameter estimation and computational resources compared to the process-based models. All types of computational models inherently contain uncertainties, and recognizing these uncertainties is important, particularly when they are used for decision making purposes.

Because all proposed soil erosion models were developed for particular purposes, application scales and environments, their optimal use lies in adhering to their original conditions and settings. Attempting to apply the selected model to different conditions may show some heavy limitations in obtaining accurate results.

## 1.1 Uncertainties and sensitivity assessment in modelling soil erosion

Several mathematical models classified as empirical, conceptual, or process-oriented have been developed to quantify the effect of soil erosion processes at different spatial and temporal scales (Merritt et al., 2003; Morgan and Nearing, 2011; Nearing, 2013). Batista et al. (2019) reported that today “there is no shortage of soil erosion models, model applications, and model users, but there is still a knowledge gap on the validity, quality, and reliability of the modelling application results”. Despite the significant progress made in model development and input parametrization, output uncertainties persist due to the non-linear relationships and thresholds at play between driving factors and the subsequent erosion processes, as well as the difficulties of upscaling model findings from the local scale to larger ones (De Vente and Poesen, 2005).

A recent global review study (Borrelli et al., 2021) systematically reviewed soil erosion modelling applications worldwide. The study conducted a statistical analysis with the aim to address identified knowledge gaps and facilitate information acquisition through a global soil erosion assessment.

Identifying sources of uncertainties involves addressing different types of causes of uncertainty when applying soil erosion models. The objective of this deliverable is to identify the different sources and their characteristics - technical (data and parameters), methodological (approach and assumptions) and epistemological (lack of knowledge, unknowns) – enhancing the understanding on how to improve the sediment connectivity within specific erosion models in selected case studies.

Both empirical and physically based models must deal with result uncertainties stemming from various causes. Such uncertainties are primarily induced by three main characteristics of the model input: i) type and quality of data sources, i.e. measured (in field or lab) or predicted/estimated (with Pedotransfer Functions, other models, etc.); ii) geographic representation type (vector or raster) and detail of inputs (scale, pixel size, etc.); iii) coefficients, indexes and parameters required to configure the model functions and/or formulas.

These sources of uncertainties are categorized as technical challenges, applicable to every type of model and of geographic context and scale. Methodological approaches and assumptions strongly related to the model's conceptual structure may often lack in addressing certain important features and processes. These shortcomings may occur because a model was originally designed for specific purposes, or due to the lack of understanding about some particular or local processes that may occur or emerge at very small scale (i.e. micro-scale erosion processes).

## 1.2 Adopted models and solutions for a "spatial distributed" evaluation

Globally, the most used erosion model is the Revised Universal Soil Loss Equation (RUSLE) (Renard et al., 1997; Borrelli et al., 2021) which is an empirical model, developed from its predecessor USLE (Wischmeier and Smith, 1978) in the United States. RUSLE was originally developed for field slope/plot scale estimation of soil loss, but has been later widely used as a spatially distributed model, where the erosion rates are predicted over spatially discrete units, such as grid cells. RUSLE has also been adapted to various parts of the world (Ghosal and Das Bhattacharya, 2020). The strength of the spatially distributed RUSLE is that it allows spatially distributed modelling of large areas with relatively modest data inputs. However, a limitation of the spatially distributed RUSLE is that it does not estimate sediment transport in the landscape between the spatial computational units, which impedes the estimation of the off-site impacts of erosion.

A promising approach for overcoming the limitation of spatially distributed RUSLE is to consider the erosion transport within the sediment connectivity framework (Bracken et al., 2015; Heckmann et al., 2018; Najafi et al., 2021) by using Index of connectivity (IC) (Borselli et al., 2008) and sediment delivery ratio (SDR) (e.g., Vigiak et al., 2012; Zhao et al., 2020) methods. This approach allows the consideration of structural sediment connectivity and the estimation of sediment delivery rates. The approach has been used, for example, by Zhao et al. (2020) to estimate catchment scale sediment delivery in China, by Foerster et al. (2014) to investigate the effect of land cover on sediment delivery in small catchments, and it is also implemented in the InVest model (Sharp et al., 2020). However, to our knowledge, this approach is not well-tested e.g. for estimating sediment delivery rates strictly at agricultural settings in northern boreal conditions in Finland.

Previous studies with this approach have focused on areas with relatively large topographic variations (e.g., Borselli et al., 2008; Gay et al., 2016; Hamel et al., 2017; Ortíz-Rodríguez et al., 2017; Zhao et al., 2020), while the connectivity in mildly undulating lowlands has been less studied. To comprehensively understand occurrence and practical implications of sediment connectivity, it is essential to study it in lowland environments. Knowledge of sediment connectivity can have implication, for example, regarding efficient targeting of buffer strips on the soil surface. In addition to these epistemic uncertainties regarding sediment connectivity in lowland environments, the related computational uncertainties – e.g. digital elevation model (DEM) processing - can also differ from those of highlands. Therefore, given the importance of understanding the uncertainties in predicted erosion rates and the benefits of including sediment transport in RUSLE, our aim is to provide 1) an assessment of prediction uncertainty of RUSLE and 2) an assessment on how sediment connectivity in agricultural environments can be considered in RUSLE. These aims were achieved by 1) literature reviews, 2) evaluation of RUSLE at experimental field sites, small catchments, and large river basins in Finland, 3) evaluation of how sediment connectivity features can currently be considered in RUSLE, and 4) implementation and testing of a sediment connectivity approach with RUSLE based on IC and SDR, using two sub-catchments in Finland as case study areas with focus on agricultural lands.

In the case study of Finland, the work presented in the document is largely based on two articles (Tähtikarhu et al., 2022; Räsänen et al., 2023) that were prepared during the project. This document contains condensed analyses and results from these papers, and more detailed descriptions can be found from them. This deliverable contains also some parts that are not included in the above mentioned two papers. The paper by Räsänen et al. (2023) was partially funded also by other sources.
In the case study of Flanders the Water and Tillage Erosion/Sediment Delivery (WaTEM/SEDEM) model was assessed and tested. This model combines a RUSLE-based erosion rate model (WaTEM) with a sediment routing algorithm and a sediment transport capacity model (SEDEM), and was widely applied before in the same Belgian environments, in Italy (Van Rompaey et al., 2005; De Vente et al., 2006) and at European level (Van Rompaey et al., 2003; Borrelli et al., 2018).
For the Italian case studies two different models were applied: RUSLE, applied at catchment scale, combined with the sediment post-processing Unit Stream Power–based Erosion Deposition (USPED) methodology (Moore and Burch, 1986; Desmet et al.,1995; Mitasova et al., 1996), considering also the erosion transport within the sediment connectivity framework - slightly different in respect to the IC-SDR model previously mentioned for Finland.
Finally, at plot scale the Watershed Erosion Prediction Project (WEPP) physically based model was tested, as well as the results of seven years in seven plots with different trials of experimental measures were compared with the model performance.

## 2. Methodology

The primary methodological approach involves the general evaluation and assessment of selected models, some of which were used in the SCALE Project case studies, regarding their potential to incorporate a series of connectivity elements. This includes both empirical and physically based models. In addition to the connectivity elements, the different indices or indicators required by the various models will also be assessed, as they are essential for the parametrization of the transport processes of sediments on the slopes and/or inside a catchment.
A first general overview of the assessed models as used by the various project partners, for their applicability at different scales, is reported in Table 1, indicating also where each model was tested (plot, catchment or wide – regional - scale).
Some models, both Physically based (PB) and Empirical (E) were tested in various case studies, and the results are reported here. For other models, only a general assessment is reported, based on an analysis of their structure and operation as found in literature and user manuals.

*Table 1. Type of evaluated models (PB = Physically based; E = Empirical) and geographic resolution assessment.*

| *MODEL* | *Type of Model* | *Parcel scale* | *Catchment scale* | *Regional scale* | *Case study for assessment* |
|---|---|---|---|---|---|
| **Open LISEM** | PB | Yes | Yes | No | No |
| **IBER** | PB | Yes | Yes | No | No |
| **EROSION 3D** | PB | Yes | Yes | No | No |
| **WEPP** | PB | Yes | Yes | No | Yes (Italy plots) |
| **MHYDAS-erosion** | PB | No | Yes | No | No |
| **RUSLE + (Ic_SDR)** | E | Yes | Yes | Yes | Yes (Finland plots and catchment) |
| **RUSLE + USPED** | E | Yes | Yes | No | Yes (Italy catchment) |
| **SWAT** | PB | No | Yes | No | No |

This project has received funding from the European Union's Horizon 2020 research and innovation programme under grant agreement N° 862695

| | | | | | |
|---|---|---|---|---|---|
| **WaTEM/SEDEM (WS-CN version)** | E | Yes | Yes | Yes | Yes (Flanders catchments) |

## 2.1 Connectivity indexes, parameters, and landscape elements

According to the list of models evaluated in relation with the connectivity of soil sediment transport inside a plot, catchment or basin, various variables inside the modelling functions were taken in account, including:

a) landscape inputs related to morphology, soil, climate, and land use: morphometric parameters, derived from a Digital Elevation Model, such as Length-slope Factor (LS), Curvature, Flow Direction, Flow accumulation, Land Cover and Management Factor (C) Support Practices (P), Climatic (Rainfall erosivity R coefficient), and soil parameters/factors, such as erodibility (K) coefficient, soil infiltrability, cohesion, roughness, etc.;
b) transport indexes and parameters: Connectivity index (IC), Erosion/Deposition Index (ED), Sediment Delivery Ratio (SDR), Sediment delivery (Q), Parcel connectivity factor (PCF), Parcel Trapping Efficiency Factor (PTEF), Transport Capacity factor (TC), Transport Capacity coefficient (kTC), Tillage transport coefficient (ktill), Transmissivity Factor (Tc);
c) landscape elements linked to and affecting connectivity rate. These elements, in almost all cases of anthropic origin, can be divided into two main categories: permanent or temporary, depending on their use over time (generally seasonal according to the cropping systems) and/or connection with the transformations of the rural/agricultural landscape (Table 2).

Not all the elements/parameters/coefficients as reported in the points a), b), and c) were effectively assessed by the modelling activity carried out in the case studies; for some of them the assessment results from literature by previous studies were reported, possibly in similar environments and geographical scales, to be comparable with the project modeling.

*Table 2. Geographic connectivity elements list, with description, category, and duration over time.*

| Connectivity element | Description | Category and duration over time |
|---|---|---|
| **Parcel borders** | Border of single parcel with different land use and/or management; generally associated with other secondary elements/coefficients (i.e. Tillage direction, Tillage transport coefficient) | Temporary – from seasonal to 5-10 years |
| **Tillage direction** | Direction of tillage for a single parcel related to the slope and parcel orientation | Temporary |
| **Upstream land use** | Land use in the upstream position related to the considered parcel, describing the topological relationships among the parcels along the stream network | Temporary, same as Parcel borders |
| **Roads** | Every type of roads inside the catchment/basin, both dirt/gravel or asphalted roads, of any amplitude | Considered as permanent (almost more than 20 years) |
| **Ditches** | Narrow channels dug into the soil, used both for drainage of the runoff water alongside a road or the edge of a field | Permanent, connected with the river network as artificial channels |
| **Sewer system** | System to convey sewage or surface runoff (stormwater, meltwater, rainwater) using sewers. It encompasses components such as receiving drains, manholes, pumping stations, storm overflows | Permanent |
| **Watercourses** | Permanent rivers and/or artificial water channels | Permanent |
| **Terraces** | Plane surfaces/strips built-up by earth movements generally delimited by stony walls | Permanent |

This project has received funding from the European Union's Horizon 2020 research and innovation programme under grant agreement N° 862695

| | | |
|---|---|---|
| **Temporary ditches** | Narrow channels dug in the soil, used for drainage of the exceeding rainwater (preventing free runoff) inside the fields in sloping lands, generally connected with the permanent ditches/rivers network | Temporary, seasonal, during the winter/fall rainy season |
| **Ponds** | Generally earth-made from small to big dimensions (also cement dams), working as water reservoir to multiple uses (generally for agricultural ones) | Permanent |
| **Land levelling** | Artificial land movements such as excavations to modify the original morphometric profile, soil horizons and water fluxes | Permanent |

## 2.2 Ability of different models to incorporate connectivity elements – Overview of the selected models

Based on the type of model, a revision has been made both on the case studies (Finland, Flanders and Italy) and from the literature, about the potential to incorporate the various elements of connectivity and the relative setting of the parameters/indices connected to them. The summary of the results for empirical models are reported in Table 3. For physically based models the technical evaluation was made only for WEPP in the Italian case study. For other models a general assessment based on the overview of each model characteristic was made and is reported in section 4.

*Table 3. Overview of the connectivity elements to be considered inside empirical models RUSLE and WaTEM/SEDEM (WS). (T) = temporary; (P) = permanent.*

| | **Empirical model** | | **Uncertainties (technical/methodological/epistemological)** | **Sensitivity analisys (references)** |
|---|---|---|---|---|
| ***Connectivity features*** | **RUSLE** | **WS** | | |
| **Parcel borders (T)** | Y/Y | Y | WS: Different settings of PCF, SDR. RUSLE: Connectivity Index (W coefficient settings), Connectivity Index Vs Erosion rates | Finland, Flanders and Italy case studies |
| **Tillage direction (T)** | Y/Y | Y | Lack of data | Flanders case study |
| **Tillage transport coefficient Ktill (T)** | N | Y | Few data for Belgium and Italy | Govers et al. (1994), Alba et al. (2006) |
| **Upstream land use (T)** | Y/Y | Y | WS: Settings of PTEF | Flanders case study |
| **Roads (P)** | Y/Y | Y | WS: Transport coefficient of infrastructure (current approach: no sedimentation); RUSLE: not possible to manage (not included in the model) | Flanders case study |
| **Ditches (P/T)** | N/Y | Y | Modelling transport of sediment in ditches (current approach: endpoint). Lack of data (ditches only partially known, underground pipes not known) | Flanders case study |
| **Sewer system (P)** | N/Y | Y | WS: Modelling transport of sediment in sewer system (current approach: endpoint) Lack of data (inlets not known, only strings) | Flanders and Finland case studies |
| **Watercourses (P)** | Y | Y | Lack of data | No References |

| | | | | |
|---|---|---|---|---|
| **Terraces (P)** | Y | Y | WS/RUSLE: Modeling break of slope inside DEM. Lack of data: effects on water flux and sediment transport depending on terraces morphometry and degree of conservation | Finland case study; Bazzoffi & Gardin (2011) |
| **Temporary Ditches (T)** | Y | N | RUSLE: Modeling as water preferential flux lines on the slopes; uncertainties depending on topographic arrangement (slope, distance, depth); WS: not provided | Bazzoffi et al. (2011); |
| **Ponds (P)** | Y | Y | Modelling of sediment transport in ponds (current approach WS: endpoint); DEM derived slope (WS - RUSLE) | Flanders case study; Van Rompaey et al. (2003) (EU); De Vente et al. (2006); Van Rompaey et al. (2005) (Italy) |
| **Land Levelling (P)** | N | N | DEM (slope) modified (tested only in hilly areas with permanent tree crops) | Bazzoffi & Tesi (2011) |

## 2.3 Empirical models

This type of models is referred to as “empirical” because they originate from laboratory investigations and open field experiments. They provide an estimate of the average annual soil loss. In theory, they have a limited applicability outside the conditions for which they were developed. When applied in other contexts, they should be properly recalibrated with local data and measurements. They are unsuitable for studying processes in dynamic development.
**Setting**: they allow the estimation of the soil loss by interpreting the parameters that account for all the factors influencing the process.
**Temporal scale**: they estimate the soil loss deriving from a single erosive event, from a historical series of events or on an average annual scale.
**Spatial resolution** (geographic scale): these models were originally tested on single plot at field scale, but were later applied and verified on a hydrographic basin scale with distributed approaches.
**Output**: originally, the models were developed for the estimation of the soil loss, and were later modified to estimate the production of sediments as well.
RUSLE-IC/SDR, WaTEM/SEDEM and RUSLE+USPED models were successfully tested in some experimental areas at different scales, from plot to regional scale (as reported in Table 1), with an accurate sensitivity analysis and assessment of uncertainties depending on the geographic resolution, the landscape characteristics (morphometry, soil, climate, land use, surface hydrology, etc.) by using different representation of the connectivity elements and parametrization of the related connectivity indexes.

### *2.3.1 The Revised Universal Soil Loss Equation (RUSLE) model*

The RUSLE (Renard et al., 1997) is an empirical model for predicting sheet and rill erosion by water, and it is the most widely used erosion model with an increasing trend in its use (Alewell et al., 2019; Batista et al., 2019; Borrelli et al., 2021). RUSLE is a revised version of USLE (Wischmeier and Smith, 1978; Foster et al., 1981), and it was originally developed for assessing soil loss at field slope/plot scale but has been later widely used as a spatially distributed model. The RUSLE equation is:

$$A = R \times K \times LS \times C \times P \qquad (1)$$

This project has received funding from the European Union’s Horizon 2020 research and innovation programme under grant agreement N° 862695

where A is the annual average erosion (t $ha^{-1}$ $yr^{-1}$); R is the rainfall-runoff erosivity factor (MJ mm $ha^{-1}$ $h^{-1}$ $yr^{-1}$) describing the effect of local rainfall and runoff on erosion, and is defined by the energy intensity of rainfall events; K is the soil erodibility factor (t ha h $ha^{-1}$ $MJ^{-1}$ $mm^{-1}$) describing the propensity of soil to be detached by the energy of the rainfall and runoff, and is affected by soil properties, including particle size fractions, organic matter content, soil structure, soil permeability and soil freezing; LS is the topographic factor (dimensionless) describing the effect of the slope length (L) and steepness (S) on erosion; C is the cover management factor (dimensionless) considering the effects of different cropping and tilling practices on erosion, and it is described by the prior land-use, canopy cover, surface cover, and the surface roughness; P is the support practice factor (dimensionless) accounting for the effect of various support practices on erosion, including contouring, strip cropping, terracing and subsurface drainage. For a more detailed description of RUSLE factors, see Renard et al. (1997).

The original field slope/plot scale RUSLE predicts soil loss, or the amount of sediment transported to the end of the slope (Renard et al., 1997), whereas the spatially distributed RUSLE predicts soil loss at a spatially discrete unit, such as a grid cell, but does not account for sediment transport between the spatial units. Therefore, the predictions of spatially distributed RUSLE over a landscape are gross erosion predictions. The spatial units are, however, connected in the spatially distributed computation through the LS factor accounting for the effect of slope length and steepness on erosion rate at each spatial unit.

### *Post processing methodologies to calculate/predict sediment loss*

Because of RUSLE empirical model limitations, it is not possible to evaluate directly from a RUSLE erosion map the sediment movement in the landscape by identifying the upslope erosion and the downslope deposition paths. So, it is necessary to implement some post-processing methodologies to achieve this aim. There are many available RUSLE-based methodologies to estimate/calculate the SDR as a further step to be added to RUSLE model, as well as many slightly different approaches are reported from literature to calculate/estimate SDR and consequently Sediment Yield.

Indeed, a huge number of articles used the empirical SDR-area power function to estimate SDR (Lu et al., 2006; Othman et al., 2023), and other studies used a constant number (between 0 and 1) to treat the SDR (Lu et al., 2006; Vigiak et al., 2012).

Most famous models are based on the nonlinear regression between the SDR and the basin area with the following equation (Vanoni, 1975; Sharda and Ojasvi, 2016):

$$SDR = \alpha \cdot Ab^{-\beta} \qquad (2)$$

where α and β are coefficients, and Ab is the basin area in $km^2$. The area of the basin is the most affecting factor in determining the SDR for these models (Table 4).

*Table 4. The α and β coefficients used to estimate the SDR according to the basin area with four different models SDR1-4 (From Othman et al., 2023).*

| α | β | References | Unit of the Area | Model No. |
|---|---|---|---|---|
| **0.4724** | 0.125 | Ozsoy et al., 2012; Ozsoy and Aksoy, 2015; Vanoni, 1975 | $km^2$ | SDR1 |
| **1.817** | 0.132 | Othman et al., 2021; Sharda and Ojasvi, 2016 | $km^2$ | SRD2 |
| **2.945** | 0.205 | Sharda and Ojasvi, 2016 | $km^2$ | SDR3 |
| **0.51** | 0.11 | Rosas and Gutierrez, 2020; Ouyang and Bartholic, 1997; Behera et al., 2020 | $m^2$ | SDR4 |

This project has received funding from the European Union's Horizon 2020 research and innovation programme under grant agreement N° 862695

Borselli et al. (2008) suggested a model that depends on the drainage basin's hydrological and sediment connectivity to calculate the SDR, which depends on calculating the IC. This was the approach used in the Finland case studies.

*Index of Connectivity (IC) and Sediment Delivery Ratio (SDR)*

Here an introduction is given to RUSLE and to a sediment connectivity modelling approach based on IC and SDR. While RUSLE estimates the erosion within discrete spatial units, the quantification of the consequent environmental loads requires the understanding of sediment transport from the source areas towards surface water bodies. The transport processes are wide-ranging and complex (Jarvis et al., 1999; Warsta et al., 2013; Turunen et al., 2017), but relatively simplistic models have also been developed to provide quantitative insight into the key processes and have also been combined with the RUSLE model (Zhao et al., 2020).

Combining IC (Borselli et al., 2008) with RUSLE results is among the most promising methods to analyze transport of sediment within landscapes with a relatively low amount of data (Vigiak et al., 2012). While sediment connectivity describes how sediment is transported between different areas, the model is based particularly on the concept of structural sediment connectivity (Wainwright et al., 2011) and focuses particularly on surface runoff. Structural sediment connectivity is computed based on landscape structural elements, including elevation and roughness. The concept excludes connectivity dynamics (temporal variation in the degree of connectivity), which is reasonable as the structural landscape elements can set key controls on sediment connectivity. Combining IC with RUSLE has produced promising results when evaluated using catchment-scale data and data within landscapes (Borselli et al., 2008; Hamel et al., 2017).

The IC [-] is calculated as follows:

$$IC = log_{10}\left(\frac{D_{up}}{D_{down}}\right) \tag{3}$$

where $D_{up}$ [-] is the upslope factor and $D_{down}$ [-] is the downslope factor. $D_{up}$ is calculated as:

$$D_{up} = \overline{W}\overline{S}\sqrt{A} \tag{4}$$

where $\overline{W}$ [-] is the mean weighing factor (upslope area), $\overline{S}$ [m m$^{-1}$] is the mean slope of the upslope area and $A$ [m$^2$] is the upslope area. $D_{down}$ is computed as:

$$D_{down} = \sum_{i=1}^{n} \frac{d_i}{W_i S_i} \tag{5}$$

where $d_i$ [m] is the length of $i$th pixel (along the downslope flow path), $W$ [-] is the weighing factor and $S_i$ [m m$^{-1}$] is the slope of $i$th pixel. $W$ describes the impacts of vegetation cover and land use on the connectivity. $W$ is often parametrized by using the RUSLE $C$ factor (Borselli et al., 2008). Note also that high IC values describe areas with a high degree of connectivity compared to lower IC values.

SDR from a computational grid cell to a chosen location can be described with a sigmoid-type function (Hamel et al., 2017; Zhao et al., 2020):

$$SDR_i = SDR_{max}(1 + \exp\left(\frac{IC_0 - IC_i}{K_{IC}}\right))^{-1} \tag{6}$$

where $SDR_{max}$ [-] is the max. SDR (from 0.0 to 1.0), $IC_i$ [-] is the IC value of the $i$th grid cell, $IC_0$ [-] and $K_{IC}$ [-] are empirical parameters. Sediment delivery to the chosen location can be thereafter computed as (Zhao et al., 2020):

$$Q_i = E_i\, SDR_i \tag{7}$$

where $Q_i$ [t ha$^{-1}$ yr$^{-1}$] is the sediment delivery and $E_i$ [t ha$^{-1}$ yr$^{-1}$] is the erosion in the $i$th grid cell.

This project has received funding from the European Union's Horizon 2020 research and innovation programme under grant agreement N° 862695

*Unit Stream Power-based Erosion Deposition methodology (USPED)*

Another methodology applied for the Italian case study, developed by Mitasova et al. (1996) was the USPED. Both USLE and RUSLE consider erosion only along the flow line, without the influence of flow convergence/divergence, and the equations can be properly applied only to areas experiencing net erosion. Depositional areas should be excluded from the study area. Therefore, direct application of USLE to complex terrain within geographic information system (GIS) is rather restricted. This method is currently implemented in GRASS GIS as a sequence of scripts both for preparing DEM, soil depth and bedrock depth.

The basic equation for the USLE and RUSLE models is Eq. (1), where the values for the factors are determined from various maps, tables, and nomographs based on field measurements (Haan et al. 1994, Renard et al. 1997). An important modification of the USLE/RUSLE backbone used by the USPED was derived by Moore and Burch (1986) and applied by Desmet et al. (1995) and Mitasova et al. (1996). Such modification involves replacement of the LS factor with the upslope contributing area, which allows the model to predict increased erosion due to concentrated flow without the need to define these areas as inputs for the model a priori. An analog LS is computed for each grid cell as:

$$LS = A\ m\ (\sin\beta)\ n \qquad (8)$$

where A is the upslope contributing area per unit width, β is the slope angle, and $m$ and $n$ are constants depending on the type of flow and on the soil properties. Where rill erosion dominates, these parameters are usually set to $m$ = 1.6 and $n$ = 1.3; where sheet erosion prevails, they are set to $m = n$ = 1.0 (Moore and Wilson 1992; Foster 1994). Moore and Burch (1986) further proposed that a modified USLE can be used as a proxy for sediment flow and sediment transport capacity. Using this concept, the USPED model computes both erosion and deposition as a change in sediment transport capacity across a GIS grid cell. In complex topography, sediment flow is represented as a bivariate vector field with the magnitude given by A and the direction given by the water flow direction. Change in sediment flow is then derived as a divergence, leading to a computationally simple formulation for estimating the net erosion or deposition rates (Warren et al. 2000, Mitasova and Mitas 2001).

The USLE or RUSLE parameters are used to incorporate the impact of soil and cover and obtain at least a relative estimate of net erosion and deposition. Estimation of sediment flow was assumed at sediment transport capacity as:

$$Tc = R*K*C*P*A^{m} * (\tan S)^{n} \qquad (9)$$

where Tc = Transport Capacity (kg $m^{-1}$ $sec^{-1}$), R = Rainfall intensity factor (MJ mm $ha^{-1}$ $h^{-1}$ $yr^{-1}$), K*C*P ~ Kt = mitigating effects of soil type, vegetation cover, and land-use practices (dimensionless), A = upslope accumulated area per contour (cell) width ($m^2$ $m^{-1}$ = m), S = topographic slope (°), $m$ = transport coefficient for upslope area (dimensionless), $n$ = transport coefficient for slope (dimensionless).

Net erosion and deposition rates are then computed across the entire DEM as change in sediment flow in the x and y directions across a cell, as follows:

$$ED = \delta(Tc * \cos\alpha)/\delta x + \delta(Tc * \sin\alpha)/\delta y \qquad (10)$$

where ED is net erosion or deposition rate for sediment and α is the topographic aspect (i.e., direction of slope) for a cell. Whether flowing water will erode or deposit sediment in a particular cell is determined by the change in sediment flow (transport capacity) from one cell to the next. If the transport capacity increases (e.g., due to an increase in the steepness of the slope or amount of flowing water), more sediment will be trained and erosion will occur; if the transport capacity decreases (e.g., due to a decrease in slope or water flow) sediment will be deposited.

This project has received funding from the European Union's Horizon 2020 research and innovation programme under grant agreement N° 862695

*USPED temporal simulation on multi-years scale*

Further data to be calculated by GRASS GIS routines to run the simulation for a period of N years (N>1) are:

**Estimation of soil depth and bedrock depth** - Soil depth is important in the routine, as it provides a depth-based limitation on the amount of erosion that can occur at any cell. The depth of soil available to erode is the difference between the current surface elevation (DEM) and the bedrock elevation map "*initbdrk*". The simplest way to estimate the bedrock elevation map is to subtract a constant from the starting DEM map used for *elev* using *r.mapcalc*. A more complex bedrock topography can be estimated using the add-on module *r.soildepth*. In either case, it is important to use the same DEM to derive the bedrock elevations as you will use for the initial starting topography in the simulation.

**Computation of elevation changes from one year to the next** - To compute the new surface elevation after erosion and deposition have occurred, it is necessary to add this year's ED map to last year's DEM, checking first if the amount of erodible soil in a given cell is less than the amount of calculated erosion. The cell will be prevented from eroding more than this amount. If some soil depth remains in the cell, and if the amount of erosion is more than the amount of soil, the routine will remove all the remaining soil and stop. Otherwise, it will remove the amount of calculated erosion. If there is deposition, then it will be added on top of the current depth of sediment (even if no sediment is currently in the cell).

Finally, this routine is sensitive to edge effects carried forward from calculation of slope or other neighborhood routines used earlier in the module. To prevent null cells at the edges of the maps, (the edge cells have no upstream cell, so get turned null), the initial DEM is patched underneath. Thus, the perimeter cells will never change in elevation throughout the simulation. Users are therefore strongly suggested to use a watershed boundary for their input maps (e.g., extracted from *r.watershed*, and then clipped with the map calculator), as cells at the watershed boundary should not change much in elevation in real world scenarios over the time spans of landscape evolution intended to be modeled with this module (100 to 1000 years).

### *2.3.2 The Water and Tillage Erosion/Sediment Delivery (WaTEM/SEDEM) model*

The WaTEM/SEDEM erosion model is based on the WaTEM (Water and Tillage Erosion Model) (Van Oost et al. 2000) and the SEDEM (Sediment Delivery Model) (Van Rompaey et al. 2001) models. The accurate definition of the connectivity in sediment transport modelling is crucial to determine the effect of off-site sediment damages (e.g., watercourses, sewers, ditches, residential area, vulnerable nature). Connectivity in erosion and sediment transport models is typically represented by structural landscape elements such as roads, small landscape elements or sewers, as well as connectivity parameters, determining the amount of sediment transported in relation to the landscape characteristics. In the pixel-based erosion and sediment transport model WaTEM/SEDEM the defined connectivity parameters are the transport capacity parameters on the one hand and connectivity/trapping efficiency parameters on the other hand. These parameters determine the extent to which sediment is transported from one pixel to another, yet do not define the transport direction, which is defined by the structural landscape elements and the topography (DTM). In WaTEM/SEDEM the amount of transport is limited by the TC, which is determined by the sediment holding capacity of the discharge (Wainwright et al., 2015):

$$TC = kTC \; EPR \qquad (11)$$

where kTC is the transport capacity coefficient (m) and EPR is the potential erosion due to concentrated drainage in channels (rill erosion, $kg.m^{-2}\ year^{-1}$). The transport capacity coefficient is a measure for the sediment transitivity (meters per pixel) of a landscape element. In the current setup

This project has received funding from the European Union's Horizon 2020 research and innovation programme under grant agreement N° 862695

of the WaTEM/SEDEM model for Flanders, two landscape elements are defined: elements with a high (〖kTC〗_high, i.e. for agriculture) and low (〖kTC〗_low, used for grassland and forest) transitivity.
The PCFs and the PTEFs are two other parameter groups that determine the amount of transport. Both vary as a function of the landscape elements. The PCFs are defined as the amount of upstream area that is transferred from one to another specific land use, while the PTEF for a given land use expresses the percentage contribution of one pixel to the downstream pixels, as a function of the specific land use of the pixel without considering the land use of the downstream pixels. In WaTEM/SEDEM the PCF is defined for agriculture, grass strips and forest, while the PTEF is defined for agriculture, pasture (grassland) and forest.
The eight parameters mentioned are set for the WaTEM/SEDEM model in the context of Flanders (20 m) (Gobeyn et al., in preparation), as shown in Table 5.

*Table 5. Settings of parameters inside WaTEM/SEDEM for kTC, PCF and PTEF in the context of Flanders case study (for a 20m pixel resolution)*

| WaTEM/SEDEM Parameters set for Flanders Catchments |
|---|
| 〖kTC〗_low: 1 m |
| 〖kTC〗_high: 9 m |
| 〖PCF〗_cropland: 90 % |
| 〖PCF〗_grasstrips: 100 % |
| 〖PCF〗_forest: 30 % |
| 〖PTEF〗_crop: 0 % |
| 〖PTEF〗_pasture : 75 % |
| 〖PTEF〗_forest: 75 % |

The application in the Flanders case studies was aimed to identify the most important connectivity parameters (sensitivity analysis) and to quantify the effect of the uncertainty of the parameters on the model output. A sensitivity analysis is the study of the variation in a model output that can be partitioned between different sources of parameters. The analysis aims to identify the most influential parameters given an output variable of interest. An uncertainty analysis is used to measure the effect of the parameter uncertainty on the model output. It is important to emphasize that sensitivity and uncertainty analyses are closely related. In this study we distinguish the purposes of the analyses: in the sensitivity analysis we want to identify the most determining parameters, while in the uncertainty analysis we want to know the effect of the most determining parameters on the output.
It should be noted that in this study no sensitivity analysis is performed on the WaTEM/SEDEM model structural elements (roads, small landscape features, sewerage), although these elements are known to be crucial to describe connectivity in the landscape (Batista et al., 2021).

## 2.4 Physically based models

### *2.4.1 The Watershed Erosion Prediction Project model (WEPP)*

The WEPP model represents a new erosion prediction tool based on fundamentals of stochastic weather generation, infiltration theory, hydrology, soil physics, plant science, hydraulics, and erosion mechanics. It was a product of soil erosion research made by the National Soil Erosion Research Laboratory of the USDA - Agricultural Research Service (ARS), West Lafayette, IN. Software, documentation and particular tools are available at https://www.ars.usda.gov/midwest-area/west-lafayette-in/national-soil-erosion-research/docs/wepp/.

This project has received funding from the European Union's Horizon 2020 research and innovation programme under grant agreement N° 862695

As reported in the User Manual – Chapter 1 – Overview of WEPP model (Flanagan et al., 1995) "the hillslope or landscape profile application of the model provides major advantages over existing erosion prediction technology. The most notable advantages include capabilities for estimating spatial and temporal distributions of soil loss (net soil loss for an entire hillslope or for each point on a slope profile can be estimated on a daily, monthly, or average annual basis), and since the model is process-based it can be extrapolated to a broad range of conditions that may not be practical or economical to field test. In watershed applications, sediment yield from entire fields can be estimated." The different approaches at Landscape, Plot and Watershed levels are shortly reported in Figure 1.

Processes considered in hillslope profile model applications include rill and interrill erosion, sediment transport and deposition, infiltration, soil consolidation, residue and canopy effects on soil detachment and infiltration, surface sealing, rill hydraulics, surface runoff, plant growth, residue decomposition, percolation, evaporation, transpiration, snow melt, frozen soil effects on infiltration and erodibility, climate, tillage effects on soil properties, effects of soil random roughness, and contour effects including potential overtopping of contour ridges. The model accommodates the spatial and temporal variability in topography, surface roughness, soil properties, crops, and land use conditions on hillslopes. In watershed applications, the model allows linkage of hillslope profiles to channels and impoundments. Water and sediment from one or more hillslopes can be routed through a small field scale watershed. Almost all the parameter updating for hillslopes is duplicated for channels. The model simulates channel detachment, sediment transport and deposition. Impoundments such as farm ponds, terraces, culverts, filter fences and check dams can be simulated to remove sediment from the flow (Flanagan et al., 1995).

The WEPP erosion model computes soil loss along a slope and sediment yield at the end of a hillslope. interrill and rill erosion processes are considered. interrill erosion is described as a process of soil detachment by raindrop impact, transport by shallow sheet flow, and sediment delivery to rill channels. Sediment delivery rate to rill flow areas is assumed to be proportional to the product of rainfall intensity and interrill runoff rate. Rill erosion is described as a function of the flow's ability to detach sediment, sediment transport capacity, and the existing sediment load in the flow.

The appropriate scales for application are tens of meters for hillslope profiles, and up to hundreds of meters for small watersheds. For scales greater than 100 meters, a watershed representation is necessary to prevent erosion predictions from becoming excessively large.

The WEPP model includes components for weather generation, frozen soils, snow accumulation and melt, irrigation, infiltration, overland flow hydraulics, water balance, plant growth, residue decomposition, soil disturbance by tillage, consolidation, and erosion and deposition. The model includes options for single storm, continuous simulation, single crop, crop rotation, irrigation, contour farming, and strip cropping.

This project has received funding from the European Union's Horizon 2020 research and innovation programme under grant agreement N° 862695

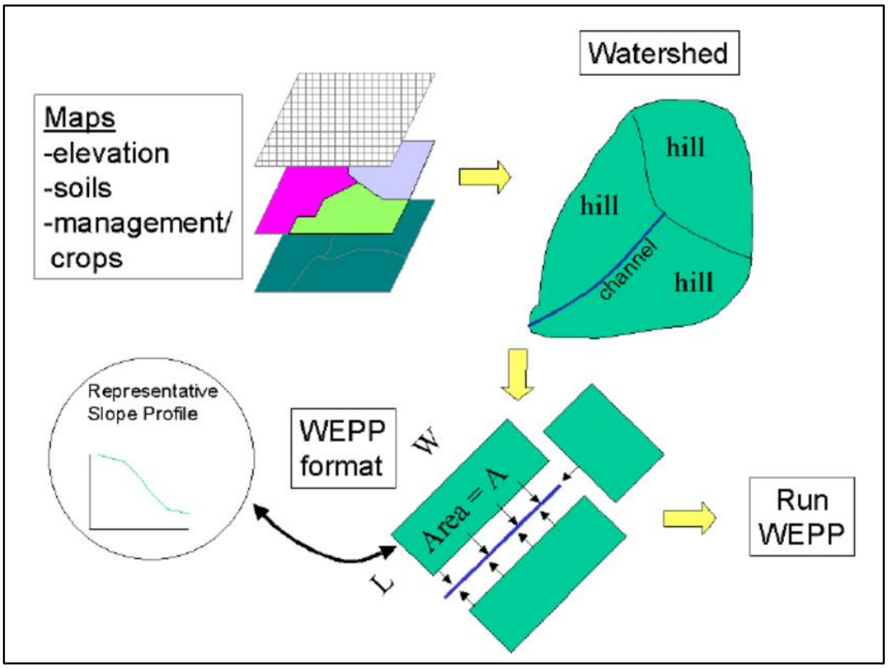


*Figure 1. Steps in discretizing a watershed for a WEPP model simulation at watershed and parcel levels (From Flanagan et al., 2000).*

# 3. Evaluation of uncertainties and sediment connectivity on case studies

In this chapter the results of the assessment and evaluation of uncertainties of some selected empirical and physically based models applied in the case studies of Finland, Flanders and Italy at catchment and plot/field scale are presented. For all the case studies a first preliminary description about the initial settings and calibration activity, according to the local scale and data sources availability, of the input parameters used is reported. Then the model's performance by assessing the uncertainties according to the sediment erosion measured yields is reported, as well as the model sensitivity following the parametrization adopted.

## 3.1 Finland case study (LUKE)

### *3.1.1 Introduction*

The prediction uncertainties were evaluated through a review of scientific literature and a case study at seven experimental fields in Finland, and by comparing RUSLE's predictions at small agricultural catchments and large basin in Finland against observed sediment loads in rivers and streams. The sediment connectivity approach was based on connectivity index and sediment delivery computations, and it was implemented and evaluated using two agricultural catchments in Finland as case study areas. The evaluation showed that RUSLE performs similarly to other erosion models in predicting long-term average erosion rates, but the errors in absolute erosion rates are large. At catchment and basin scales RUSLE was able to rank areas according to the magnitude of observed sediment loading. This suggests that RUSLE is most likely best used for relative comparison of erosion rates (e.g., between areas and scenarios) instead of for accurate estimation of absolute erosion rates. For considering sediment connectivity features, spatially distributed RUSLE was found to be highly limited, and therefore additional methods are needed. The implemented sediment connectivity approach suggests that it may provide new avenues for modelling sediment connectivity in agricultural environment based on RUSLE. For example, the approach reveals how different parts of the fields are connected to ditches, streams, and rivers, which may support evaluation of erosion mitigation strategies over different spatial scales. The information can be important from the point of view of targeting sediment load mitigation measures. However, further research is needed on more reliable parametrization of the approach and on the implementation of water protection measures (e.g., grassed riparian buffer zones) in the model. Altogether, the results suggest that the uncertainty assessment is highly important for understanding usefulness and applicability of model predictions, and the sediment connectivity approach may improve the understanding of erosion and its management in agricultural settings. Our results decreased epistemic uncertainties related to the role of sediment connectivity in lowland environments and increased understanding of technical uncertainties related to the model-based analyses.

### *3.1.2 Calibration and setting of parameters of RUSLE model for Finland*

First, literature on the performance and uncertainty of RUSLE was reviewed to gain a general understanding on the capacity to predict observed erosion rates, and to compare the performance of RUSLE with other commonly used models. The literature review was not systematic or exhaustive, and focused on more recent applications of RUSLE. After the review, RUSLE was subjected to evaluation in Northern boreal conditions of Finland, and its performance and uncertainty was evaluated at field parcel, small catchment, and large river basin scales.

RUSLE was first developed at 2×2 m resolution for agricultural lands. The R factor was taken from a measurement-based 1×1 km resolution European scale data (Panagos et al., 2015a); the K factor was established using Finnish soil database with 1:200000 scale and was supplemented with soil specific K factor values (Lilja et al., 2017a, 2017b); the LS factor was computed from 2 m resolution LiDAR-based DEM (National Land Survey of Finland, 2020) using the method by Desmet and Govers (1996). The C factor values for different crop and management cases were calibrated against erosion measurements from seven field sites using the least squares method. In P factor calculation only subsurface drainage was considered – a value of 0.6 was used, following Renard et al. (1997) and Lilja et al. (2017a). Thus, the model was subjected only to calibration, since the measured data was inadequate for a separate validation. The development of RUSLE factors data is described in more detail in Räsänen et al. (2023).

The study field sites included Aurajoki, Gårdskulla, Hovi Liperi, Kotkanoja, Nummela and Toholampi (Table 6, Figures 2 and 3) with year-round erosion measurements. The field sites were under different crop and management practices, including spring cereals (wheat, oat, barley) with conventional autumn ploughing, shallow autumn stubble tillage, autumn cultivator tillage, no autumn tillage (winter-time stubble) and direct sowing (winter-time stubble); winter cereals (wheat, rye); perennial grass; and perennial pasture. The sum of erosion via surface runoff and subsurface drainage flow was considered in the evaluation, given that the majority of the eroded material in subsurface drainage is observed to originate from soil surface (Øygarden et al., 1997; Uusitalo et al., 2001; Foster et al., 2003; Turunen et al., 2017). The length of measurement periods for each crop and management type varied from 3-10 years.

The RUSLE setup was aimed at testing its feasibility for national scale modelling, therefore national scale datasets were used, although more precise data were available for the test field parcels (e.g., for soils). The field parcel scale evaluation is described in more detail in Räsänen et al. (2023), which was partially prepared within the SCALE project.

*Table 6. Characteristics of the seven field sites used in the calibration and evaluation of RUSLE (From Räsänen et al., 2023).*

| Field | Description | More detailed field description and data sources |
|---|---|---|

| | | |
|---|---|---|
| Aurajoki (F1) | Southwestern Finland (60.4815°N 22.3678°E), slope 7.0%, Stagnosol (clay), experimental field with 12 plots (each 18×51 m), data period 1989-2002 | Puustinen et al. (2005); Finnish Environment Institute (2019) |
| Gårdskulla (F2) | Southern Finland (60.1766°N, 24.1726°E), slope 5.0%, Stagnosol (clay), single field (4,7 ha), sub-surface drained, data period 2011-2020 | Turunen et al. (2017) |
| Hovi (F3) | Southern Finland (60.4232°N, 24.3711°E), slope 1.7%, Stagnosol (clay), section of a larger field (12 ha), sub-surface drained, data period 1990-2001 | Bengtsson et al. (1992); Finnish Environment Institute (2019) |
| Kotkanoja (F4) | Southern Finland (60.8157°N, 23.5110°E), slope 2.6% Stagnosol (clay), experimental field with 4 plots (33×132 m each), sub-surface drained, data period 1993-2010 | Uusitalo et al. (2018); Finnish Environment Institute (2019) |
| Liperi (F5) | Eastern Finland (62.5297°N, 29.3669°E), slope 1.0%, Stagnosol (silt), experimental field with 4 plots (20×126 m each), sub-surface drained, data period 1989-1999 | Kukkonen et al. (2004); Puustinen et al. (2010) |
| Nummela (F6) | Southern Finland (60.8660°N, 23.4300°E), slope 0.8%, Stagnosol (clay), experimental field with 4 plots (total area 9 ha), sub-surface drained, data period 2007-2016 | Äijö et al. (2018) |
| Toholampi (F7) | Central-Western Finland (63.8209°N, 24.1598°E), slope 1.0%, Regosol (sand), experimental field with 16 plots (16×100 m each), sub-surface drained, data period 1997-2009 | Turtola and Kemppainen (1998); Finnish Environment Institute (2019) |

*Figure 2. The experimental field of Kotkanoja with year-round erosion measurements from four plots (Image: Google Earth).*

The catchment and basin scale analyses were performed by comparing the total gross erosion estimates (t yr$^{-1}$) of the spatially distributed RUSLE for the agricultural lands to total suspended solid (TSS) measurements from rivers in respective catchments and basins. The TSS measurements are expected to well reflect the agricultural loading to rivers, as in Finland the landscape is mostly forested with low erosion rates, and in agricultural catchments the TSS loads originate mainly from agricultural lands. The catchments and basins selected for the analysis did not include significant lakes, reservoirs, or dams, which could have a large impact on sediment transport within the watercourses. This resulted in the selection of five small catchments (5.3 to 15.2 km$^2$) and 14 large river basins (566 to 3095 km$^2$) with measured data spanning from one to three decades (Table 7). The share of agricultural land varied from 11% to 63%. The TSS measurement data were taken from Finnish Environment Institute (2019). It is, however, important to recognize that the spatially distributed RUSLE does not model the

This project has received funding from the European Union's Horizon 2020 research and innovation programme under grant agreement N° 862695

catchment scale erosion-transport-deposition process, and therefore the catchment and basin scale evaluation are only indicative on the RUSLE's capacity to distinguish between broader regions with different erosion rates.

*Table 7. Total suspended solid (TSS) measured data from small catchments and river basins (Finnish Environment Institute, 2019) used for testing RUSLE.*

| Catchment/River basin | Area [km²] | Agricultural land [%] | Data period [years] | Measured average TSS load [kg ha$^{-1}$ yr$^{-1}$] |
|---|---|---|---|---|
| **Small catchments** | | | | |
| Haapajyrä (C1) | 6,09 | 57 | 28 | 104 |
| Latosuonoja (C2) | 5,32 | 17 | 25 | 52 |
| Löytäneenoja (C3) | 6,24 | 63 | 26 | 101 |
| Ruunapuro (C4) | 5,39 | 21 | 27 | 104 |
| Savijoki (C5) | 15,21 | 39 | 28 | 338 |
| **River basins** | | | | |
| Aurajoki (B1) | 874 | 36 | 27 | 364 |
| Ilolanjoki (B2) | 309 | 25 | 20 | 129 |
| Koskenkylänjoki (B3) | 895 | 30 | 16 | 198 |
| Lapväärtinjoki (B4) | 1 098 | 13 | 28 | 66 |
| Lestijoki (B5) | 1 373 | 11 | 23 | 53 |
| Loimijoki (B6) | 3 095 | 36 | 9 | 217 |
| Mustijoki (B7) | 783 | 30 | 23 | 225 |
| Närpiönjoki (B8) | 992 | 21 | 23 | 61 |
| Paimionjoki (B9) | 1 088 | 42 | 28 | 427 |
| Porvoonjoki (B10) | 1 273 | 27 | 23 | 220 |
| Pyhäjoki (B11) | 3 712 | 11 | 29 | 49 |
| Uskelanjoki (B12) | 566 | 43 | 20 | 547 |
| Vantaanjoki (B13) | 1 686 | 23 | 29 | 215 |
| Virojoki (B14) | 357 | 13 | 16 | 76 |

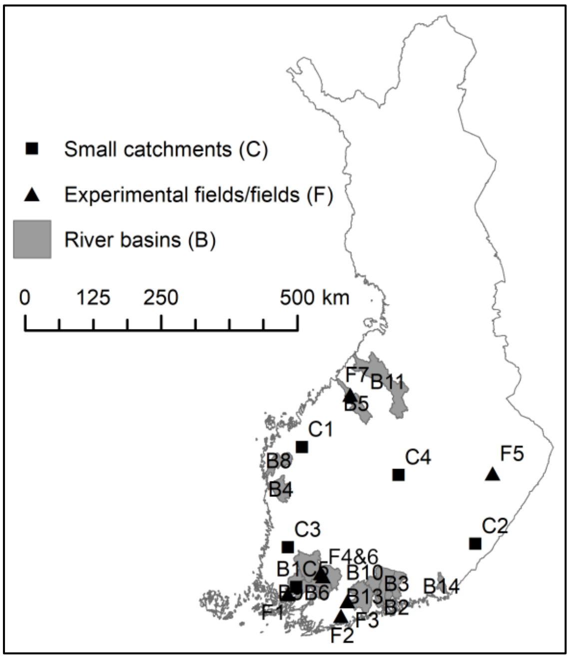


*Figure 3. Location of the experimental field sites (F1-7), small catchments (C1-5) and river basins (B1-14) with measured erosion loads (kg ha$^{-1}$ yr$^{-1}$, t yr$^{-1}$) used for the evaluation of RUSLE.*

### 3.1.3 Implementation of sediment connectivity for Finland case study

The inclusion of sediment connectivity features in RUSLE was evaluated both at field slope/plot scale and at a broader extent. Connectivity features were identified in the original RUSLE handbook (Renard et al., 1997) and additional connectivity features relevant for spatially distributed RUSLE were identified.

First large-scale structural connectivity estimate in Finland was conducted at agricultural lands of two topographically contrasting sub-catchments. RUSLE data of Räsänen (2021) was combined with IC (Eq. 3) and SDR (Eq. 6) to estimate the sediment delivery (Eq. 7) from the field parcels. Furthermore, we estimated the proportion of field areas that are structurally connected to open ditches and streams, based on flow direction and flow accumulation computations (Kebede et al., 2021). The computations were subjected to sensitivity analyses and were done with the ArcGIS software (Borselli et al., 2008). The computations were conducted at the spatial resolution of 2×2 $m^2$. The data and the analyses are shortly presented below and are described in more detail in Tähtikarhu et al. (2022).

The studied sub-catchments of Aurajoki (60.12°N, 23.74°E) and Mustionjoki (60.53°N, 22.44°E) are located in southwestern Finland. The Mustionjoki sub-catchment has an area of 116 $km^2$ while the area of the Aurajoki sub-catchment is 147 $km^2$. Clay soil was the dominating soil type at both sub-catchments. The topography of the Mustionjoki sub-catchment was gently undulating (mean slope 4.9%), while the topography of the Aurajoki sub-catchment was gentle with steep slopes near the streams and rivers (mean slope 2.7%). Spring and winter cereal production are the dominant agricultural activities within the sub-catchments (about 60% of the agricultural land area, according to data from Finnish Food Authority), but also perennial grasses and hay-type crops were grown. The agricultural fields are typically well drained in Finland, typically surrounded by open ditches, and artificial subsurface drainage is a common practice.

Agricultural field parcel borders were taken from the field parcel data of the Finnish Food Authority. The data contains vectorized field parcels and covers nearly all the agricultural lands of Finland. The average parcel area was 2.8 ha and 3.4 ha at the Aurajoki and Mustionjoki sub-catchments, respectively. The parcel boundaries typically closely match with the open ditches or stream locations. Thus, in our computations, the ditches and streams were represented by pixels which were located adjacent to the parcel boundaries.

Differences in elevation were described by a 2×2 $m^2$ lidar-based DEM, taken from National Land Survey of Finland (NLS, 2017). The root mean square error (RMSE) of the DEM is <0.3 m on slopes ≤47%. Only 0.5% of the studied land area had slopes >47%. Mean RMSE has been shown to be 0.11 m, being lower on the mildest slopes (Oksanen, 2013). DEMs typically include topographical depressions (sinks) of different sizes. Some sinks are too small to practically induce structural disconnectivity, and some sinks are caused by inaccuracies in the data. Since the sinks can influence the connectivity computations, we determined threshold values which distinguish which sinks can practically induce structural disconnectivity. Sinks with a lower depth than a threshold value were considered as small depressions or noise and were thus filled in the DEM. We estimated 0.1 m to be a plausible threshold value (Tähtikarhu et al., 2022). However, to understand the sensitivity of our results to the choice of the threshold, we produced 4 different DEMs with the threshold values of 0.05, 0.10, 0.15 and 0.2 m, and they are hereafter called DEM5, DEM10, DEM15 and DEM20, respectively.

The IC (Eq. 3), sediment delivery (Eq. 7) and connected field area computations were subjected to sensitivity analyses. Firstly, all computations were conducted with the four different DEMs (DEM5-DEM20) to produce a range of possible connectivity scenarios. Secondly, the sensitivity of the results to ditch width variability and possible inaccuracies in ditch locations was studied with two additional scenarios. In these two scenarios, the ditches were widened 2 and 3 pixels (4 and 6 m) and the scenarios are hereafter called DITCH4 and DITCH6, respectively. Finally, we also studied the sensitivity of the results to parameter variations. The empirical parameters in Eq. 6 were determined based on previous studies and local observations. The parametrizations (P1-P7) are shown in Table 8 (see Tähtikarhu et al., 2022 for further details).

*Table 8. Parametrizations in the sensitivity analysis (sediment delivery computations).*

| Parametrization | P1 | P2 | P3 | P4 | P5 | P6 | P7 |
|---|---|---|---|---|---|---|---|
| **Description** | Widely used literature value | Literature value | Literature value | Literature value | Reflects local data | Reflects local data | Reflects local data |
| $IC_0$ | 0.5 | 0.5 | 0.5 | 0.1 | -4.7 | -3.3 | -5.7 |
| $K_{IC}$ | 2.0 | 1.8 | 3.5 | 2.0 | 1.0 | 1.0 | 1.0 |
| $SDR_{max}$ | 0.8 | 0.8 | 0.8 | 0.8 | 0.8 | 0.8 | 0.8 |

While the results were computed at the 2×2 $m^2$ pixel scale, the IC and Q were aggregated to field parcel scale. The aggregation was conducted by calculating mean values for each field parcel. The field parcel scale is of particular interest, being a typical scale for agricultural and erosion management choices.

### 3.1.4 Prediction uncertainty of RUSLE for Finland

*Literature review*

RUSLE has been evaluated in a large number of studies (Alewell et al., 2019; Batista et al., 2019; Borrelli et al., 2021), and probably the most extensive evaluations have been done in the United States, where the model was developed, but evaluations have been performed also in various other parts of the world. Moreover, several model adaptations have been done for different climate and soil conditions (Ghosal and Das Bhattacharya, 2020), and remote sensing-based data is increasingly used to derive model parameters in spatially distributed approaches (Phinzi and Ngetar, 2019).

RUSLE and the predecessor USLE have been evaluated against extensive measurement data from large number of rainfall-runoff plots. Risse et al. (1993) compared the performance on USLE against over 1700 years of data from 208 rainfall-runoff plots in USA, determining a Nash-Sutcliffe model efficiency (NSE) of 0.75 for average annual erosion, and an average prediction error of 39% of the measured erosion. Rapp (1994) compared similarly the performance on RUSLE against over 1700 years form 206 rainfall-runoff plots in USA, and determined the NSE to be 0.73. Tiwari et al. (2000) compared the performance of WEPP, USLE and RUSLE against over 1600 years of data from rainfall-runoff plots in USA, and found NSE values of 0.71, 0.80 and 0.72 for the models, respectively. The averages of the prediction errors were 38%, 33% and 54% of the measured erosion, respectively. Some studies have also reported the tendency of RUSLE to over-predict low average annual soil losses and to under-predict high average annual soil losses (Kinnell, 2010; Zhang et al., 1996). Larger share of the evaluation has been performed in USA, but studies show that when USLE-type models are appropriately parametrized their uncertainties are not larger outside USA (Stolpe, 2005; Kinnell, 2010; Meusburger et al., 2010; Yue et al., 2016).

Batista et al. (2019) further reviewed erosion models and compared MMF, PERSERA, RUSLE, RUSLE2, USLE, USLE-M, USLE-MM and WEPP models and did not find systematic differences in model performances in predicting long-term average erosion rates. These authors also found that calibration of model parameters is an important means for improving model performance. It is also the general understanding in literature that more complex models (including process-based) do not systematically outperform each other regarding erosion predictions, and that models should be evaluated against fit-for-purpose tests (Govers, 2011; Alewell et al., 2019; Batista et al., 2019; Borrelli et al., 2021). Govers (2011) further argues that such models may have already reached the upper limit of erosion predictability.

This project has received funding from the European Union's Horizon 2020 research and innovation programme under grant agreement N° 862695

### 3.1.5 Results on uncertainty assessment

The evaluation at the seven field sites (Räsänen et al., 2023) showed that RUSLE predictions were close to measured erosion at five out of seven field sites. At the two field sites with heavy clay soils – Nummela and Kotkanoja – the erosion was underestimated. The $R^2$ for the 20 crop management cases was 0.76 (p-value <0.000), and NSE was 0.72 (Figure 4). The average error of the predictions was -133 kg ha$^{-1}$ yr$^{-1}$ and the 5$^{th}$ and 95$^{th}$ percentiles of the errors were -634 and 141 kg ha$^{-1}$ yr$^{-1}$ (Table), the mean absolute error (MEA) was 190 kg ha$^{-1}$ yr$^{-1}$, and the RMSE was 336 kg ha$^{-1}$ yr$^{-1}$. The long-term average erosion estimates were also within the ranges of measured annual erosion rates, except for Nummela and partially for Kotkanoja (Table 9).

*Table 9. Measured average and estimated erosion rates at the seven field sites. The range of measured annual erosion rates are in brackets (From Räsänen et al., 2023).*

| Crop and tillage management | Field | Treatment | Duration (yr) | Measured erosion (kg ha$^{-1}$ yr$^{-1}$) | Estimated erosion (kg ha$^{-1}$ yr$^{-1}$) | Error (kg ha$^{-1}$ yr$^{-1}$) | Relative error (%) |
|---|---|---|---|---|---|---|---|
| **Cereals with autumn ploughing** | Aurajoki | Normal ploughing | 9 | 2100 (980-4640) | 2213 | 113 | 5 % |
| | Liperi | Normal ploughing | 10 | 125 (67-163) | 146 | 21 | 16 % |
| | Toholampi | Normal ploughing | 10 | 380 (88-661) | 329 | -51 | -13 % |
| | Kotkanoja | Normal ploughing | 10 | 968 (435-1996) | 489 | -479 | -49 % |
| | Hovi | Normal ploughing | 12 | 640 (198-1858) | 638 | -2 | 0 % |
| **Cereals with reduced autumn tillage** | Aurajoki | Shallow stubble tillage | 4 | 1420 (650-2930) | 1699 | 279 | 20 % |
| | Aurajoki | Cultivator | 5 | 1760 (1120-3330) | 1699 | -61 | -3 % |
| | Kotkanoja | Shallow stubble tillage | 5 | 987 (552-1313) | 379 | -608 | -62 % |
| | Nummela | Cultivator | 7 | 1246 (324-2330) | 125 | -1121 | -90 % |
| **Winter cereals** | Aurajoki | Winter wheat | 9 | 1555 (780-3540) | 1566 | 11 | 1 % |
| | Liperi | Winter rye | 3 | 90 (49-130) | 103 | 13 | 14 % |
| **Cereals with winter-time stubble** | Aurajoki | No autumn till | 9 | 790 (270-1500) | 754 | -36 | -5 % |
| | Liperi | No autumn till | 4 | 80 (33-98) | 50 | -30 | -38 % |
| | Toholampi | No autumn till | 4 | 195 (76-456) | 112 | -83 | -43 % |
| | Aurajoki | Direct sowing | 5 | 620 (430-950) | 754 | 134 | 22 % |
| | Kotkanoja | Direct sowing | 3 | 541* | 168 | -373 | -69 % |
| **Perennial grass** | Aurajoki | Grass ley | 4 | 570 (500-620) | 571 | 1 | 0 % |
| | Liperi | Grass ley | 8 | 55 (17-160) | 38 | -17 | -32 % |
| | Kotkanoja | Grass ley | 6 | 631 (383-1239) | 262 | -369 | -58 % |
| **Perennial pasture** | Gårdskulla | Pasture | 9 | 720 (137-1151) | 720 | 0 | 0 % |

For further analyzing of the model errors at field parcel scale, a gamma distribution was fitted to the model errors. This provided a preliminary probability distribution for the prediction errors of the calibrated RUSLE. The resulting error distribution had an average of -134 kg ha$^{-1}$ yr$^{-1}$ and the 5$^{th}$ and 95$^{th}$ percentiles of the error distribution were -711 and 218 kg ha$^{-1}$ yr$^{-1}$.

The catchment and large basin scale comparisons revealed strong correlations between RUSLE predictions and TSS measurements. In large basins the $R^2$ was 0.90 (n = 14, p-value <0.000) and the Kendall's tau was 0.78 (p-value <0.000) (Figure). In small catchments, $R^2$ was 0.49 (p-value = 0.1896), but Kendall's tau rank correlation was 1.00 (n = 5, p-value = 0.0167), which indicates higher uncertainty in absolute erosion estimates, but perfect correlation in the ranking of the catchments by the estimated erosion.

This project has received funding from the European Union's Horizon 2020 research and innovation programme under grant agreement N° 862695

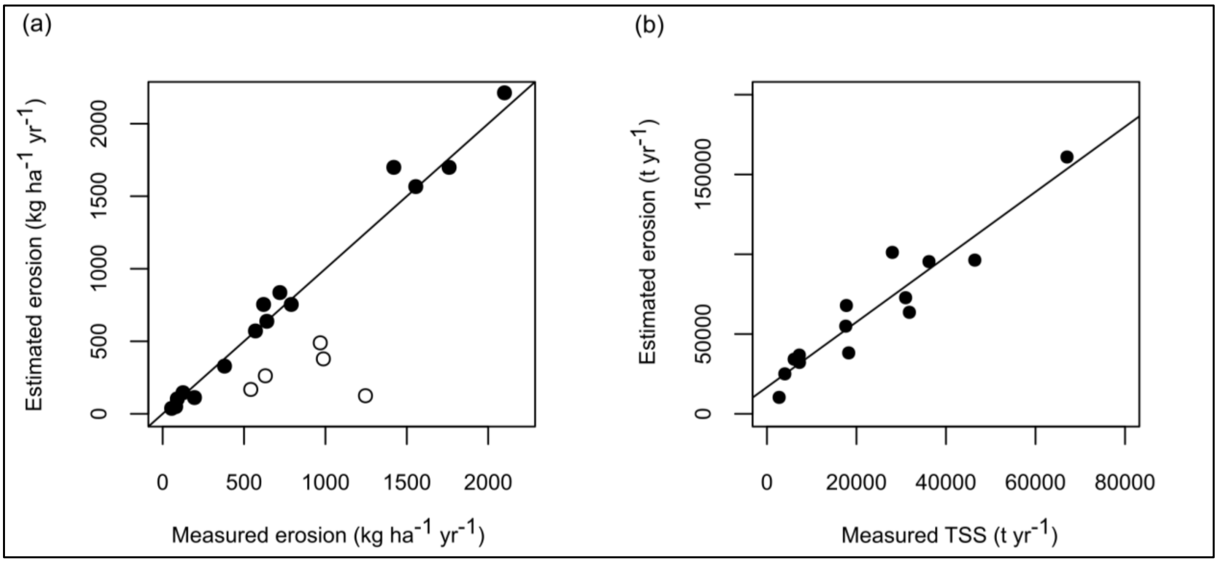


*Figure 4. RUSLE performance at a) seven experimental fields and b) 14 river basins. In tile A, the two fields with model underestimations are shown with empty circles (Kotkanoja and Nummela) and a diagonal line (1:1) is shown. In tile B, linear regression fit is shown.*

### 3.1.6 Sediment connectivity features in RUSLE

The RUSLE is originally used to predict soil loss or sediment delivery at the end of field slope and does not include sediment connectivity descriptions. The original handbook (Renard et al., 1997) demonstrates how different crop and tillage practices, contour tillage, cross-slope strip cropping, buffer strips, filter strips, terraces, and subsurface drainage can be implemented in the model and how they affect the soil loss or the sediment delivery to the end of the slope (Table 10).

The spatially distributed RUSLE, in turn, predicts gross erosion and lacks the description of sediment transport and deposition among the computational spatial units, which notably limits the possibilities for considering structural sediment connectivity. Therefore, many of the features in the original field slope/plot scale RUSLE involving sediment transport cannot be considered, or can be considered only partially, in the spatially distributed RUSLE (Table 10). For example, in the case of buffer strips, their sediment retention cannot be considered, but the effect on erosion generation in their own area can be considered.

In the spatially distributed RUSLE the LS factor is the only element connecting different computational spatial units, and therefore it is the main entry point for considering connectivity within the RUSLE framework. According to Desmet and Govers (1996), hydrologically isolated areas (in terms of surface runoff) can be considered in the LS factor by calculating the factor separately for the hydrologically isolated land units. For example, field parcels are often surrounded by open ditches, leading to hydrological isolation. Also, surface runoff in certain land covers (e.g., forest) can be considered minimal or non-existent, which may require the consideration of hydrological isolation, e.g. when fields are situated downslope a forest (Desmet and Govers, 1996). However, isolation of different land covers is often partial and its consideration in the LS factor is not well developed.

Structural sediment connectivity may also be considered by modifying the DEM underlying the LS calculation. For example, the DEM can be modified to contain ditches and embankments, which in turn will affect the computation of the LS factor and consequently the estimated gross erosion. The feasibility of the DEM modification, however, depends on the resolution of the DEM. High-resolution DEMs provide more opportunities.

Otherwise, spatially distributed RUSLE is a highly limited model for considering structural sediment connectivity, and its use is mainly limited to estimation of gross erosion and the effect of different land

This project has received funding from the European Union's Horizon 2020 research and innovation programme under grant agreement N° 862695

covers and soil management types on gross erosion. For further consideration of sediment transport or structural connectivity elements in spatially distributed RUSLE, additional approaches are needed to supplement the RUSLE framework. The difference between field slope/plot scale and spatially distributed RUSLE, in terms of sediment connectivity are further described in Table 10.

*Table 10. Comparison of field slope/plot scale and spatially distributed RUSLE in terms of type of predicted erosion and possibility to consider erosion measures and connectivity features.*

| | Field slope/plot | Landscape (spatially distributed) |
|---|---|---|
| **Type of erosion** | | |
| Net erosion | Yes | No |
| Gross erosion | No | Yes |
| **Measures and connectivity features** | | |
| Crop/land cover | Yes | Only the effect on gross erosion can be considered |
| Tillage | Yes | Only the effect on gross erosion can be considered |
| Contour tillage | Yes | Only the effect on gross erosion can be considered if tillage direction is exactly according to contours. Off-grade contouring cannot be considered |
| Cross-slope strip cropping | Yes | Only the effect on gross erosion can be considered |
| Buffer strips | Yes | Only the effect on gross erosion can be considered |
| Filter strips | Yes | Only the effect on gross erosion can be considered |
| Terraces | Yes | Can be considered only if terraces are hydrologically isolated, potentially if the flow pathways between terraces can be described in DEM/LS factor and there is no partial reduction of connectivity in the flow pathways |
| Subsurface drainage | The reduction effect on net erosion can be considered, but RUSLE does not include description of transport via sub-surface drainage | The reduction effect on gross erosion can be considered, but RUSLE does not include description of transport via sub-surface drainage |
| Hydrological isolation (surface runoff) of land units | Yes | Yes |
| Topographical features through DEM modification | Can be considered to some extent | Yes |

### 3.1.7 Implementation of sediment connectivity in RUSLE

*Literature review*

IC computations have been previously conducted mainly in areas with relatively large topographic variations (Borselli et al., 2008; Gay et al., 2016; Hamel et al., 2017; Ortíz-Rodríguez et al., 2017; Zhao et al., 2020). The modelling approaches and applied data of the computations often differ and therefore are not directly comparable. However, for reference, Zhao et al. (2017) reported IC values of -10.3 - 5.3, Gay et al. (2016) reported mean values of -3.9 - 10.0 and Cantreul et al. (2017) reported

This project has received funding from the European Union's Horizon 2020 research and innovation programme under grant agreement N° 862695

median values of -8.0 - -6.5. These values demonstrate considerable variability in the degree of connectivity within different catchments.

The IC computations have been previously validated by using field measurements within the studied landscapes. For example, Borselli et al. (2008) found a relationship between computed and empirical (within landscape) connectivity indices. Also Martini et al. (2022) evaluated IC with empirical data within a landscape and suggested that the index can reasonably describe structural connectivity but presents challenges in describing functional connectivity in a mountainous landscape. The combination of IC and sediment delivery computations has been also evaluated using catchment scale data. Vigiak et al. (2012) reported relative RMSE values of 0.10 - 0.34 [-] between computed and measured sediment deliveries at sub-catchment scale. Hamel et al. (2017) evaluated the model in 28 different catchments and reported an overall $r^2$ of 0.47 between the computed sediment deliveries and measured or simulated (reference model) values. Hamel et al. (2017) further stated that major differences among the studied sites were captured by the model. Zhao et al. (2020) also reported a relationship with $r^2 = 0.63$ between measured and computed sub-catchment scale sediment deliveries. Aneseyee et al. (2020) reported a $r^2$ of 0.79 between computed and measured sub-catchment scale sediment deliveries. Also, Gashaw et al. (2021) showed that annual catchment-scale sediment export can be reasonably described with the model. Note also that the above-mentioned studies differ in terms of applied data and modelling choices and thus are not directly comparable.

It has also been recognized that DEM resolution and quality can influence the results. Borselli et al. (2008) mentioned that DEM quality and resolution can have an impact on IC computations. Their influence on computational results have also been systematically studied (Hamel et al., 2017; Cantreul et al., 2017). For example, Hamel et al. (2017) showed how sediment deliveries may correlate with DEM resolution, but DEM resolution did not have a consistent effect on sediment delivery among sites, which underlines the need to understand the location-specific differences. Also, the role of parametrization has been recognized. For example, Hamel et al. (2015) showed how sediment delivery estimates can vary due to uncertainties in parametrization.

### 3.1.8 Results

The results are shown in detail in Tähtikarhu et al. (2022) and a summary is presented here. The conducted computations showed how the pixel scale (2×2 m2) IC values within the two sub-catchments largely overlapped. The values varied between -8.6 - -1.2 in the Mustionjoki and -8.1 - -0.4 in the Aurajoki sub-catchment. The distributions were centred around the median values (-6.0 - -5.9 at Mustionoki and –5.9 - -5.8 at Aurajoki subcatchment) and were slightly skewed. At both sub-catchments, the IC values correlated with log-transformed erosion values (Pearson r = 0.58 - 0.59). Moreover, IC values typically formed tree-like drainage networks within field parcels and thus were not evenly distributed within the landscape. Impacts of the computational scenarios (DEM5-20 and DITCH4-6) on the results were low compared to the variability in the IC values within the DEM10 scenario. The distributions and relationships were qualitatively similar at the parcel scale as compared to the pixel scale.

Most of the agricultural areas within the sub-catchments were connected to the ditches and streams surrounding the field parcels. The share of connected field areas was sensitive to the sink treatment scenario and the share of connected area varied from 65% to 92% at Mustionjoki and from 78% to 97% at Aurajoki sub-catchment in the computational scenarios (DEM5-DEM20 and DITCH4-DITCH6). Disconnected field areas were mostly due to depressions on the soil surface, and they were sporadically located within the sub-catchments.

Parcel scale sediment delivery magnitudes with the different parametrizations P1-P7 varied by several orders of magnitude. This demonstrates that the computed sediment delivery magnitude predictions include high uncertainties. The parcel index of connectivity values correlated significantly with the erosion values (Pearson r ≥0.49) at both sub-catchments (Figure 5).

This project has received funding from the European Union's Horizon 2020 research and innovation programme under grant agreement N° 862695

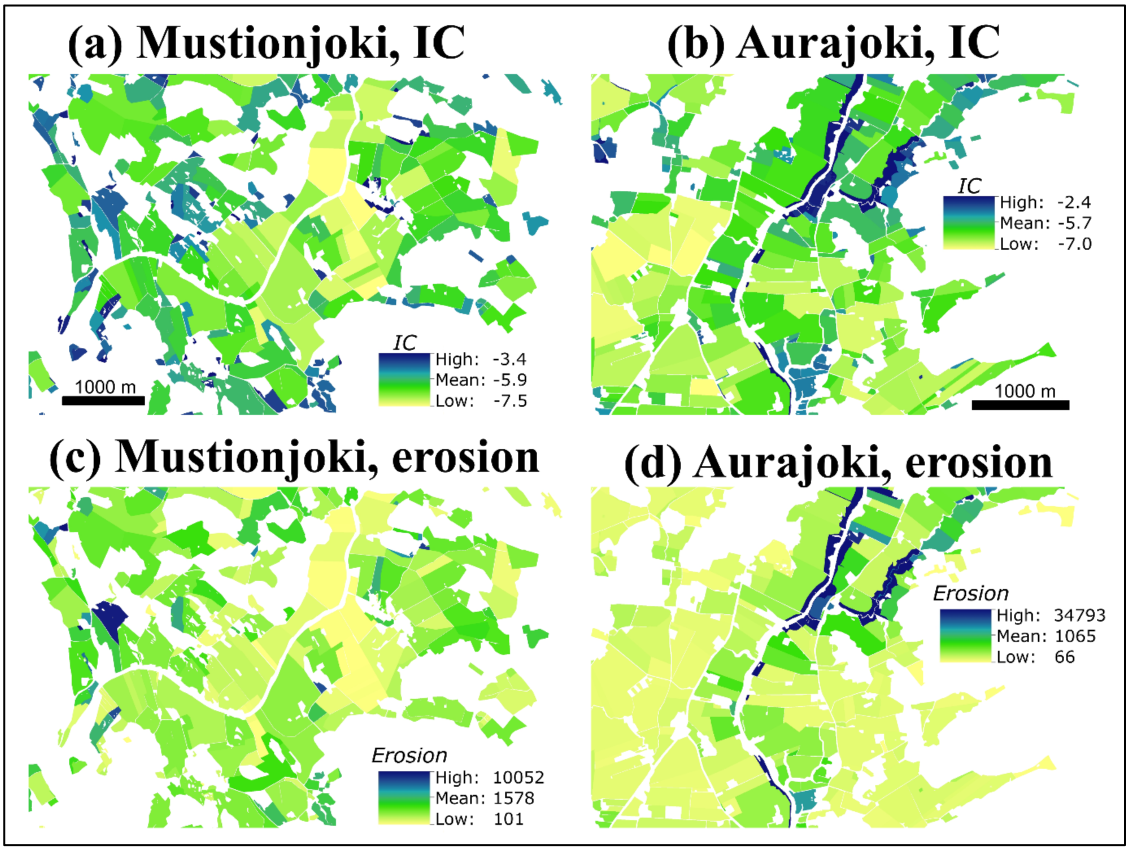


*Figure 5. A representative snapshot on the spatial distribution of the mean plot-scale index of connectivity (IC) and erosion values (RUSLE) at the (a) Mustionjoki and (b) Aurajoki sub-catchments (From Tähtikarhu et al., 2022).*

Finally, we analyzed rank correlations between the calculated parcel scale sediment deliveries in different scenarios. The rank correlations between the sediment delivery results of parametrizations P1-P7 were high (Spearman $r_s$ >0.95, p-value <0.01). Thus, the model produced consistent relative estimates of sediment delivery of the field parcels although the absolute delivery magnitudes were uncertain.

### *3.1.9 Sources of uncertainty in RUSLE*

These findings from field parcel scale by Räsänen et al. (2023) are in line with findings and conclusions in literature. For example, Rapp (1994) and Tiwari et al. (2000) report NSE values of 0.72 - 0.75 for USLE and RUSLE, whereas the NSE in Räsänen et al. (2023) was 0.72. A review by Batista et al. (2019) provided also that the mean performance of non-calibrated and calibrated RUSLE was $-\log_{10}(2- \text{NSE}) = -0.45$ and $(-\log_{10}(2- \text{NSE}) = -0.10$, whereas in Räsänen et al. (2023) the correspondent value was -0.11. The literature further shows that the absolute prediction errors of RUSLE are generally large. Risse et al. (1993) and Tiwari et al. (2000) report average errors of 39% for USLE and 54% for RUSLE, respectively, whereas the average error in Räsänen et al. (2023) was 25%. The findings on catchment scale by Räsänen et al. (2023) are in agreement with the general understanding that erosion models, including RUSLE, are generally capable of ranking areas according to their erosion rates if good quality input data is available (Batista et al., 2019).

The uncertainty in RUSLE's predictions is expected to originate from multiple sources. These uncertainties can be categorized to i) *technical uncertainties* originating from input data parameter values, and parameter estimation methods; ii) *methodological uncertainties* originating from model structure and assumptions; and iii) *epistemological uncertainties* originating from lack of knowledge.

This project has received funding from the European Union's Horizon 2020 research and innovation programme under grant agreement N° 862695

The data for R was developed for the whole Europe and for Finland for a relatively short time period (2007-2013), and its representativeness of local conditions is not well understood. The K data was also based on a national scale soil map at 1:200000, with soil class specific K values, which excludes more local variations in soil properties. The RUSLE factors can also be estimated with different methods with differing assumptions, and in these methods the aspects influencing the erosion process can be selectively considered. For example, the LS factor was calculated with the method of Desmet and Govers (1996) with rill/interrill ratio of 1, whereas different methods and parameter values result in different magnitudes of predicted erosion (Hrabalíková and Janeček, 2017). Also, the observational erosion data for optimizing model parameters and evaluating the model predictions are known to contain uncertainties (Batista et al., 2019). In this study, the erosion measurements from the experimental field sites were from different locations and from different time periods, the data periods were short for individual crop and management cases (3-10 years), and a certain degree of subjectivity was needed in data preparation to account for missing data, etc.

The model structure of spatially distributed RUSLE was also found inadequate for accurately including subsurface drainage and comparing model predictions to observed erosion. The observed erosion is often based on sediment measurements at the outlet of the experimental area, whereas the spatially distributed RUSLE does not include sediment transport or deposition, which significantly impedes the model evaluation. This was the case with evaluation of RUSLE at the experimental field parcels of this study. Most of the experimental field sites of this study were also subsurface drained and most of the sediment loads were observed in subsurface drainage flow. According to the research, soil material in subsurface drainage flow originate mainly from the soil surface (Øygarden et al., 1997; Foster et al., 2003; Turunen et al., 2017; Uusitalo et al., 2018), but RUSLE does not have a process description for accounting this. In the evaluation, RUSLE predictions were simply compared to the sum of observed surface and subsurface sediment loads at the field outlets.

The lack of knowledge was significant in the consideration of erosion reduction effect of subsurface drainage. In literature, a broad range of estimates have presented this reduction effect, and these range from 16% to 84% (Schwab et al., 1977, 1980; Bottcher et al., 1981; Istok and Kling, 1983; Bengtsson et al., 1984, 1988; Formanek et al., 1987; Bengtsson and Sabbagh, 1990; Grazhdani et al., 1996), whereas there is no data on this for Finnish conditions. This uncertainty also propagated to the C factors as they were optimized against observed erosion rates using uncertain P value (0.6) for subsurface drainage. The correctness of the spatial patterns of the predicted erosion also could not be evaluated, as there was no observational data for this. A limited understanding of the uncertainties in individual RUSLE factors was also found to impede the general understanding of uncertainties in model predictions.

### *3.1.10 Interaction of RUSLE with sediment connectivity*

Our results also imply that the variability of IC in agricultural areas may be typically larger within a sub-catchment than between sub-catchments in Finland, even though a higher number of catchments would be needed to reach more robust conclusions. We showed that most of the field parcel area can be structurally connected to the surrounding open ditches and streams. Previously, there have been major epistemological uncertainties regarding the role and magnitude of sediment connectivity in environmental load generation. Despite the modest topographical variations of the studied catchments, the IC values for agricultural lands in Finland were proportional to those found in other lowland environments (Cantreul et al., 2017).

Our results have practical implications regarding design and targeting of environmental protection measures. The largest share of the field areas was found to be connected to the ditches and streams via surface runoff, and therefore buffer strips and grassed waterways may have an important role in sediment load mitigation at large scale, if they are well targeted and can affect the water quality of concentrated surface runoff fluxes. Previous studies have focused on showing the impacts of such measures in field scale (Uusi-Kämppä and Jauhiainen, 2010; Uusi-Kämppä et al., 2000). Our findings are important in terms of reducing epistemic uncertainties related to the large scale and parcel scale connectivity of sediment loads via surface runoff.

Another practically relevant finding was that, despite differences in the parametrization of the sediment delivery model, it produced consistent information on the ranking of the field parcels in terms of relative sediment delivery. This means that the model may be useful for the prioritization of field parcels for targeted environmental protection measures (e.g., wintertime vegetation cover). Previously, also Hamel et al. (2017) suggested that the approach can be useful, particularly regarding the prioritization of the targeting of environmental protection measures. Note, however, that there were marked technical uncertainties regarding the computed sediment delivery magnitudes (parameter uncertainty).

The uncertainties could be reduced by using local sediment delivery data for model calibration and validation. Furthermore, while the study considered structural connectivity, studying the connectivity dynamics would further improve the understanding on connectivity and could decrease epistemological and methodological uncertainties regarding temporal variability of connectivity. Previously, Martini et al. (2022) showed that dynamic connectivity may differ from the structural connectivity in a mountainous landscape. However, in the gently undulating catchments of southern Finland water levels on the field surface (during ponding or overland flow events) are typically low and consequently the structural elements are likely to set key controls on surface runoff routing.

We also assessed technical uncertainties due to input data uncertainty, namely DEM sink processing and ditch width/locations. These uncertainties were small compared to the variability in the IC values within the sub-catchments. However, the share of connected field area was clearly affected by the DEM sink treatment. These results show the importance of DEM processing and quality when estimating the share of connected field area.

It is also noteworthy that our analysis and most of the previous analyses have focused particularly on sediment connectivity via surface runoff. More comprehensive connectivity assessment would require consideration of vertical connectivity of small or colloidal soil particles through the soil to subsurface drains and thereafter directly to surface water (Turtola et al., 2007; Warsta et al., 2013; Turunen et al., 2017). Practically, such vertical connectivity can bypass any disconnectivity elements (e.g. buffer strips) on soil surface. However, the consideration of sediment connectivity via surface runoff has practical importance since surface runoff quality and routing can be partly controlled by elements on the soil surface.

Overall, the applied methods provide a possibility to generate large scale and consequently enhance systemic evaluation and discussion on the impacts of connectivity on the targeting of environmental protection measures.

### *3.1.11 Conclusions and future research needs*

Reliability of the IC computations would benefit from validation of the model results using data from the lowland conditions. Extensive within-field observations (Borselli et al. 2008) would be potentially highly informative in terms of validation. Also, field-scale sediment load data (Turtola et al. 2007) could be used for the parametrization and validation of the sediment delivery model in different conditions. Comparison of the structural connectivity estimates with dynamic model simulations (Warsta et al. 2013) could increase understanding of functional sediment connectivity. Furthermore, the applied model (Eq. 3-7) could be used to quantitatively and systematically evaluate the impacts of targeted water protection measures on sediment delivery (Foerster et al., 2014).

The evaluation of RUSLE's prediction uncertainty showed that RUSLE has skill in predicting erosion rates at field parcel scale with different cover and management practices, but the prediction errors in absolute erosion rates were large. RUSLE was, however, found to perform similarly as erosion models in general in predicting long-term average erosion rates. At larger spatial scales, RUSLE was able to

rank small agricultural catchments and large river basins against measured TSS in rivers and streams, despite not having a description of landscape scale sediment transport in the model structure.
The calibration of model parameters against measured erosion rates was also found to be useful approach for improving the model parametrization when the data is limited, although calibration is not a common practice within the RUSLE framework. However, a proper evaluation of the uncertainties of RUSLE was found challenging due to limited knowledge on the variability of model parameters. Over larger spatial scales the model evaluation remains also a challenge, given that spatially distributed RUSLE provides gross erosion estimates and suitable observational landscape scale data for evaluation is rarely available.
Altogether, the uncertainty assessment suggests that RUSLE is most likely best used for relative comparison of erosion rates, for example between areas and scenarios, instead of for accurate estimation of absolute erosion rates. Also, it is suggested that an uncertainty assessment should consider the variability and potential range of model parameter values already in a development stage of model parameters, and should implement a systematic assessment framework (e.g., probability-based) for comprehensive understanding of prediction uncertainties and their sources.
The evaluation of sediment connectivity in RUSLE, in turn, showed that spatially distributed RUSLE is highly limited in terms of connectivity features, and additional methods are needed to incorporate connectivity in RUSLE. The main limitation is that the sediment transport between the modelled spatial units is not included in the model structure, and consequently the model provides gross erosion estimates over larger landscapes. This limits the use of RUSLE when off-site impacts of erosion are of interest, and also complicates the evaluation of the RUSLE against observed erosion as the observations are often based on measurements at the outlet of the study area.
The implementation of sediment connectivity approach in RUSLE provided interesting and promising results which reduced epistemic uncertainties related to the role of connectivity via surface runoff in lowland environments of Finland. At the case study catchments, the approach provided improved understanding of the degree of sediment connectivity between and within field parcels. For example, most of the field areas and high erosion areas are generally well connected to rivers, streams, or ditches. Moreover, the analyses provided insights on sediment delivery and connectivity pathways, which may be useful for targeting erosion mitigation measures. In the case study settings, the approach was also found to be relatively insensitive for variation in parameter values when comparing ranking of field parcels in terms of sediment delivery. However, the estimated sediment delivery magnitudes were highly sensitive to parameter variations. Altogether, the combination of sediment connectivity indices and RUSLE can provide new avenues for the use of RUSLE in sediment connectivity assessments in agricultural environment, but further research is needed for a better understanding. We also identified and listed means to further improve the conducted estimates.

## 3.2 Flanders case study (VPO)

### *3.2.1 Calibration and parameters setting of WaTEM/SEDEM model for Flanders*

*Study area*

For Flanders, the sensitivity and uncertainty analyses were conducted in two catchments, Molenbeek and Maarkebeek. The Molenbeek catchment is located in the south-eastern part of Flanders between 50°46’59”N, 5°10’78”E and 50°41’39”N, 5°06’03”E. The catchment encompasses about 3060 ha, consisting of a rolling topography between the altitudes of 55 to 145 m a.s.l.. The Maarkebeek catchment is located in the south to south-western part of Flanders between 50°49'54.072"N, 3°43'4.483"E and 50°45'45.915"N, 3°35'19.465"E. This catchment is about 5000 ha and stretches over hilly terrain with altitudes between 10 and 160 m a.s.l..

This project has received funding from the European Union’s Horizon 2020 research and innovation programme under grant agreement N° 862695

*Datasets and model parameters*

The input data for the sensitivity and uncertainty analyses are the official data sets as used for erosion modelling by the government of Flanders. This data consists of public and private data sources, such as DEM, Land Cover Map, Infrastructure Reference Map (publicly available), sewer inventories, and Parcel map of Agricultural Fields (private data). The used data is further specified in the SCALE database (only project internal access at cloud.baw.at, produced for SCALE WP2-D1).

For the analyses, the output of the WaTEM/SEDEM model as calibrated for Flanders is used as a reference for model performance. This model calibration had the main purpose of fitting the kTC to in-field sediment measurements, measured in 26 catchments throughout Flanders.

The WaTEM/SEDEM model used in this study was configured for Flanders with the specific scenario, in which a crop specific land use and all the known erosion control measures in the catchments are used. As the aim of this study is to investigate the impact and uncertainty of the TC, the PCF and the PTEF parameters on the modelled output, all other parameters of the WaTEM/SEDEM model were kept the same as for the model calibration, with the exception of the investigated parameters. In the reports of Deproost et al. (2018a, 2018b), the main input and parameter selection for the WaTEM/SEDEM model in Flanders, on which this model was based, are mentioned. In the attachment the used “user choices” from the WaTEM/SEDEM model are given.

### 3.2.2 Sensitivity analysis

*Morris Screening*

For the sensitivity analysis, the Morris's Elementary Elements Screening (EE) method is chosen, because it estimates global sensitivities in a relative manner (ranking) (Van Hoey, 2016). The EE method aims to estimate the global sensitivity of parameters by defining a number of trajectories over the parameter space, and to compute the mean and standard deviation of the model output over these trajectories.

In Figure 6 and Figure 7 this approach is exemplified. Assuming that the analysis wants to measure the sensitivity of the model output for two parameters $\theta_1$ and $\theta_2$, in the first figure the parameter is perturbed with an elementary unit (assume this is $\Delta\theta_1$). This perturbation with $\Delta\theta_1$ is repeated four times given different start values for $\theta_1$ and $\theta_2$. The four sets of parameters are used to compute a model output, and the mean ($\mu_{EE_{\theta 1}}$) and standard deviation ($\sigma_{EE_{\theta 1}}$) on the model output change ($EE_{\theta 1}$) is computed. This mean and standard deviation is an estimate of the global sensitivity of the model output to changes in parameter $\theta_1$. This procedure can be repeated for parameter $\theta_2$, in which the parameter is perturbed with $\Delta\theta_2$ (Figure 7, left). Yet, by combining step 1 (perturbation with $\Delta\theta_1$) and 2 (perturbation with $\Delta\theta_2$), defined as the Morris sampling scheme, one can limit the number of required computations (Figure 7, right) – in this example - from 16 to 12.

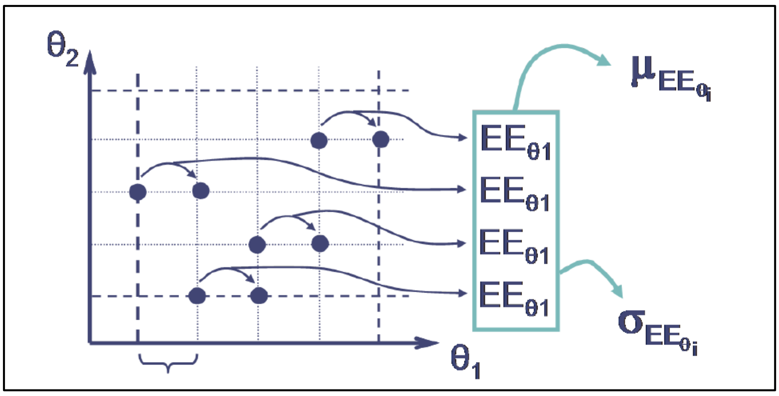


*Figure 6. Illustration of EE method, where $EE_{\theta 1}$ represents the model output change for a disturbance of the input parameter $\theta_1$ by a value of $\Delta\theta_1$ (From Nopens, 2010).*

This project has received funding from the European Union’s Horizon 2020 research and innovation programme under grant agreement N° 862695

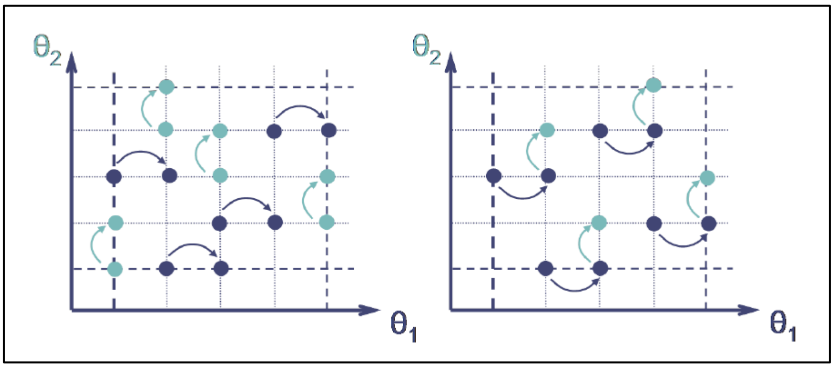


*Figure 7. Right: Illustration of EE method, for a disturbance of the input parameter $\theta_2$ by a value of $\Delta\theta_2$. Left: Example of the combination methodology where both parameters $\theta_1$ and $\theta_2$ are perturbed. (From Nopens, 2010).*

The advantages of this method are:
- the method is easy to understand and to apply;
- the analysis starts from a local point of view but is global by starting from different initial points in the parameter scheme;
- simulations are reused by using the Morris sampling scheme, declining the number of required simulations and lowering the runtime.

The disadvantages of this methods are:
- needs to define the number of samples (Vanrolleghem et al., 2015);
- the EE method has been identified as less performant in identifying the most influential parameters compared to other methods (i.e. FAST, Vanrolleghem et al., 2015);
- the EE of the several parameters can be analyzed only in a relative manner;
- in its simplest form, only uniform elementary effects can be considered, i.e. $\Delta\theta_i$ is considered to be constant.

The parameter values are sampled from a uniform distribution, with following boundaries:
- $kTC_{low}$: *[0, $kTC_{high}$] m*
- $kTC_{high}$: *[0, 20] m*
- $PC_{cropland}$: *[80, 100] %*
- $PC_{grasstrips}$: *[80, 100] %*
- $PC_{forest}$: *[20, 40] %*
- $PTEF_{crop}$: *[0, 20] %*
- $PTEF_{pasture}$ *: [65, 85] %*
- $PTEF_{forest}$: *[65, 85] %*

A total number of 100 samples was generated (100 trajectories, leading to >1000 simulations). The Morris EE method is applied for the WaTEM/SEDEM model based on the available data on specific yearly land cover and crop rotations and current ECM for the year 2019 in both study areas (Molenbeek and Maarkebeek), at a resolution of 5 and 20 m, using the *pycnws* version 0.5.4. The variables of interest are:
- total amount of sediment load to the river;
- total amount of net erosion;
- total amount of net deposition;
- total amount of sediment load to ditches and sewers.

The sensitivity analysis was conducted by using the open source package SALib (Usher et al., 2021).

This project has received funding from the European Union's Horizon 2020 research and innovation programme under grant agreement N° 862695

*Results*

The results of the sensitivity analysis for the Molenbeek and Maarkebeek case studies (20 and 5 m resolution) are presented in Figure 8 to Figure 11 On the X-axis one can find the mean of the EE, while on the Y-axis the variation is found. The higher the standard deviation and mean, the more influential the parameter is considered. From these figures, it is observed that the $kTC_{high}$ is estimated to be the most influential parameter for WaTEM/SEDEM, both for Maarkebeek and Molenbeek. Other parameters that are observed to be influential – to a lower extent – are the $kTC_{low}$ and PTEF for cropland. Note that differences are observed depending on the catchment and resolution, yet the conclusions are fairly similar. The results show that the TC parameter for agricultural land use is by far the most influential parameter. This supports the findings of Verstraeten et al. (2006b) and Deproost et al. (2018a, 2018b) in which only the capacity parameters are calibrated, without considering other parameters. Note also that the boundaries of the connectivity and efficiency parameters are set relatively narrow, yet this is because there is no indication for a larger range to be used. At this point of the study, a variation of 10 % around the standard set value is assumed adequate.

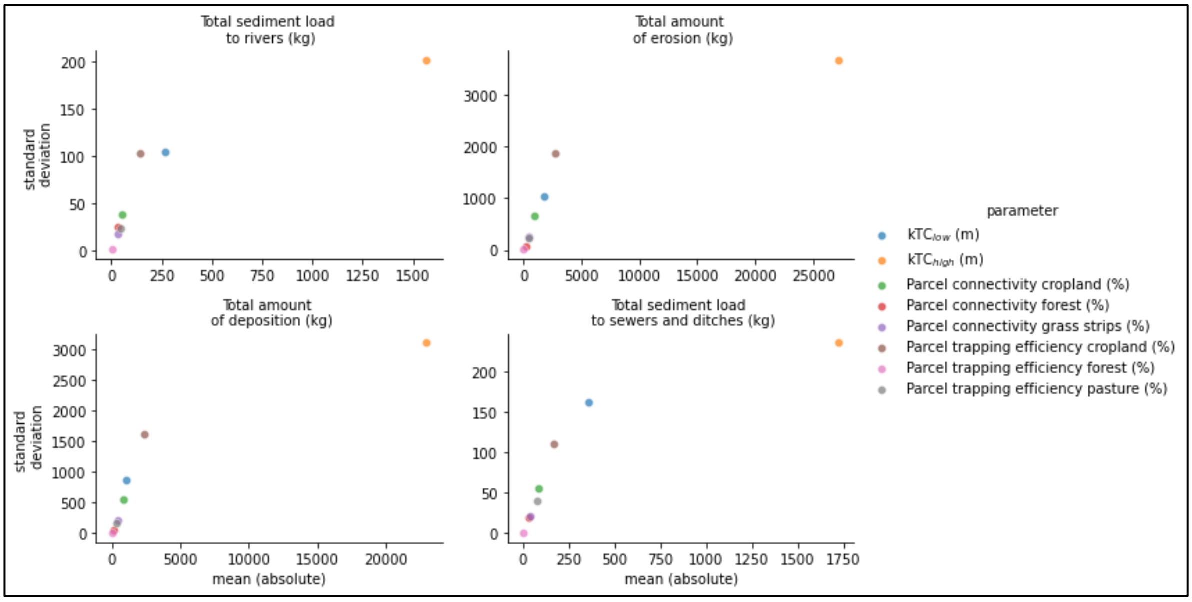


*Figure 8. Summary of Morris analysis for Molenbeek (20 m). Standard deviation of the distribution as a function of the absolute mean of the EE.*

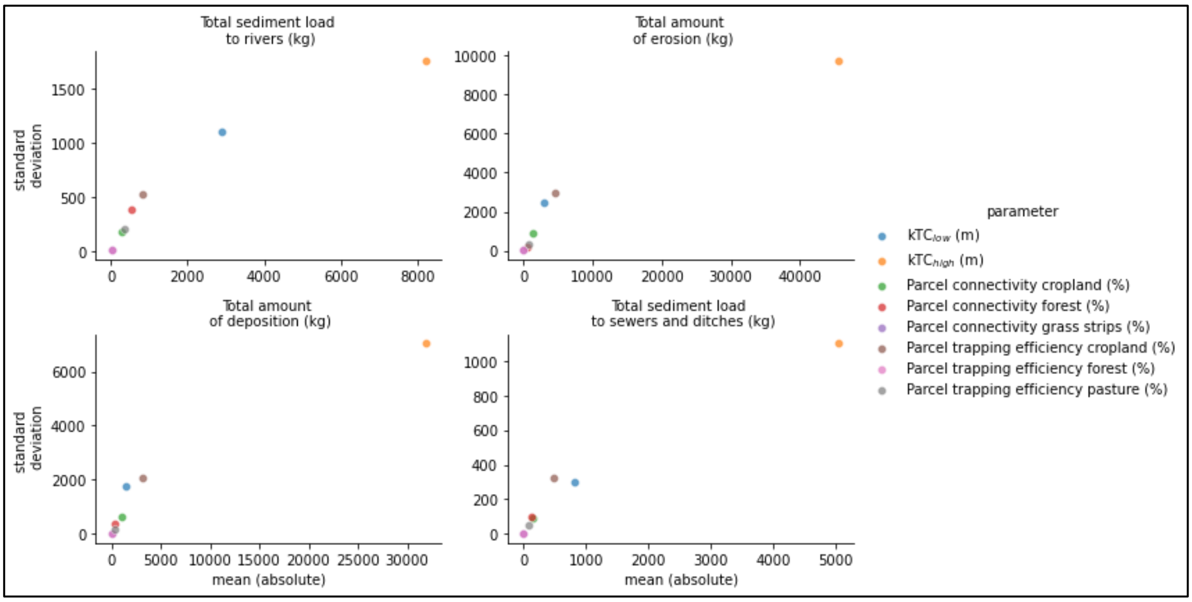


*Figure 9. Summary of Morris analysis for Maarkebeek (20 m). Standard deviation of the distribution as a function of the absolute mean of the EE.*

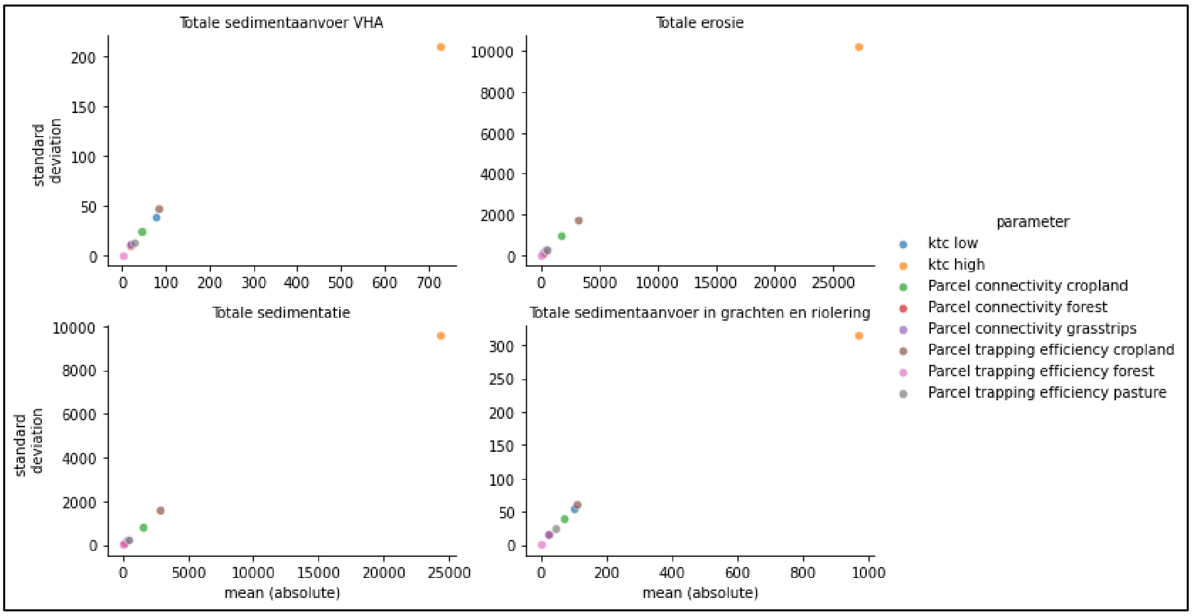


*Figure 10. Summary of Morris analysis for Molenbeek (5 m). Standard deviation of the distribution as a function of the absolute mean of the EE.*

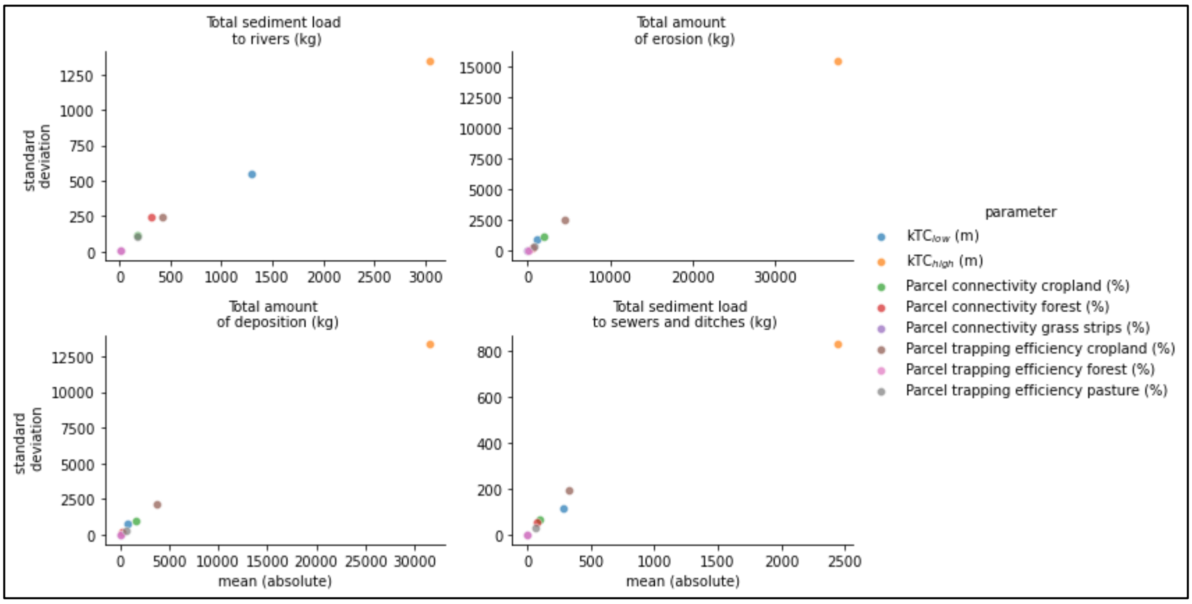


*Figure 11. Summary of Morris analysis for Maarkebeek (5 m). Standard deviation of the distribution as a function of the absolute mean of the EE.*

### *3.2.3 Uncertainty analysis*

In this part of the study, the subject of the uncertainty analysis will be the parameter uncertainty. Parameter uncertainty is defined as the uncertainty associated to the parameter values. This uncertainty originates from the calibration process, in which uncertainty in the calibration data and methods exists. Parameters are supposed to be invariant in the chosen context (Flanders) and algorithm description. As such, they are not supposed to change as an effect of causal relations in the model. This implies that they depend on the chosen model relations/equations (more explicitly: the WaTEM/SEDEM model) and on the chosen context, i.e. in this case the geographic context (Flanders). If the model relations/equations (e.g. redefinition of the routing algorithm) change, one needs to redefine the most optimal parameter set.

The uncertainty inspected here is categorized as aleatoric uncertainty. We define aleatoric uncertainty arising from randomness due to natural variability of observations results from spatial heterogeneity or fluctuations of quantity in time (Baudrit and Dubois, 2006). This natural variability in observations, i.e. imprecise observations, prevent us to delineate a single model parameter set with full certainty. As an alternative, we can identify a set of models (with different parameter values) that fit with the imprecise observations with a given certainty. Probability theory is typically used to represent this type of uncertainty. It is important to note that epistemic uncertainty (lack of knowledge of the process of erosion and sediment transport, see Verstraeten et al., 2007) is also an important source of uncertainty, yet the quantification/inspection is out of the scope of this study.

*Monte Carlo Simulation*

Monte Carlo simulation is a sampling method for error propagation that is not built on assumptions upon the model structure. The approach is based on repeated evaluation of the model output with multiple realizations of the model input/parameters, generated by sampling a probability distribution. A Monte Carlo analysis usually consists of the following steps (Loosvelt, 2014) (Figure 12):

1. assign a probability distribution to each parameter. In this study, we will sample a uniform distribution for sampling $kTC_{low}$ ([1, $kTC_{high}$]) and $kTC_{high}$ ([1,20]). The other parameters are sampled from a normal distribution N (mean, standard deviation) not uniform, as opposed to the sensitivity analysis, since in Morris one cannot easily sample from a normal distribution:

- $kTC_{low}$: [1, $kTC_{high}$] m
- $kTC_{high}$: [1, 20] m
- $PC_{cropland}$: $\mathrm{N}(90, 10\ \%)$
- $PC_{grasstrips}$: $\mathrm{N}(90, 10\ \%)$
- $PC_{forest}$: $\mathrm{N}(30, 10\ \%)$
- $PTEF_{crop}$: $\mathrm{N}(10, 10\ \%)$
- $PTEF_{pasture}$ : $\mathrm{N}(75, 10\ \%)$
- $PTEF_{forest}$: $\mathrm{N}(75, 10\ \%)$

2. determine the realization of the model parameters from their probability function;
3. evaluate the model output for each of the realization/sample of the model parameters;
4. repeat steps 2 to 4 by repeated sampling and repeated computation, until the variation reaches a stable level;
5. compute an empirical distribution for the realization of the model output.

The analysis is performed with the *pycnws* 0.5.4 release for the Molenbeek and Maarkebeek for a similar scenario as the sensitivity analysis (reality based land cover, crop rotation and ECM's for 2019 on scale 20 and 5 m).

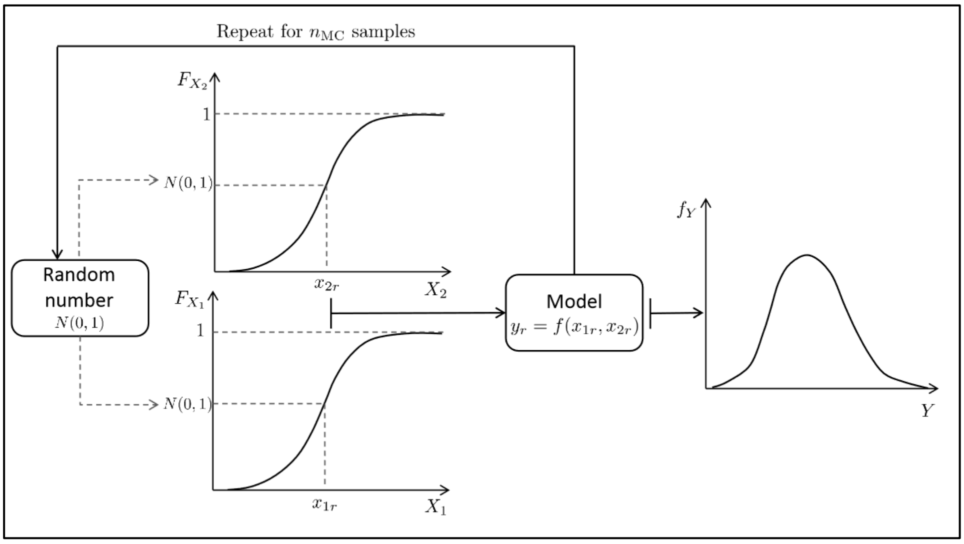


*Figure 12. Illustration of Monte Carlo simulations (From Loosvelt, 2014). In this example figure, $X_1$ and $X_2$ are two parameters that are sampled (e.g. $kTC_{low}$ and $kTC_{high}$) given a random sampler (left part). Both the parameters are sampled and fed to the model $y_r$ (in this report: WaTEM/SEDEM) to simulate an output ($Y$, e.g. total sediment load to river). By performing repeated sampling, one can compile a distribution for $y$: $F_Y$ (right part). Note that the random sampler can be a uniform sampler (as is the case for $kTC_{low}$ and $kTC_{high}$), but also a normal sampler (PTEF and PC).*

### Results

In Figure 13 and 14 the results of the uncertainty analysis for the Molenbeek (20 m) and Maarkebeek (20 m) are given. The optimal values determined in the calibration (
Table ) (Gobeyn et al, in preparation) are indicated on the plots in orange. It is important to note that any parameter set for which the $kTC_{high}$ and $kTC_{low}$ both agree with the optimal values listed in Table 11 are identified as optimal sets, irrespective of the connectivity or efficiency values. The results show that the values for all output variables of interest have a large spread (note that total net erosion is always expressed as soil loss, thus negative). Our previous analysis shows that this spread can be explained by changes in $kTC_{high}$ value. The spread on the results for the optimal parameter sets are relatively small, even when the connectivity and efficiency parameters are varied. As such, one can

This project has received funding from the European Union's Horizon 2020 research and innovation programme under grant agreement N° 862695

conclude that the identification of multiple optimal parameter sets is possible with the available data (Gobeyn et al., in preparation) with a relatively small amount of uncertainty as a result. As an example, the optimal parameter sets give rise to a range of 750 to 900 tons and 4000 to 5500 tons sediment transport to the river for the Molenbeek and Maarkebeek, respectively. This analysis shows that absolute amounts can be considered in case these uncertainty bounds are reported to stakeholders as a means of decision making under uncertainty.

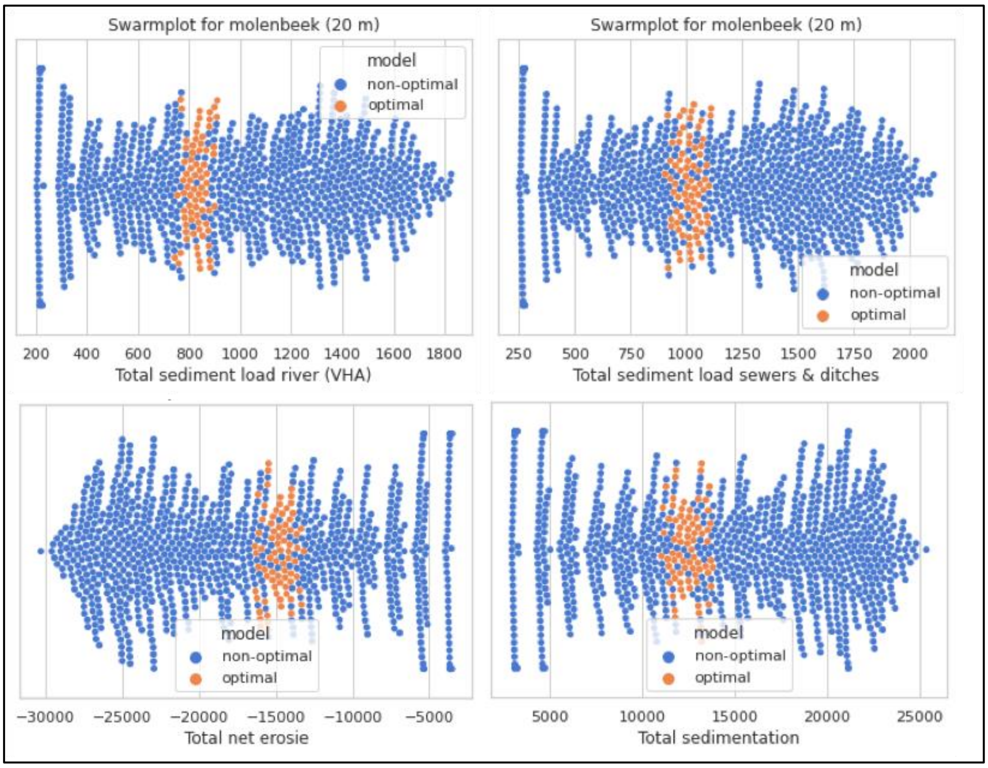


*Figure 13. Distribution of output variables for non-optimal and optimal solutions for the Molenbeek (20 m) (in tons).*

This project has received funding from the European Union's Horizon 2020 research and innovation programme under grant agreement N° 862695

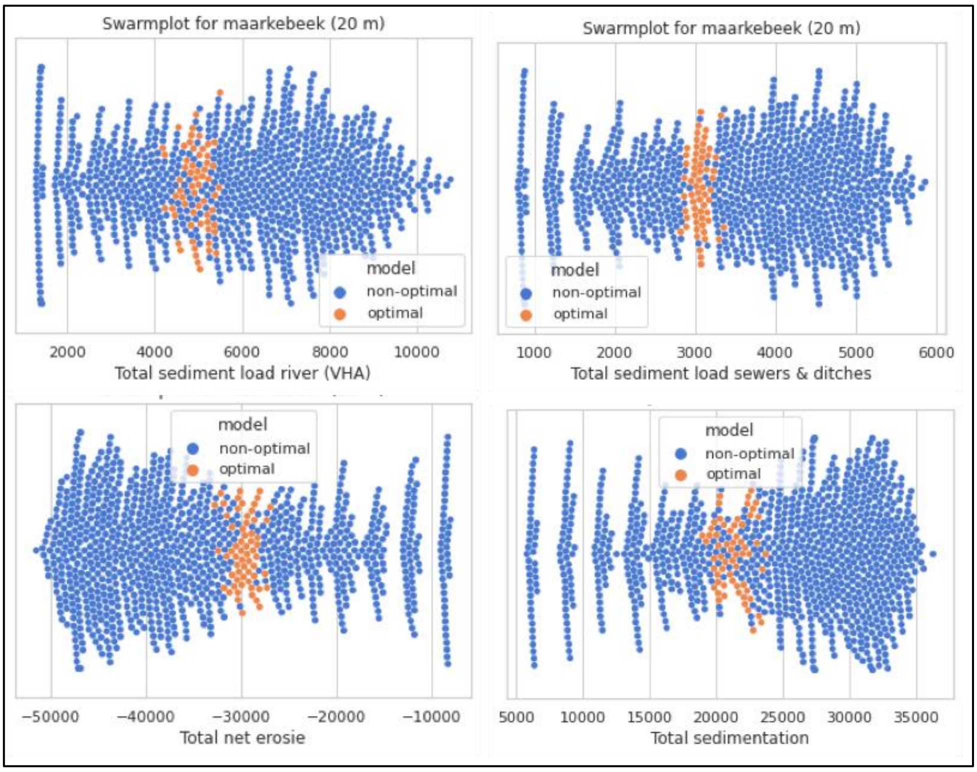


*Figure 14. Distribution of output variables for non-optimal and optimal solutions for the Maarkebeek (20 m) (in tons).*

*Table 11. Optimal parameter sets for 20 m (identified in Gobeyn et al. (in preparation)*

| $kTC_{low}$ (m) | $kTC_{high}$ (m) |
|---|---|
| 1 | 9 |
| 2 | 9 |
| 3 | 9 |
| 4 | 8 |
| 4 | 9 |
| 5 | 8 |
| 6 | 8 |
| 7 | 8 |

## 3.3 Italian case study (CREA)

The two case studies reported here are related to two different exercises made at Capriggine watershed (1), and at Vicarello field experimental plots (2), at different scales and with two different modelling approaches, applying in the first case the empirical RUSLE+USPED model, and in the second one the physically based WEPP model.

### *3.3.1 Catchment scale: RUSLE+USPED model*

The Capriggine watershed (10.9057 E, 43.4717 N) is a sub-basin of the Era River Basin, that is one of the most important contributors of Arno River. The Era River valley has a surface of 648 km$^2$ made up of 15 municipalities in the Province of Pisa, and extends from Volterra to Pontedera. Capriggine

watershed, whose surface extends for 33.3 $km^2$, includes a series of hilly reliefs between 110 and 625 m a.s.l., with slope range from 0 to 51.4%, and mean slope value of 15.2% (±6.3 st.dev.). Soils on marine Pliocene deposits of the lower hills, mainly Calcaric Regosols and subordinately Vertic Cambisols, are present; on the clay/sandstone/and conglomerates hills mainly Hypercalcic Calcisols and subordinately Calcari Stagnic Cambisols are present; in the other small areas with claystones and siltstones Skeletic Calcaric Regosols, Calcari Endostagnic Cambisols and Eutric Cambisols are present.
Land use on the upper part with higher slopes of the catchment is mainly woodland, with some vineyards and olive groves, the lowest with lower slopes is managed by croplands,
There are common phenomena of mass and rill erosion favored by tillage along the maximum slope direction. Previous studies indicate that interrill, rill and channel erosion processes are predominant on mass movements. Reduction in the number of smalls farms during the last decades has led to the elimination of the pre-existing drainage system, stone walls or hedges, the latter also used to delimit farm boundaries. The increase in construction of new road infrastructures and small artificial reservoirs for the storage of irrigation water (despite of Cavalcanti big earth Dam, ten more small ponds, at the level of single farm, were mapped in land use parcel map) contribute to the decrease of the hydrologic connectivity.
Simulations with the RUSLE+USPED methodology have been carried out on a cumulative sequence of eight years (2016-2022), taking into account the starting date of new DEMs release (Lidar from Tuscany Region and Sentinel from Copernicus EU consortium).

### *Calibration and setting of parameters of RUSLE+USPED model for Italy*

The RUSLE+USPED approach conceptually provides a modelling mode with two temporal ways, both for a single year and for a series of consecutive years, during which the thickness of the eroded sediments is calculated for each year starting from the first year of simulation. Subsequently, the DEM is then "adjusted" automatically by the model through the calculation of the eroded soil thickness by the respective cell based on the bulk density provided as a input data in the "soil" layer.
In this case study, the simulation was tested on an eight-year period from 2015 to 2022. The start date was decided based on the date of release of the available DEM. Results related to uncertainties and sensitivity assessment of the model were conducted by evaluating the final Transmissivity coefficient (Tc) and Erosion/Deposition (ED) output, according to the equations (9) and (10) provided by the model.
The ED values were expressed in each pixel of the simulated output raster as positive for deposition and negative for erosion. Thus, the values for each geographic element considered and the whole catchment (or sub-catchment) were retrieved by cumulating them as algebraic sum for each of the parcel and/or geographic elements considered.

### *Setting of DEM, R, K, C and P factors*

With reference to the modelling produced by RUSLE+USPED, and to the evaluation of accuracy and uncertainty of the results, four different scenarios has been applied to the case study, obtained from two different DEMs respectively at 2 and 2.5 m, and from two different exits of erosion-deposit related to: i) the last year of simulation; ii) the average of the eight years of simulation (for each pixel).

### *DEM resampling*

To obtain a proper run of RUSLE+USPED model, a resampling of DEM was necessary. Indeed, the model manual states "*It is vitally important that the starting input DEM be hydrologically valid and at an appropriate raster resolution. Resolution should be scaled to the size of the region being modelled, with the caveat that the assumptions of the way the transport equations are implemented will start to break down at larger cell resolutions. As a rule of thumb, cell resolution should be <= 10m. This can be achieved through resampling/interpolation from coarser data sets (e.g., a 30m SRTM DEM). If* *interpolation is used, it is best to use an interpolation procedure that will result in relatively smooth interpolated DEM with minimal depressions*."

Thus, the two DEMs used (2.5 and 2 m) were obtained respectively from a) EU-DEM V1.1, with 25 m resolution, and b) TinItaly at 10 m (Tarquini et al., 2012), by resampling with B-Spline interpolation method on SAGA GIS (Conrad et al., 2015; Version 7.3.0), to avoid these errors in running the model.

**Rainfall erosivity** (R factor): the R factor was calculated, as requested by the USPED model, as single value (average/year) for all the temporal simulations. Climate data sources were retrieved from the AGRI4CAST (Joint Research Centre - Agri4cast Resources Portal, 2024), that provides the climate daily data with a 25x25 km grid for all Europe from 1976 to 2023. Capriggine basin was included mostly in one unique Agri4cast cell; to calculate R the method by Bazzoffi (2007) was adopted, reporting a summary of soil erosion modelling and measured approaches for Italy. The method allows to calculate R on an annual basis, as the average of six different functions proposed by different Authors, as reported in Table 12.

*Table 12. Different functions proposed to calculate the average R value on an annual basis. P is the mean annual precipitation (mm) and F* is the Fournier Index (mod. by Arnoldus, 1977).*

| *Function* | *Reference* | *Method* |
|---|---|---|
| $R = [(4.17*F) - 152]*17.02$ | Arnoldus (1980) | Based on Fournier Index (F) |
| $R = 0.302*F^{1.93}$ | Arnoldus (1977) | Based on Fournier Index (F) |
| $R = 0{,}739*F^{1.847}$ | Renard and Freimund (1994) | Based on Fournier Index (F) |
| $R = 0{,}0483*P^{1.61}$ | Renard and Freimund (1994) | Based on annual precipitation (P) |
| $R = 38.46 + 3.48*P$ | Lo et al. (1985) | Based on annual precipitation (P) |
| $R = 3.82*F^{1.41}$ | Yu and Rosewell (1996) | Based on Fournier Index (F) |
| Modified Fournier Index | $F = \left(\sum_{j=1}^{12} p_j^2\right)/P$ | p = monthly precipitation |

C and P factors were estimated based on the 2019 land use parcels digital map of Regione Toscana (http://www502.regione.toscana.it/geoscopio/usocoperturasuolo.html) at 1:10000 scale, as summarized below.

**Cover and management factor** (C factor): the C factor was calculated on the basis of the Italian estimation tables as reported by Bazzoffi (2007), with an approximate evaluation of the annual C factor, according to different Italian land use and management classes for GIS applications of RUSLE model, as summarized in Table 13.

*Table 13. Main values of C factor according to the main Land use categories (From Bazzoffi, 2007).*

| Land Use | C Factor | | |
|---|---|---|---|
| | *Average* | *Min* | *Max* |
| Arable lands and permanent tree plantations (vineyards, olive groves, fruit) | 0.244 | 0.005 | 0.400 |
| Woodlands, shrubs, abandoned areas | 0.127 | 0.012 | 0.800 |

**Soil conservation practices factor** (P factor): due to the lack of local data on the conducting practices of the various crops adopted, reference was made to the P factor calculated on the basis of the analysis at European member States level carried out by Panagos et al. (2015b) following the CAP rules support

This project has received funding from the European Union's Horizon 2020 research and innovation programme under grant agreement N° 862695

practices (compulsory for farmers to receive incentives under the CAP-GAEC), taking in account three different sub-factors to prevent soil erosion: i) contour farming sub-factor (farmers apply certain field practices as ploughing or planting along contours, perpendicular to the normal flow direction of runoff); ii) grass margins sub-factor (known as strip cropping sub-factor and buffer strips); and iii) stone walls sub-factor (known as terrace sub-factor). A final overall P factor was estimated for all the EU Countries. For Italy it is assumed as average = 0.9519. In the Capriggine catchment it was applied only for the arable lands, not for woodland, permanent grassland and mediterranean shrubs (all the Corine codes 3).

**Soil erodibility** (K factor): the K factor was evaluated on the basis of the digital soil map given by Regione Toscana (http://www502.regione.toscana.it/geoscopio/pedologia.html) at 1:10000 scale, and associated soil benchmark profiles for each Soil Typological Unit reported on the Cartographic Units of the soil map.

For K factor calculation the formula proposed by Torri et al. (1997) was applied, obtained from a regression carried out on 207 case studies with a global dataset:

K=0.0293 (0.65 – Dg + 0.24 (Dg2)) exp {- 0.0021 OM/C - (0.00037 (OM/C)2) - 4.02 C + 1.72 C2} (12)

where Dg is the logarithm of the average geometric diameter of the three granulometric fractions (sand, silt and clay), defined by:

$$D_g = \exp\left[\sum f_i \log_{10}\left(\sqrt{d_i\, d_{i-1}}\right)\right] \tag{13}$$

where, for each of the three granulometric components, $f_i$ is the corresponding fraction, $d_i$ is the maximum diameter in mm and $d_{i-1}$ the minimum, according to the following scheme:

| *Texture Class* | *$d_i$ (mm)* | *$d_{i-1}$ (mm)* |
|---|---|---|
| Clay | 0.002 | 0.00005 |
| Silt | 0.05 | 0.002 |
| Sand | 2 | 0.05 |

The K factor was then calculated based on the soil map of Tuscany, with 31 different map units, of which 21 with a single type of soil and 10 with 2 types of soil (dominant and secondary, soil complex). In the latter case, the K was calculated as the weighted average of the different K factors, with respect to the percentage of geographic extension of the individual superficial horizon (topsoil). K variability and relative uncertainty was assessed comparing different available methods from literature. Despite so many different methodologies and functions developed until today, we compared three different methodologies among the most used actually in Italian landscapes, i.e. the original K function developed by Wischmeier and Smith (1978), and other two proposed by Renard et al. (1997), the first one (Renard 1) tested on a global dataset of 225 case study and the second one (Renard 2) on a dataset of 182 measures coming from the U.S. only.

In Table 14 the best results for the K values of the soils in the Capriggine basin are reported.

*Table 14. Statistics of deviations as average of the K estimation for 21 different soils of the Capriggine basin related to original K determined according to Wischmeier and Smith (1978).*

| Statistics | Wischmeier K values | Renard 1 | Renard 2 | Torri et al. |
|---|---|---|---|---|
| **mean** | 0.0340 | 7% | 23% | 4% |
| **min** | 0.0188 | -39% | -36% | -42% |
| **max** | 0.0501 | 106% | 135% | 23% |

This project has received funding from the European Union's Horizon 2020 research and innovation programme under grant agreement N° 862695

**Setting *n* and *m* coefficients in Eq. 8 and 9**: the exponents *m* and *n* are used to influence the behaviour of the transport equations by differentially weighting the influence of upslope accumulated area: *m* represents the depth of flow, while *n* represents the influence of local slope. Depending on how they are weighted, transport estimates can be made for overland flow processes, rilling and gullying, or channelized flow (Mathier et al., 1989; Peckham, 2003; Kwang and Parker, 2017).
As this is largely an experimental process, the specifics of this scaling are exposed to the user via the m and n variables. The user can define the scalar relationship of *m* to surface flow accumulation, and *n* to local slope.
Values of *m* and *n* are generally thought to be between 2 and 1, but experimental trials suggests that they should scale inversely with increasing depth of flow (*m*) and scale inversely with increasing local slope (*n*). Proposed values (Mitas and Mitasova, 1998) are $m = 1.6$, $n = 1.3$ for prevailing rill erosion, while $m = n = 1$ for prevailing sheet erosion; in our setting we adopted the initial settings of $m = 1.2$ (scalable to 1) and $n = 1.3$ (scalable to 1), according to our range of slopes.

### *Hydrological issues related to DEM structure for Ponds/Dams*

With reference to the model request of a hydrological filled DEM to avoid errors in computational processes for the RUSLE+USPED equations, the problem of DEM arrangement to represent the ponds/dams surface and ending artificial morphology (bridle) has to be solved, so to be considered inside the flow accumulation computation as an endpoint in terms to collect sediments. Consequently, the representation of ponds/dams present in the catchment (Calvalcanti dam and 10 small ponds on the slopes) inside the DEM was solved by considering the water surface as a flat area, and assign the same value of elevation to the correspondent DEM cells. Subsequently, the routine DEM filling was launched considering the ponds/dams as sinks to be filled. In this way we ensured that the model considered these areas as collecting water fluxes, according to the flow accumulation pattern (Figure 15) until the border of the artificial lake; accordingly, the *flowacc* value is then = 0 for all the water surfaces.

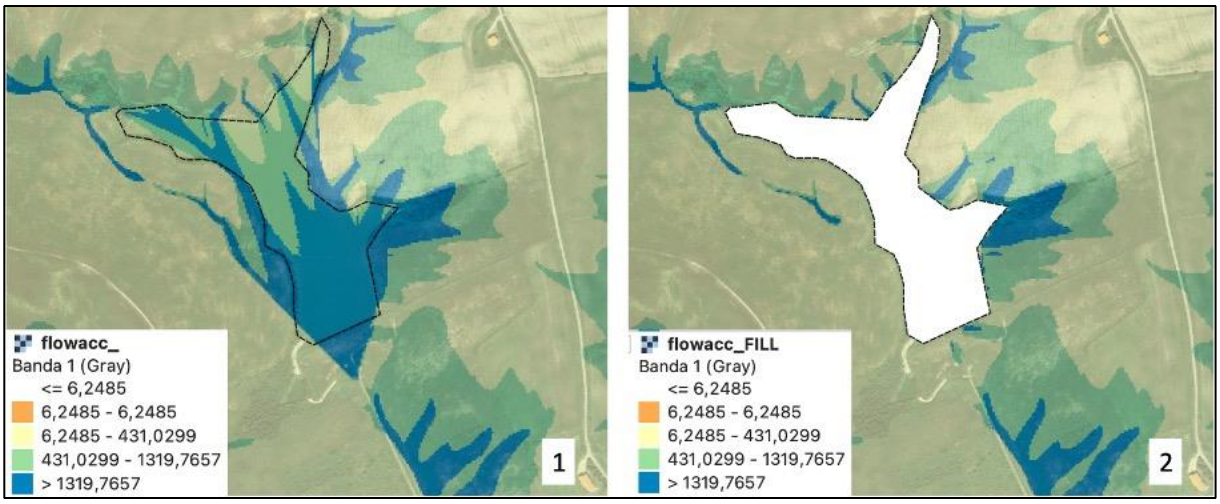


*Figure 15. Flow accumulation pattern before (1) and after (2) the DEM modification for Cavalcanti dam, simulating the lake surface like a sink (Flat area with flowacc = 0).*

### *Prediction uncertainty for Italian case study - Capriggine watershed*

First, the calibration of the predictive model was carried out through the comparison with the data obtained from a series of sediment filling measures from a Cavalcanti dam survey relating to the upstream basin, which represents a sub-basin of Capriggine catchment (Figure 16). On Cavalcanti dam, built in 1954, a series of bathymetric reliefs with sonar profiling of the seabed and density of the

This project has received funding from the European Union's Horizon 2020 research and innovation programme under grant agreement N° 862695

sediment captured were conducted, to establish the thickness of the sediments compared to the compact bottom of the lake. This methodology has made it possible to have measures of the quantity of cumulated sediments per year, considering the capture effect of the dam as if it was a measure at the exit of the underlying basin, as reported in Bazzoffi and Pellegrini (1992a).
The Cavalcanti dam has a 62.36 ha surface upslope catchment and is representative of most of the hilly surveys within the Capriggine basin, both as morphology/morphometry, slopes, types of soils and of land uses, and management practices.

*Figure 16. Cavalcanti dam and upstream sub-basin borders in green dot-dashed line (right) and their location inside the Capriggine catchment (left, in the red square).*

From the analysis of the two cumulative measures carried out in 1980 and 1990, and with reference to the topography of the pre-existing valley floor in 1954 (the year of construction of the dam), it was possible to obtain annual values of sediment from erosion captured by the dam itself. A series of measures of 140 samples taken on filling sediments allowed also to determine the average sediment apparent density (as dry weight/moist total volume – g cm$^{-3}$), and to report the measured values in m$^3$ as real quantities of sediment caught. The resulting value of 9.72 Mg.year$^{-1}$ is reported as an yearly average of the values measured for the period 1954-1980 (9.79 Mg.ha$^{-1}$) and for the period 1980-1990 (9.64 Mg.ha$^{-1}$) (Bazzoffi and Pellegrini, 1992a). Considering the total surface of the upstream sub-basin, an annual average of sediment filling measure of 9.76 Mg.ha$^{-1}$ was obtained with the capture of the eroded sediment, which reported in terms of total sediment delivered and captured in the Cavalcanti lake was estimated at 606.14 Mg.year$^{-1}$.

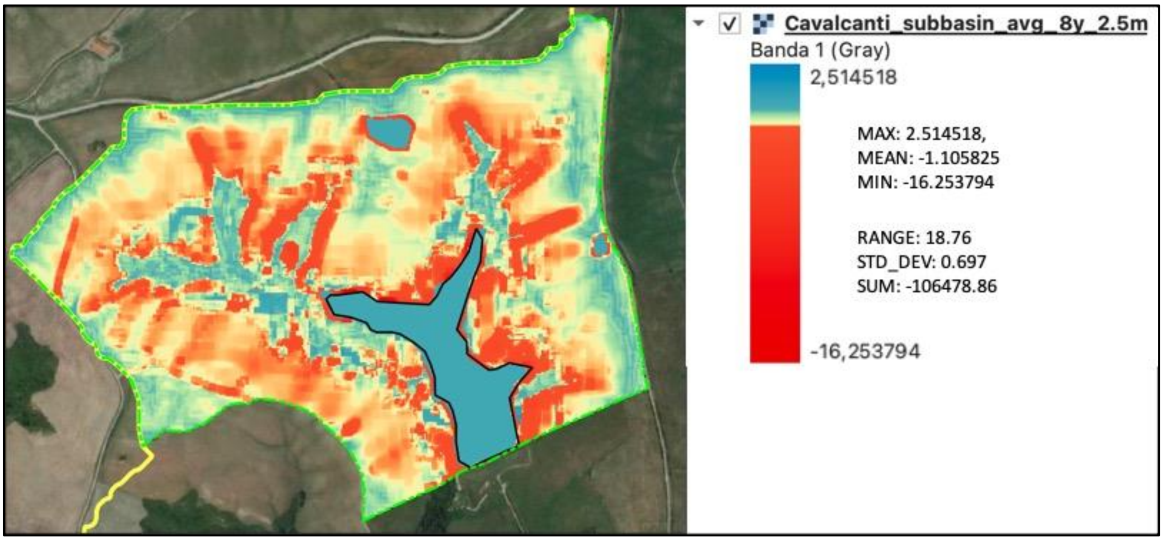


This project has received funding from the European Union's Horizon 2020 research and innovation programme under grant agreement N° 862695

*Figure 17. View of the predicted erosion/deposition values as output for the best performance scenario. In red are the negative values (erosion) and in blue the positive ones (deposition).*

Predicted cumulative values were obtained by the sum of all the ED values of the sub-catchment cells (Figure 17), transformed in total Mg values from the ED output calculated for surface units ($kg.m^{-2}$). The relative error between the predicted cumulative and the average measured values for the four different approaches adopted is reported in Table 15. Since a relative error (predicted/measured ratio) ≤20% is considered satisfactory, according to these results the best performance was obtained from the average of the eight years of simulation with the 2.5m DEM scenario.

*Table 15. Results of the relative error as predicted/measured ratio of RUSLE+USPED model runs according to 4 different scenarios using two different DEM detail (2 and 2.5 m) and simulation results over time (last year and average of eight years).*

| Scenario | Dam upstream catchment (ha) – modelled scenarios | Measured erosion (kg) | Predicted erosion (Mg) | Average/year measured sediment yield (Mg) from Bazzoffi and Pellegrini (1992a) | Measured/ predicted relative error |
|---|---|---|---|---|---|
| 1 | LEVOL_2m (LAST YEAR 8) | 180515.08 | 722.06 | 606.14 | 0.19 |
| 2 | LEVOL_2.5m (LAST YEAR 8) | 85755.33 | 535.97 | 606.14 | -0.12 |
| 3 | LEVOL_2m (AVG) | 211082.58 | 844.33 | 606.14 | 0.39 |
| 4 | LEVOL_2.5m (AVG) | 106478.86 | 665.49 | 606.14 | 0.10 |

### *Sensitivity analysis*

Sensitivity of Tc and ED results were determined in relation to the input parametrized CP, K and S factors; *m*, *n* and R were not considered, since they were imposed as constant values throughout the Capriggine catchment. The evaluation was applied on the whole pixel dataset of 53,131 simulated observations inside the catchment.

Thus, Spearman rank correlations among the inputs and both the Tc and ED results were analyzed (Table 16) for the scenario with the best performance (averaged values with 2.5 m DEM); the pairwise two-sided p-value was <0.0001 for all the considered CP, K and S factors.

The analysis of sensitivity describes the type of land use (C factor) as a more significant parameter, with better correlation both with the Tc transmission coefficient and with erosion values (expressed as negative values in USPED). The influence of both the slope and, lastly, of the soil erodibility coefficient K are present, but with lower inverse (K for Tc and slope for ED) or direct (K for ED and slope for Tc) correlations.

*Table 16. Rank corelation of the input values land cover practices (CP), soil erodibility (K), and slope (S) input factors with transmissivity coefficient (Tc) and erosion/deposition (ED) values of the best simulation with RUSLE+USPED method.*

| Factor/index | CP | K | Slope | Tc | ED |
|---|---|---|---|---|---|
| **CP** | 1.0000 | -0.2536 | -0.1965 | 0.7164 | -0.5017 |
| **K** | -0.2536 | 1.0000 | 0.0559 | -0.1478 | 0.1317 |
| **Slope** | -0.1965 | 0.0559 | 1.0000 | 0.1741 | -0.1810 |

| Pairwise two-sided p-values | CP | K | R | Slope | Tc | ED |
|---|---|---|---|---|---|---|
| **CP** | | <.0001 | NA | <.0001 | <.0001 | <.0001 |

This project has received funding from the European Union's Horizon 2020 research and innovation programme under grant agreement N° 862695

| | | | | | | |
|---|---|---|---|---|---|---|
| **K** | <.0001 | | NA | <.0001 | <.0001 | <.0001 |
| **Slope** | <.0001 | <.0001 | NA | | <.0001 | <.0001 |

*Uncertainties Results*

According to the weight and importance of input factors following the sensitivity analysis, summary statistics about relative estimates of sediment delivery of the field parcels type, produced by RUSLE+USPED, are reported as a map of the whole basin and boxplots in the Figures 18 and 20 for Tc and Figures 19 and 21 for erosion rates, according to the different Corine land cover classes of the land use parcels.

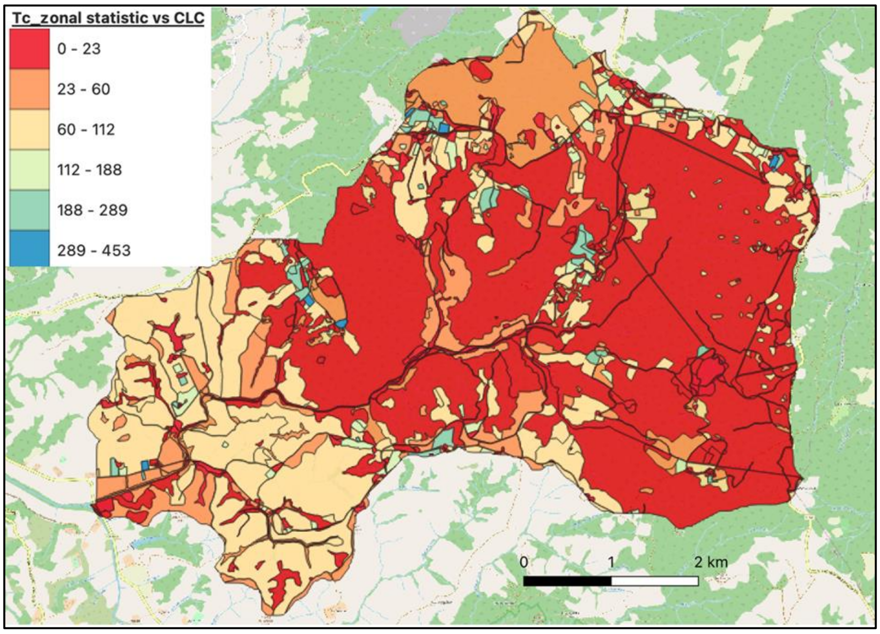


*Figure 18. A representative snapshot on the spatial distribution of the mean Transmissivity Coefficient (Tc) values for each different land cover/use parcels at the Capriggine catchment.*

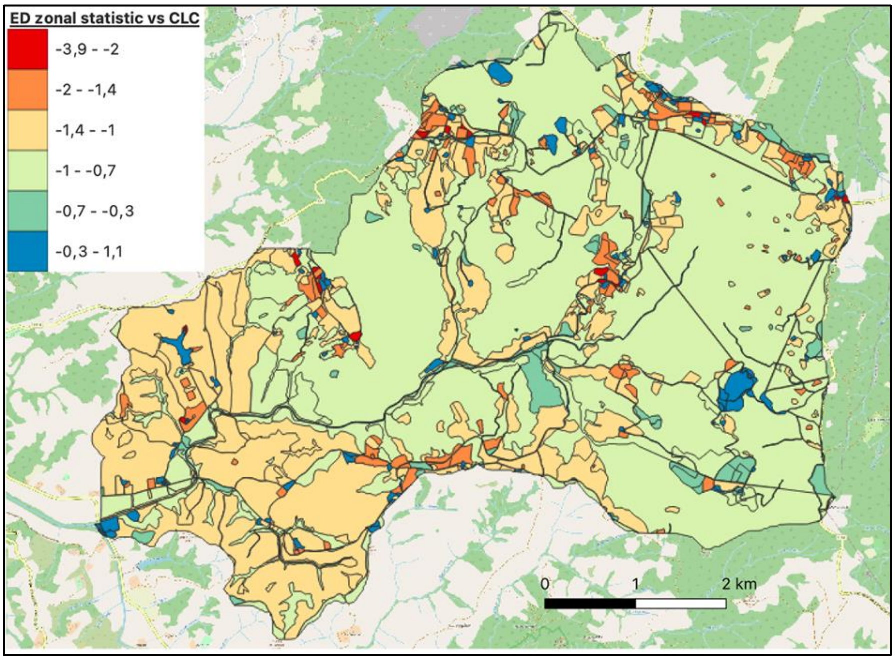


This project has received funding from the European Union's Horizon 2020 research and innovation programme under grant agreement N° 862695

*Figure 19. A representative snapshot on the spatial distribution of the mean erosion/deposition values (ED, expressed in kg m$^{-2}$) by RUSLE+USPED for each different land cover/use parcels at the Capriggine catchment.*

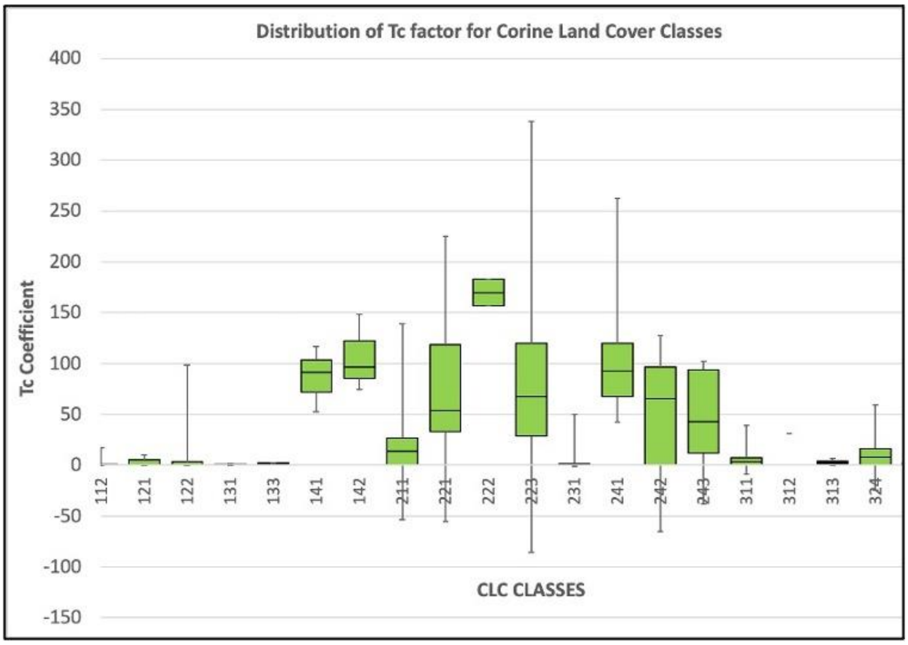


*Figure 20. Boxplots of the of the mean, range and min/max values distribution of Transmissivity coefficient (Tc) for each different land cover/use parcels at the Capriggine catchment.*

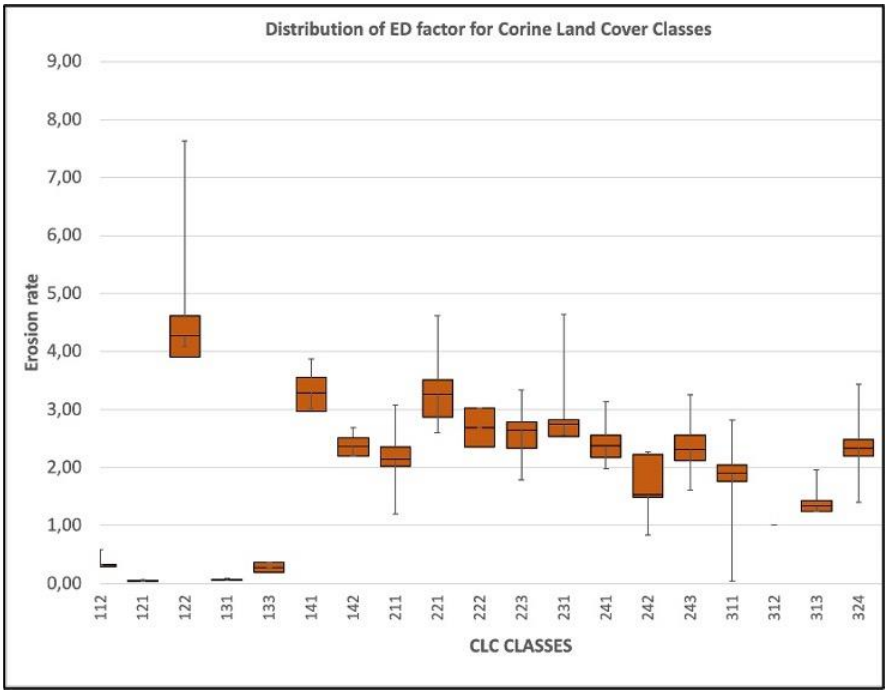


*Figure 21. Boxplots of the of the mean, range and min/max values distribution of erosion absolute rates (ED expressed in kg m$^{-2}$) by RUSLE+USPED for each different land cover/use parcels at the Capriggine catchment.*

Despite the strong correlation of the parameter "land use type" (CLC codes) with erosion, the uncertainties linked to these variations are quite high, as shown in the boxplots (Figure 20 and 21).

The Tc values distribution around the mean are very large, especially inside many agricultural areas as 'non-irrigated arable lands' (211), 'vineyards' (221), 'olive groves' (223) and other mixed areas as 'annual associated with permanent crops' (241) and 'land principally occupied by agriculture with significant areas of natural vegetation' (243). Final erosion rates show also wide ranges for the same land use types, plus the 'broad lives forest' (311) and 'transitional areas from woodland to shrub' (324). The presence of significantly different values as outliers could be related to a not proper parametrization of input factors (C, P, K, S,) and considered as a technical and methodological source of uncertainty, or may be related to the variability and non-linearity of the functions implemented inside the USPED model, as an epistemological source of uncertainty. More trials and model runs are necessary to further define this point.

### 3.3.2 WEPP model for Italian plots (field level)

*Literature review about WEPP model*

The WEPP model (Flanagan et al., 2001) is a physically based computer simulation program which has been tested and applied to estimate, both at hillslope and at watershed level, daily, monthly, annual or average annual values of runoff and soil erosion in different locations across the United States (Savabi, 1993; Savabi et al., 1995; Huang et al., 1996; Laflen et al., 2004), Mexico (Oropeza-Mota et al., 2004), United Kingdom (Brazier et al., 2000), Norway (Gronsten and Lundekvam, 2006), Australia (Rosewell, 2001), India (Pandey et al., 2009), Thailand (Onsamrarn et al., 2020) and China (Zheng et al., 2020).

Physically based models often work well even without calibration because the principles they use are assumed to be valid for a wide range of situations, including those that have not yet been observed. Therefore, one should expect their range of validity to be broader than that of other types of models (e.g., empirical or conceptual) (Guinot and Gourbesville, 2003). Tiwari et al. (2000) obtained acceptable runoff and soil loss results from uncalibrated WEPP simulations, similar to those obtained with both the USLE and RUSLE models using a part of the USLE dataset. Theoretically, physically based soil erosion models do not require calibration, since the information about its parameter values is measurable through field investigations. However, it is impossible to avoid the calibration procedure since the models are nothing more than simplifications of a real system. In this regard, Bhuyan et al. (2002) highlighted how calibration provides more exact estimates. Similarly, Yu and Rosewell (2001) suggested to calibrate the model with site-specific data whenever WEPP needs to use information related to cases not covered by the US database. Pieri et al. (2007) highlighted underestimated results when using the uncalibrated WEPP model in Italy.

During WEPP calibration, the input parameters that are most often recommended to be considered are effective hydraulic conductivity, rill erodibility, interrill erodibility and critical shear stress (Flanagan et al., 2012); anyway, these are not the only parameters to which WEPP is sensitive.

A noteworthy improvement in runoff volume predictions was obtained by Risse et al. (1994) by calibrating the effective hydraulic conductivity. Similarly, Zheng et al. (2020) achieved satisfactory predictions of soil loss on steep slopes by calibrating with effective hydraulic conductivity, rill erodibility, and critical shear stress.

However, to our knowledge there are few examples of WEPP application in the Mediterranean environment. There have been only few studies that used WEPP for modelling erosion in Sicily (Amore et al., 2004; Spadaro et al., 2004) Northern Italy (Simonato et al., 2002; Pieri et al., 2007), Tunisia (Raclot and Albergel, 2006) and Palestinian Territories (Albaradeyia et al., 2011). These authors reported generally acceptable indices of model efficiency. When input values of effective hydraulic conductivity and critical shear were adjusted, the WEPP prediction was improved. Overall, they found that WEPP has an adequate potential for simulating runoff and soil loss under Mediterranean conditions.

This project has received funding from the European Union's Horizon 2020 research and innovation programme under grant agreement N° 862695

*Sources of uncertainty in WEPP*

Usually in modelling hydrological processes using deterministic models, uncertainty arises from the structure of the model itself, from the input data and from a series of parameters used by the specific model (Lindenschmidt et al., 2007). There are many conceptual and physical parameters in the hydrological models at watershed and field slope scale (Gong et al., 2011). The conceptual parameters, such as Curve Number (CN) in the Natural Resources Conservation Service (NRCS) curve number method (NRCS, 2009), are defined as the conceptualization of a non-quantifiable process and determined by the process of model calibration. In contrast, physical parameters can be measured or estimated (Nandakumar and Mein, 1997). Some of the physical parameters vary greatly across spatial and temporal scales, and they are constrained by measurement devices, methods, and cost; it may not be easy to assign specific values, and therefore they must be determined by calibration against the measured data. It is also known that the measured erosion and runoff data used for optimizing model parameters and evaluating related predictions may have some degree of uncertainty (Batista et al., 2019). In this case study, for example, the data refers to different time periods and in one case it was necessary to make up for the lack of weather data for a two-months' time window by using data from a weather station in proximity of the experimental farm.

Due to spatial heterogeneity and high measurement costs, physical parameters are usually determined by calibrating the model to measured data (Beck, 1987; Raat et al., 2004). Accordingly, parameter uncertainty is inevitable in modelling, and should be assessed before the simulation results are used in the decision-making process.

However, when the number of parameters is large, due to the large number of subprocesses considered or to the structure of the model itself, the calibration process becomes complex and uncertainty problems appear (Rosso, 1994). Parameter uncertainty studies have been conducted in soil loss prediction (Cochrane and Flanagan, 2005), nutrient flux analysis (Miller et al., 2006), evaluation of the effects of land use change (Shen et al., 2010; Xu et al., 2011) and evaluation of the impact of climate change (Kingston and Taylor, 2010). However, parameter identification is a complex and nonlinear problem, and numerous possible solutions could be obtained by optimizing algorithms (Nandakumar and Mein, 1997). Furthermore, different sets of parameters can lead to similar predictions, a phenomenon known as equifinality (Beven and Binley, 1992).

In the specific case of the WEPP model, the input data used in the simulations are of four types: soil data, crop-management data, climatic data, and topographic data. The soil and crop-management correspond to real field data, so the source of uncertainty is assumed as related to measurement and spatial variability within the investigated area (plot or watershed). Climate and topographical data are synthetic data, and the associated uncertainties are only due to measurement errors and inaccuracy of empirical equations that calculate parameters (Chaves and Nearing, 1991).

*Model performance assessment*

The modelling efficiency can be evaluated by comparing the estimated runoff and soil loss values against the measured data. To assess the performance of the model, a single index cannot adequately reflect the relationship between the observed and the predicted data, so multiple indexes are usually used (Willmott, 1981). In this case we used:

1. the relative error (%) between the predicted and the observed value. Percentage error ≤20% are considered satisfactory according to Chung et al. (1999) in the validation of EPIC (Erosion Productivity Impact Calculator) model, a computer-based model that predicts soil loss due to water and wind erosion in response to different management options (Williams et al., 1984);
2. the efficiency index E proposed by Nash and Sutcliffe (1970), herein referred to as NS, is defined as one minus the sum of the absolute squared differences between the predicted and observed values, normalized by the variance of the observed values during the period under investigation. The range of NS lies between 1.0 (perfect fit) and −∞. Perfect model

This project has received funding from the European Union's Horizon 2020 research and innovation programme under grant agreement N° 862695

performance is indicated by an NS value of 1. An efficiency value lower than zero indicates unacceptable model performance. Values between 0.0 and 1.0 are commonly considered as acceptable. Values of NS >0.75, the model simulations are considered "very good", for values in the range of 0.65-0.75, 0.50-0.65 and <0.50 the model simulations are considered "good", "satisfactory" and "unsatisfactory", respectively (Moriasi et al., 2007);

3. the main limit of the NS efficiency index is because the differences between the observed and predicted values are squared. As a result, larger values in the time series gain excessive weight, while smaller values are irrelevant (Legates and McCabe, 1999);
4. the RMSE measures the average difference between the values predicted by a model and the actual values. It provides an estimation of how well the model can predict the target value (accuracy). RMSE values can range from zero to positive infinity and use the same units as the outcome variable. Perfect model performance is indicated by an RMSE value of zero. The lower the value of the RMSE, the better the model performance is;
5. the Relative Root Mean Square Error (RRMSE), representing the aggregate magnitude of the prediction errors relative to the mean of observations, is calculated by dividing the RMSE by the mean value of the observed data. Model performance is considered "excellent", "good", "fair" and "poor" when RRMSE is <10%, between 10 and 20%, between 20-30% and >30%, respectively (Jamieson et al., 1991).

We evaluated the performance of the WEPP model in simulating runoff and soil erosion from field plots under different soil use and management systems by comparing predictions with observations before and after model calibration. The model was tested using data from a study carried out in Italy in the early nineties of the last century, aimed to quantify the effects of different soil uses on surface runoff and soil loss at plot and small catchment scale.

The hillslope routines of WEPP were used for the overland flow portion of a watershed area. The smallest possible watershed includes one hillslope. Runoff characteristics, soil loss and deposition are calculated on each plot with the hillslope component of the model. The model was subjected only to calibration as we think the measurement data were not sufficient for separate validation.

The plots from which the data used to validate the WEPP model come from, were in the S. Elisabetta experimental farm (Vicarello, Municipality of Volterra, Pisa) of the CREA Agriculture and Environment Research Centre (Firenze, Italy). According to Pinna (1977), the climate of the site is classified as Csa (mesothermic, humid, mediterranean). The mean annual temperature is 12.7°C, ranging between extreme values of -10°C and +40°C. The mean annual rainfall is 678 mm, with precipitation concentrated in spring and autumn (Bazzoffi and Pellegrini, 1992b). Potential evapotranspiration, following Thornthwaite, is 569 mm.

The plots were arranged in two randomized blocks of 5 plots 75 m long and 15 m wide (Figure 22).

*Figure 22. Panoramic view of the experimental plots setup.*

Each plot was equipped with an electronic Fagna-type hydrological unit (Figure 23) for runoff and soil loss measurement and sampling (Bazzoffi, 1994).

*Figure 23. The Fagna-type measurement device.*

Near the plots, an electronic meteorological station collected data about rainfall, solar radiation, air humidity, air temperature, wind velocity and direction (Figure 24). The electronic tipping bucket rain gauge collected rainfall data with a resolution of 0.2 mm.

This project has received funding from the European Union's Horizon 2020 research and innovation programme under grant agreement N° 862695

*Figure 24. The electronic meteorological station.*

In the trial five treatments were compared: 1) winter wheat (*Triticum durum* Desf.), 2) alfalfa (*Medicago sativa* L.) meadow, 3) agropastoral system with sulla (*Hedysarum coronarium* L.) and grazing saltbush (*Atriplex halymus* L.), 4) 20-year-old Mediterranean maquis, and 5) continuous fallow. Model simulations considered runoff volume, soil loss, climate, soil properties and crop management data of three years (1994, 1995 and 1996) for the winter wheat and alfalfa treatment, 4 years (1994-1997) for the agropastoral system and 2 years (1998 and 1999) for the Mediterranean maquis. In these years, the recorded runoff events were 33, 34, 56 and 37 for cereal, alfalfa, agropastoral system and Mediterranean maquis soil use, respectively. In this evaluation exercise data from continuous fallow plots were not used.

The soil of the plots (Figure 25 and Table 17), derived from Pliocene clayey marine deposits, has a silty clay loam texture, and is classified as a Vertic Xerochrept, clayey-fine, mixed, mesic (calcaric) according to Soil Taxonomy (Delogu and Lulli, 1982), or Vertic Cambisol (IUSS-WRB, 2015)

This project has received funding from the European Union's Horizon 2020 research and innovation programme under grant agreement N° 862695

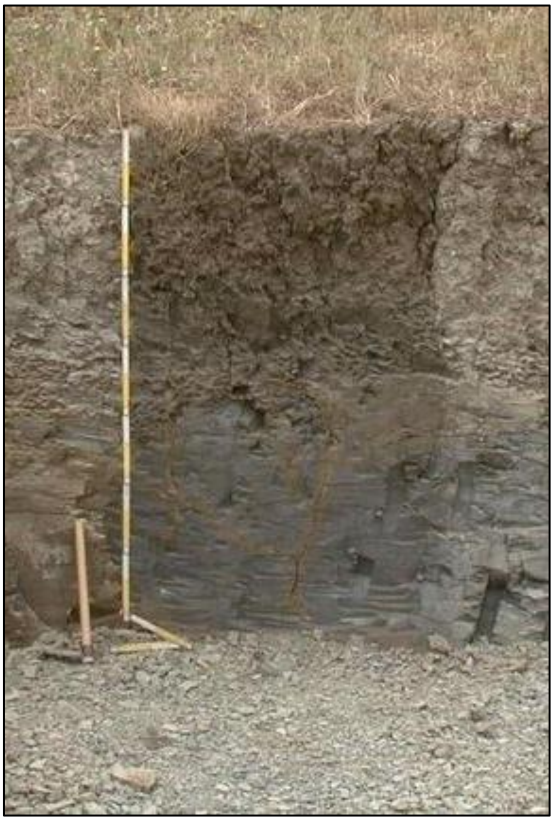

*Figure 25. Soil profile in the experimental area, classified as Vertic Cambisol (IUSS-WRB, 2015).*

*Table 17. The main physical and chemical characteristics of the soil in the experimental area.*

| Soil horizon | Depth( mm) | Sand (g kg$^{-1}$) | Clay (g kg$^{-1}$) | Silt (g kg$^{-1}$) | Organic matter range (%) | CEC (meq/100g) | Rock (%) |
|---|---|---|---|---|---|---|---|
| Ap1 | 130 | 121 | 329 | 550 | 1.2 - 6 | 25.2 | 0 |
| Ap2 | 250 | 210 | 380 | 410 | 1.1 - 3.5 | 27 | 0 |
| Ap3 | 450 | 300 | 365 | 335 | 0.87 - 2.0 | 28 | 0 |
| BCw | 750 | 135 | 435 | 430 | 0.74 - 1.0 | 28 | 0 |
| Ckr | 950 | 135 | 550 | 315 | 0.69 - 1.0 | 28 | 0 |

Soil Organic matter content was monitored at different horizons depths, according to the parcel land use, showing a wide range of values for the topsoil horizons, from low values in cereals and alfalfa to very high values in the agropastoral and Mediterranean maquis plot trials (Table 18).

This project has received funding from the European Union's Horizon 2020 research and innovation programme under grant agreement N° 862695

*Table 18. Average organic matter content (%) in different soil horizons under different treatments.*

| | | Soil use | | | |
|---|---|---|---|---|---|
| **Soil horizon** | **Depth (mm)** | **Cereal** | **Alfalfa** | **Agropastoral** | **Med. maquis** |
| **Ap1** | 130 | 1.2 | 1.5 | 2.0 | 6.0 |
| **Ap2** | 250 | 1.1 | 1.2 | 1.6 | 3.5 |
| **Ap3** | 450 | 0.9 | 0.9 | 0.9 | 2.0 |
| **BCw** | 750 | 0.7 | 0.7 | 0.7 | 1.0 |
| **Ckr** | 950 | 0.7 | 0.7 | 0.7 | 1.0 |

Shrinking and swelling phenomena dominate the soil hydrological behavior. In winter it has an extremely low infiltration capacity, with runoff coefficient up to 0.85 (Mbagwu and Bazzoffi, 1987). In summer, on the contrary, cracks determine a high infiltration rate, and runoff coefficient approaches zero (Lulli and Ronchetti, 1973).

*Setting of input data and calibration of parameters for model simulations*

As requested by the WEPP model, parameters were set to fill the 4 type modules: Climate (file .cli), Soil (file .sol), Slope (file .slp) and Management (file .rot).

Thus, for the different land uses tested, the model required a specific setting of some input parameters. The "Soil file" was created through the soil file builder in the WEPP interface and included the soil type and the soil texture with the corresponding soil depth for each layer. All the plots considered in this evaluation were represented as a single overland flow element with uniform slope gradient and width. "Slope files" held slope gradient, length, and width for each plot.

The "Management" input file holds the diverse types of parameters describing the different crops, tillage implements, tillage sequences, harvest operations, management practices, etc. Also, the calendar of cultivation operations (e.g., soil tillage, sowing, mowing, and harvesting date) as conducted in the experimental farm was inserted in this file. However, in the WEPP database library it was not always possible to find an exact correspondence regarding, for example, the type of tool used for soil tillage (e.g., type of harrow) or the soil use (e.g., in the choice of the land use we used "Shrub-Perennial" and "Tree-20yr-forest" to reproduce the conditions of agropastoral cropping system and Mediterranean maquis, respectively). Whenever possible, the default values of the WEPP database library have been modified.

The soil characteristics used to create the "Soil file" through the file builder in the WEPP interface are reported in Table 17 and Table 18.

The other parameters in the soil input file, namely the baseline interrill erodibility (ki), baseline rill erodibility (kr), baseline critical shear stress ($\tau c$), and baseline effective hydraulic conductivity (ke) were set to zero (0.0), allowing WEPP to calculate them internally (Flanagan and Livingston, 1995).

Earlier studies showed that the WEPP model is sensitive to kr, ki, ke and $\tau c$ (Brunner et al., 2004; Zheng et al., 2020). The determination of these parameters is objectively difficult and uncertain, in particular about soil erodibility parameters. This is due both to the limited availability of such data for specific types of soil and to the high spatial variability associated with them. It is also for these reasons that we decided to use only critical shear stress and effective hydraulic conductivity in the calibration phase; in relation to these parameters. In fact, earlier site-specific observations and measurements were available (Torri et al., 1987), which could make the identification of the values to be used for model calibration less random.

This project has received funding from the European Union's Horizon 2020 research and innovation programme under grant agreement N° 862695

In Table 19 the mean values of the main parameters used in the different calibrated simulations are listed. Ki and Kr are the values internally calculated by the model, while Ke and τc have been changed according to earlier site-specific observations and measurements.

*Table 19. Mean values of the main parameters used in the different calibrated simulations.*

| Soil use | Adjusted Ki (millions kg $s^{-4}$) | Adjusted Kr (x 1000 s $m^{-1}$) | Adjusted tc (Pascal) | Effective hydraulic conductivity (mm $hr^{-1}$) |
|---|---|---|---|---|
| **Cereal** | 1.056 | 1.113 | 5.8 | 2.38 |
| **Alfalfa** | 0.273 | 0.392 | 6.0 | 2.63 |
| **Agropastoral** | 0.151 | 0.211 | 6.8 | 2.51 |
| **Med. maquis** | 0.124 | 0.211 | 5.5 | 2.98 |

### *Performance of the WEPP model in runoff and soil loss simulations*

Tables 20 and 21 summarize the results of the simulations carried out for the different soil uses with the uncalibrated and calibrated model, also including the relative error calculation.

Comparing the data generated by the uncalibrated model highlighted how, in such a pedoclimatic environment, WEPP tends to overestimate both runoff and erosion values for each cropping system in the entire observation period (see the mean relative errors reported in Table 20).

Only for alfalfa, an underestimation of runoff was observed (Table 20). The highest relative errors are recorded, both for runoff and erosion, for the Mediterranean maquis; however, in absolute terms, we are facing with very low soil erosion values (0.23 Mg $ha^{-1}$).

Taking into consideration the single treatments and analyzing what happened in the different years, as well as in the whole monitoring period, we can observe that, as regards cereals (Table 20; Figure 27), a runoff overestimation it is observed only in 1994, characterized by rainfall values quite like the long-term ones (680 mm; Bazzoffi and Pellegrini, 1992b), but also by a higher erosivity with respect to the long-term mean value (1067 MJ mm $ha^{-1}$ h) (Table 22; Figure 26).

*Table 20. Results of the simulations carried out with the uncalibrated model.*

| Year | Soil use | | Runoff meas. | Runoff est. | Runoff relative error | Eros. meas. | Eros. est. | Eros. relative error |
|---|---|---|---|---|---|---|---|---|
| | | | *(mm)* | *(mm)* | *%* | *(t/ha)* | *(t/ha)* | *%* |
| 1994 | Cereal | | 59.7 | 176.1 | 195.0 | 10.9 | 273.1 | 2405.5 |
| 1995 | Cereal | | 38.5 | 34.7 | -9.9 | 0.87 | 23.7 | 2624.1 |
| 1996 | Cereal | | 206.1 | 202.7 | -1.6 | 19.6 | 290.1 | 1380.1 |
| | | **mean** | **101.4** | **137.8** | **61.2** | **10.5** | **195.6** | **2136.6** |
| | | | | | | | | |
| 1994 | Alfalfa | | 108.1 | 100.2 | -7.3 | 20.5 | 9.9 | -51.7 |
| 1995 | Alfalfa | | 115.4 | 24.9 | -78.4 | 1.8 | 0.1 | -94.4 |
| 1996 | Alfalfa | | 220.3 | 142.3 | -35.4 | 2.2 | 18.8 | 754.5 |
| | | **mean** | **147.9** | **89.1** | **-40.4** | **8.2** | **9.6** | **202.8** |
| | | | | | | | | |
| 1994 | Agropastoral | | 18.6 | 43.1 | 131.7 | 0.8 | 1.6 | 100.0 |
| 1995 | Agropastoral | | 27.9 | 28.2 | 1.1 | 0.2 | 1.4 | 600.0 |
| 1996 | Agropastoral | | 152.6 | 164.4 | 7.7 | 1.6 | 13.2 | 725.0 |
| 1997 | Agropastoral | | 75.5 | 46.5 | -38.4 | 0.3 | 1.8 | 500.0 |
| | | **mean** | **68.7** | **70.6** | **25.5** | **0.7** | **4.5** | **481.3** |
| | | | | | | | | |
| 1998 | Med. maquis | | 1.9 | 33.6 | 1668.4 | 0.0064 | 0.19 | 2868.8 |
| 1999 | Med. maquis | | 2.9 | 116.9 | 3931.0 | 0.0083 | 0.26 | 3032.5 |
| | | **mean** | **2.4** | **75.3** | **2799.7** | **0.0074** | **0.23** | **2950.6** |

This project has received funding from the European Union's Horizon 2020 research and innovation programme under grant agreement N° 862695

*Table 21. Results of the simulations carried out with the calibrated model.*

| Year | Soil use | | Runoff meas. | Runoff est. | Runoff relative error | Eros. meas. | Eros. est. | Eros. relative error |
|---|---|---|---|---|---|---|---|---|
| | | | *(mm)* | *(mm)* | *%* | *(t/ha)* | *(t/ha)* | *%* |
| 1994 | Cereal | | 59.7 | 137.1 | 129.6 | 10.9 | 153.5 | 1308.3 |
| 1995 | Cereal | | 38.5 | 33.1 | -14.0 | 0.9 | 6.0 | 589.7 |
| 1996 | Cereal | | 206.1 | 163.8 | -20.5 | 19.6 | 43.1 | 119.9 |
| | | **mean** | **101.4** | **111.3** | **31.7** | **10.5** | **67.5** | **672.6** |
| | | | | | | | | |
| 1994 | Alfalfa | | 108.1 | 86.9 | -19.6 | 20.5 | 1.6 | -92.2 |
| 1995 | Alfalfa | | 115.4 | 40.1 | -65.3 | 1.8 | 0.1 | -94.4 |
| 1996 | Alfalfa | | 220.3 | 203.8 | -7.5 | 2.2 | 2.1 | -4.1 |
| | | **mean** | **147.9** | **110.3** | **-30.8** | **8.2** | **1.3** | **-63.6** |
| | | | | | | | | |
| 1994 | Agropastoral | | 18.6 | 41.9 | 125.3 | 0.8 | 0.4 | -55.0 |
| 1995 | Agropastoral | | 27.9 | 37.9 | 35.8 | 0.2 | 0.1 | -50.0 |
| 1996 | Agropastoral | | 152.6 | 193.7 | 26.9 | 1.6 | 6.5 | 306.3 |
| 1997 | Agropastoral | | 75.5 | 36.7 | -51.4 | 0.3 | 0.2 | -45.5 |
| | | **mean** | **68.7** | **77.6** | **34.2** | **0.7** | **1.8** | **39.0** |
| | | | | | | | | |
| 1998 | Med. maquis | | 1.9 | 38.9 | 1947.4 | 0.0064 | 0.2 | 3025.0 |
| 1999 | Med. maquis | | 2.7 | 129.5 | 4696.3 | 0.0083 | 0.2 | 1948.2 |
| | | **mean** | **2.3** | **84.2** | **3321.8** | **0.0074** | **0.2** | **2486.6** |

*Table 22. Annual rainfall depth and erodibility during the trial period.*

| | **Annual rainfall** | **Erosivity** |
|---|---|---|
| **Year** | (mm) | (MJ mm.ha$^{-1}$ h) |
| 1994 | 659.8 | 2175.6 |
| 1995 | 652.8 | 681.7 |
| 1996 | 1003.2 | 2521.2 |
| 1997 | 644.2 | 971.9 |
| 1998 | 697.8 | 1467.8 |
| 1999 | 779.8 | 751.2 |

This project has received funding from the European Union's Horizon 2020 research and innovation programme under grant agreement N° 862695

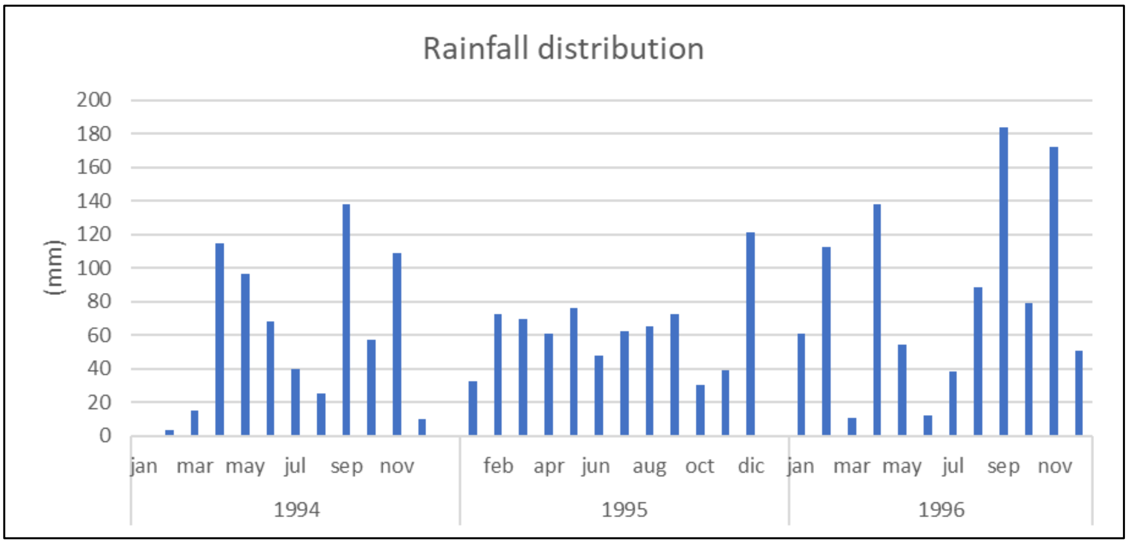


*Figure 26. Monthly rainfall distribution during the period 1994-1996.*

The large clods produced with deep ploughing resist even after repeated intense rainfall events (summer thunderstorms), thus ensuring a high soil surface storage capacity, higher than that estimated by the model. Furthermore, also the deep and wide cracks developed during the dry season persist. Due to this fact, in this pedological environment surface runoff is almost never recorded during summer; the measured runoff volumes were in fact not very high since the cracks network drained the rainwater and any incipient surface runoff in deep.

The year 1996 is also characterized by a rainfall erosivity higher than the long-term average, but the more abundant rainfall, particularly in the summer period (Figure 26), contributed to reducing soil cracks formation.

As far as erosion is concerned, the model always overestimates it: when erosivity is higher with respect to the long-term average (1994 and 1996), the measured and estimated erosion values are higher compared to 1995, but the relative error in 1996 is considerably lower with respect to 1994, since soil loss is also indirectly related to the degree of soil cracking. This different soil behavior, which the model seems unable to take into consideration, led to an overestimation of runoff and erosion in 1994, in which the soil cracking phenomenon was probably more pronounced (Figure 27 and 28).

In 1996 the higher-than-average rainfall, especially in the summer period, probably contributed to reduce soil cracking; the model seems to be able to consider the meteorological trend, estimating runoff and soil loss values with the lowest relative error over the three years.

This project has received funding from the European Union's Horizon 2020 research and innovation programme under grant agreement N° 862695

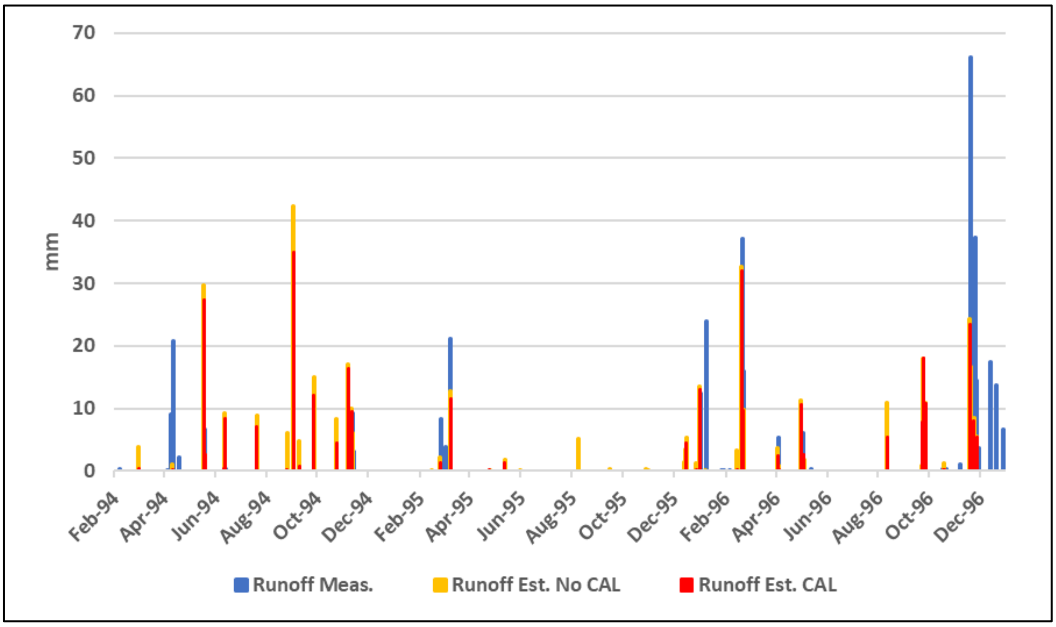


*Figure 27. Runoff amount measured and simulated by uncalibrated and calibrated model in plots under cereal.*

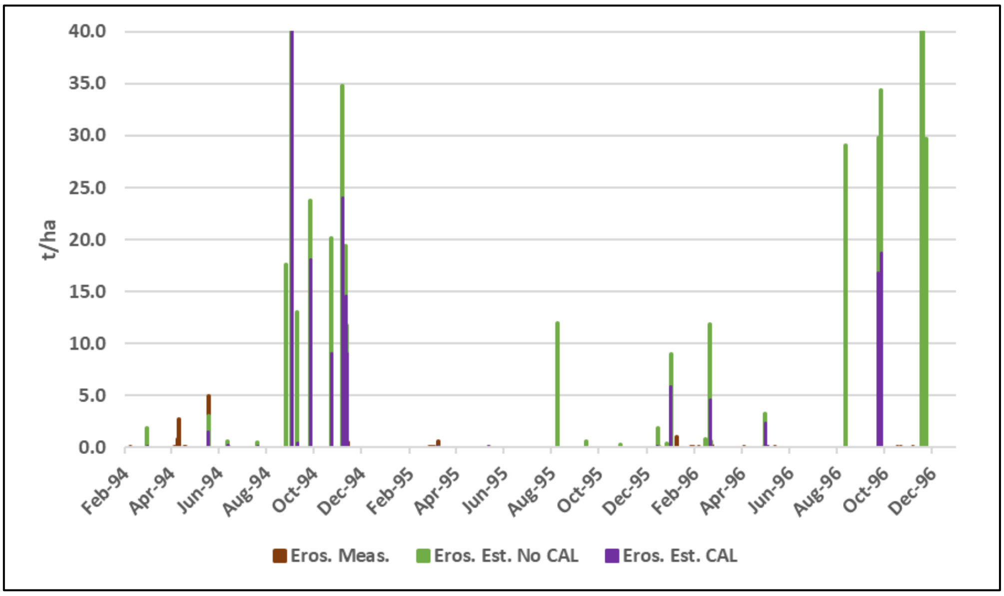


*Figure 28. Soil loss amount measured and simulated by uncalibrated and calibrated model in plots under cereal.*

Alfalfa is a crop less sensitive to erosion. In this case, WEPP as previously reported, predicts runoff values lower than the measured ones. Overall, the erosion is overestimated; however, this is due exclusively to the soil loss predicted in 1996, higher than the measured one, in particular during the spring of 1996, characterized by remarkably high rainfall (Figure 29 and 30). On the contrary, WEPP underestimated erosion in spring 1994, which was really high due to suboptimal soil conditions (high moisture) when the crop was seeded. In this latter case, WEPP was not able to adequately simulate the behavior of the crop (growth phase) following a delayed sowing.

This project has received funding from the European Union's Horizon 2020 research and innovation programme under grant agreement N° 862695

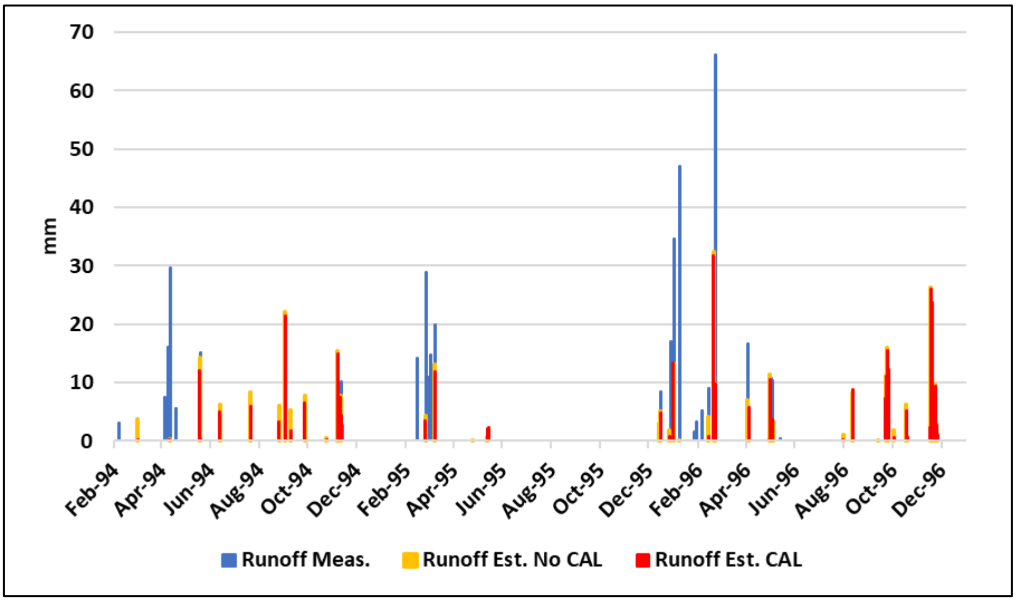


*Figure 29. Runoff amount measured and simulated by uncalibrated and calibrated model in plots under alfalfa.*

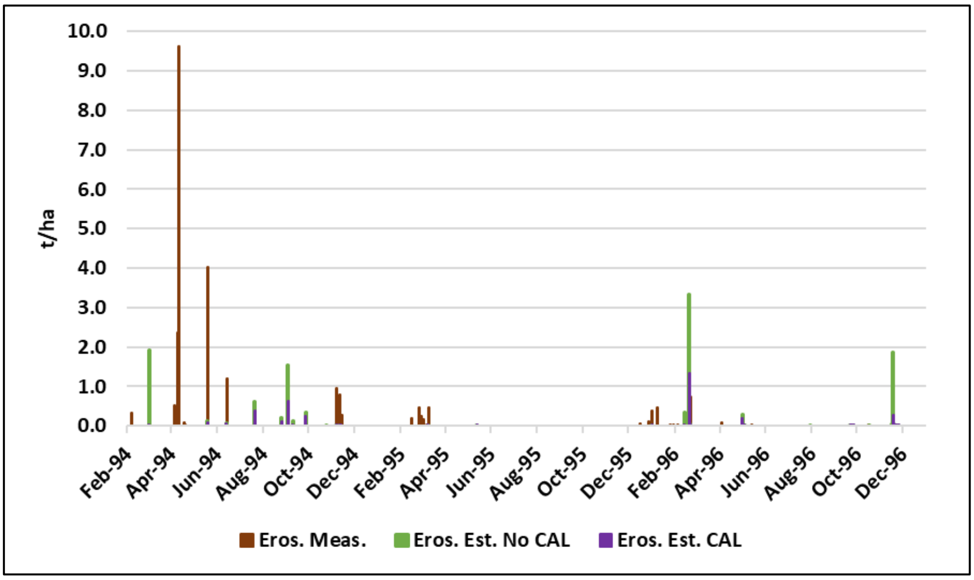


*Figure 30. Soil loss amount measured and simulated by uncalibrated and calibrated model in plots under alfalfa.*

Even with a protective land use such as agropastoral system (grazing shrubs and legume meadows), WEPP generally overestimates runoff and soil loss (Table 20; Figure 31 and 32). The overestimated erosion is however modest (1.6 $Mg.ha^{-1}$) on average for the years 1994, 1995 and 1997; only in 1996 WEPP overestimated soil loss by 11.6 $Mg.ha^{-1}$, almost entirely due to an incorrect estimate of erosion in February 1996, difficult to justify with a soil use in which, in addition to shrubs, there was a dense herbaceous cover (2-year-old sulla meadow). The model overestimates also the runoff volume, but the overall relative error is lower with respect to those of other land uses.

This project has received funding from the European Union's Horizon 2020 research and innovation programme under grant agreement N° 862695

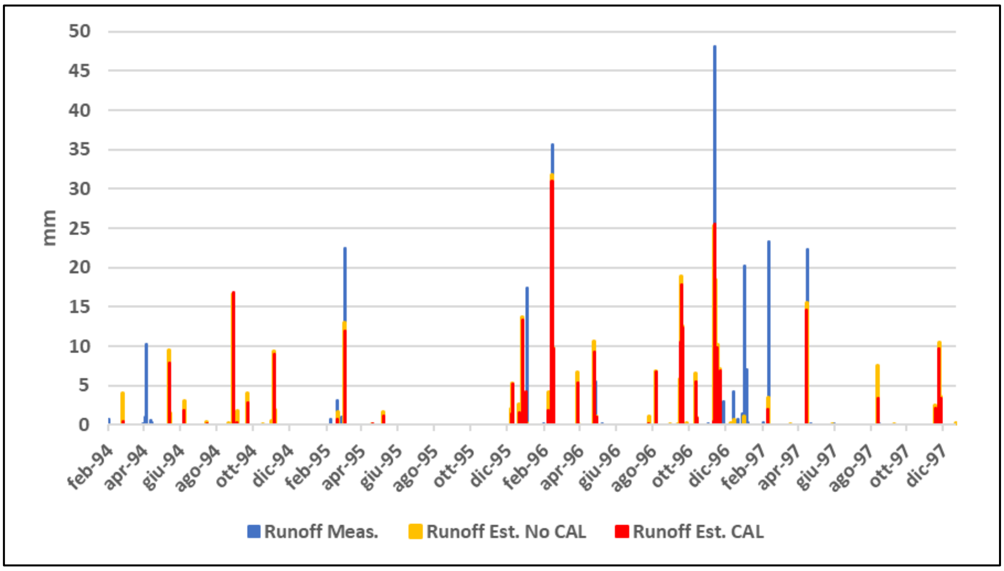


*Figure 31. Runoff amount measured and simulated by uncalibrated and calibrated model in plots under agropastoral land use.*

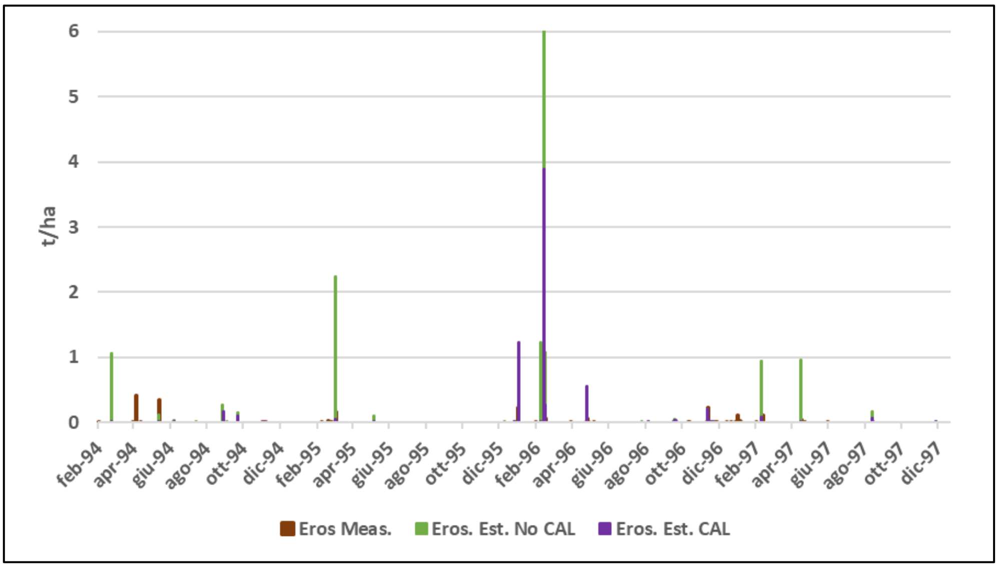


*Figure 32. Soil loss amount measured and simulated by uncalibrated and calibrated model in plots under agropastoral land use.*

Finally, in the Mediterranean maquis, although the relative percentage error is the highest, the runoff values and even more the erosion values, both measured and estimated, are very low. In the two years of observation they appear to be more affected by the amount of total rainfall rather than by its erosivity, confirming the excellent protective capacity of the Mediterranean maquis.

This project has received funding from the European Union's Horizon 2020 research and innovation programme under grant agreement N° 862695

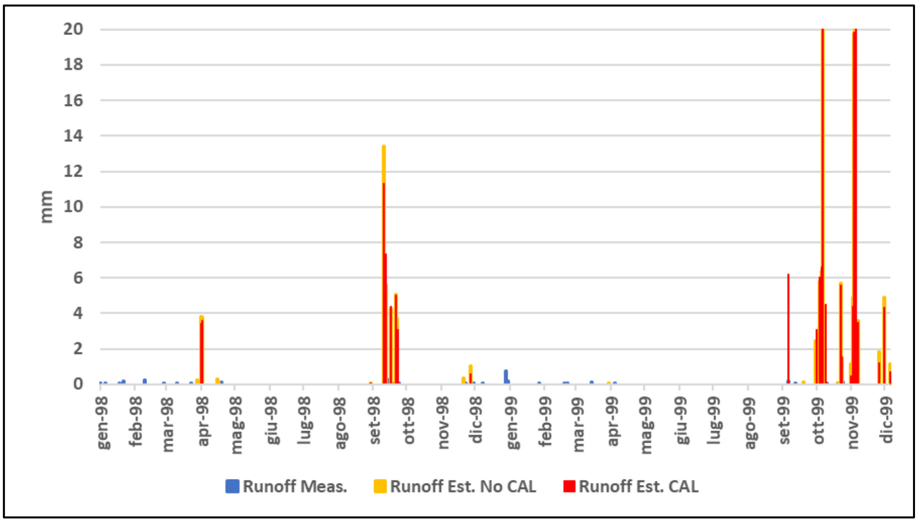


*Figure 33. Runoff amount measured and simulated by uncalibrated and calibrated model in plots under Mediterranean maquis.*

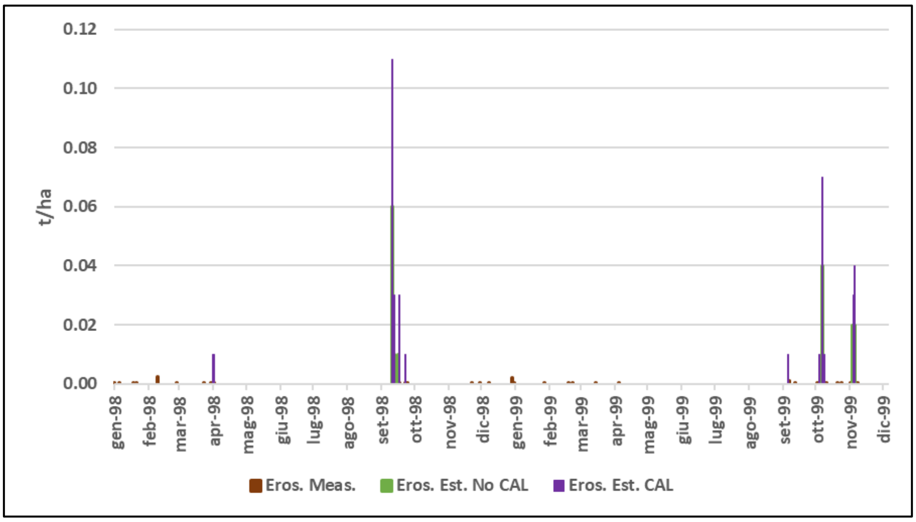


*Figure 34. Soil loss amount measured and simulated by uncalibrated and calibrated model in plots under Mediterranean maquis.*

In Table 21 and Figures 27, 28, 29, 30, 31, 32, 33 and 34 the results obtained after model calibration are reported. The main objective of the calibration was to improve the estimation of soil loss; and this was achieved for all soil uses.

In general, the model always overestimates erosion, except for alfalfa; in this case, however, the absolute value of the relative percentage error is considerably reduced. The calibration did not have the same generalized effect on runoff, improving its estimate in cereal and alfalfa, but not in the more protective ones (agropastoral and Mediterranean maquis).

Overall, however, both with the uncalibrated and calibrated model, percentage relative error values lower than 20 - the limit value for considering the error “satisfactory” according to Chung et al. (1999) - were never recorded. In Table 23 the results of model performance as evaluated by the other statistical indexes are reported.

This project has received funding from the European Union’s Horizon 2020 research and innovation programme under grant agreement N° 862695

*Table 23. Results of the model performance as evaluated by different statistical indexes.*

| | | | Uncalibrated | | | | | | Calibrated | | | | | |
|---|---|---|---|---|---|---|---|---|---|---|---|---|---|---|
| | | | Runoff | | | Erosion | | | Runoff | | | Erosion | | |
| Year | Soil use | | NS | RMSE | RRMSE % | NS | RMSE | RRMSE % | NS | RMSE | RRMSE % | NS | RMSE | RRMSE % |
| 1994 | Cereal | | -5.2 | 13.2 | 22.1 | -481.7 | 24.7 | 226.6 | -4.9 | 11.5 | 19.3 | -204.3 | 16.1 | 147.7 |
| 1995 | Cereal | | -0.5 | 7.0 | 18.2 | -83.6 | 3.9 | 448.3 | -0.9 | 7.6 | 19.7 | -100.6 | 1.5 | 172.4 |
| 1996 | Cereal | | -1.0 | 13.1 | 6.4 | -192.8 | 31.0 | 158.2 | -0.5 | 16.2 | 7.9 | 0.4 | 4.7 | 24.0 |
| | | **mean** | **-2.2** | **11.1** | **15.5** | **-252.7** | **19.9** | **277.7** | **-2.1** | **11.8** | **15.6** | **-101.5** | **7.4** | **71.1** |
| | | | | | | | | | | | | | | |
| 1994 | Alfalfa | | -1.6 | 11.6 | 10.7 | -0.4 | 2.5 | 12.2 | -1.1 | 10.2 | 9.4 | -0.2 | 2.2 | 10.6 |
| 1995 | Alfalfa | | -0.8 | 12.1 | 10.5 | -0.1 | 0.2 | 11.1 | -0.9 | 12.2 | 10.6 | -0.4 | 0.2 | 10.6 |
| 1996 | Alfalfa | | -0.3 | 15.9 | 7.2 | -145.2 | 1.8 | 81.8 | -0.6 | 17.7 | 8.0 | -2.3 | 0.3 | 12.7 |
| | | **mean** | **-0.9** | **13.2** | **9.5** | **-48.6** | **1.5** | **35.0** | **-0.9** | **13.4** | **9.3** | **-1.0** | **0.9** | **10.8** |
| | | | | | | | | | | | | | | |
| 1994 | Agrop. | | -3.6 | 4.7 | 25.3 | -4.6 | 0.3 | 31.3 | -4.1 | 5.1 | 27.4 | -0.3 | 0.1 | 15.0 |
| 1995 | Agrop. | | -0.6 | 7.0 | 25.1 | -67.5 | 0.3 | 165.0 | -0.8 | 7.0 | 25.0 | -0.3 | 0.0 | 20.0 |
| 1996 | Agrop. | | -0.3 | 10.1 | 6.6 | -102.0 | 10.1 | 631.3 | -0.3 | 10.4 | 6.8 | -22.2 | 0.6 | 39.0 |
| 1997 | Agrop. | | -0.5 | 8.8 | 11.6 | -76.2 | 0.3 | 96.7 | -0.6 | 10.4 | 13.8 | -0.8 | 0.1 | 15.2 |
| | | **mean** | **-1.3** | **7.6** | **17.1** | **-62.6** | **2.7** | **231.0** | **-1.5** | **8.2** | **18.2** | **-5.9** | **0.2** | **28.4** |
| | | | | | | | | | | | | | | |
| 1998 | Maquis | | -951.1 | 2.4 | 126.3 | -1321 | 0.0 | 312.5 | -1611 | 3.2 | 166.3 | -173 | 0.0 | 312.5 |
| 1999 | Maquis | | -3660.9 | 8.8 | 303.4 | -2362 | 0.0 | 241.0 | -3708 | 8.9 | 329.6 | -118 | 0.0 | 241.0 |
| | | **mean** | **-2306.0** | **5.6** | **214.9** | **-1842** | **0.0** | **276.7** | **-2659.3** | **6.0** | **248.0** | **-1458.1** | **0.0** | **272.1** |

Table 23 displays the overall results about uncertainty evaluation of uncalibrated and calibrated WEPP model in predicting runoff volume and soil loss in different years and diverse soil uses by the selected statistical indexes.

Negative values of NS efficiency index identify an unacceptable performance of the model, both for runoff and erosion estimation. When the input values of effective soil hydraulic conductivity and critical shear strength were adjusted, although the NS index shows an improvement, limited exclusively to the estimate of erosion, the values always remain unacceptable (<0). The only value higher than zero is recorded when using the calibrated model relative to the estimate of erosion in cereals in 1996. Even in this case, however, the value of the NS index remains unsatisfactory (0.4).

Regarding the RMSE, there is a slight, generalized deterioration in the performance of the calibrated model in relation to the runoff estimate for all the soil uses.

In estimating erosion, after model calibration the RMSE values are reduced, reaching average values close to 0 in the most protective land uses (alfalfa, agropastoral and Mediterranean maquis).

In runoff estimation the RRMSE highlights a substantially identical performance of the uncalibrated and calibrated model; in particular, the performance is "excellent" for alfalfa, "good" for cereal and agropastoral and "poor" for Mediterranean maquis.

Regarding the estimation of soil loss, RRMSE indicates a poor performance of the uncalibrated model for all the land uses. After calibration the model performance improves, reaching RRMSE values considered "good" for alfalfa and "fair" for agropastoral soil use.

This project has received funding from the European Union's Horizon 2020 research and innovation programme under grant agreement N° 862695

*Conclusions*

The predictive performance of the WEPP model about runoff volume and amount of eroded soil was evaluated in a soil environment of central Italy characterized by fine-textured soil with vertic properties using six years of field data.

Both the estimated runoff and soil loss data highlight an unsatisfactory predictive capacity of the uncalibrated model, as proven by the negative values of the NS efficiency index.

The comparison between the quantity of eroded soil, simulated by the uncalibrated WEPP, and the measured one, highlights how in such a pedological environment the model overestimates soil loss.

The improvement in the predictive performance of the model after calibration, shown by the RRMSE values considered “good” and “fair” for conservative land uses, seems to prove a satisfactory reliability of the WEPP model in identifying management scenarios able to counteract soil loss.

Future WEPP application efforts need an in-depth assessment and proper calibration and parametrization of the erodibility and effective hydraulic conductivity parameters to improve erosion prediction in environments characterized by the presence of soils with a similar hydrological behaviour.

# 4. Optimized parametrization strategies to manage connectivity elements inside models for different scales and environments

This section summarizes the findings of both the case studies and the previous literature studies, in order to suggest some “optimal” parametrization strategies emerged from the model assessment. The suggestions on how to optimally configure and set the model parameters (minimizing uncertainties) will be reported for different data categories: the input data, the parameters/coefficients (for setting transmissivity or related to land parcel management and field plots), and the connectivity elements. If possible, a distinction is made among various scales of application, from plot to catchment and/or regional scale. As a reference to the various models used, the application of RUSLE-ID-SDR method (Finlandia case studies) is indicated with RUSLE1, while the RUSLE+USPED method (Italian case study) is indicated with RUSLE2.

For all the considered elements, it is possible to define geographic detail thresholds, which should be used depending on the working scale of the model: this is an explicit approach, introducing the elements with their own geographies in the model, or an implicit approach (lumped), where “some or all relevant connectivity links and properties are represented through proxies, and processes have been parametrized to include connectivity” (Nunes et al., 2018). In Figure 35, this distinction is shown between the explicit and implicit representation of these elements in accordance with the geographic scales at which models allow to incorporate the type of representation.

This project has received funding from the European Union’s Horizon 2020 research and innovation programme under grant agreement N° 862695

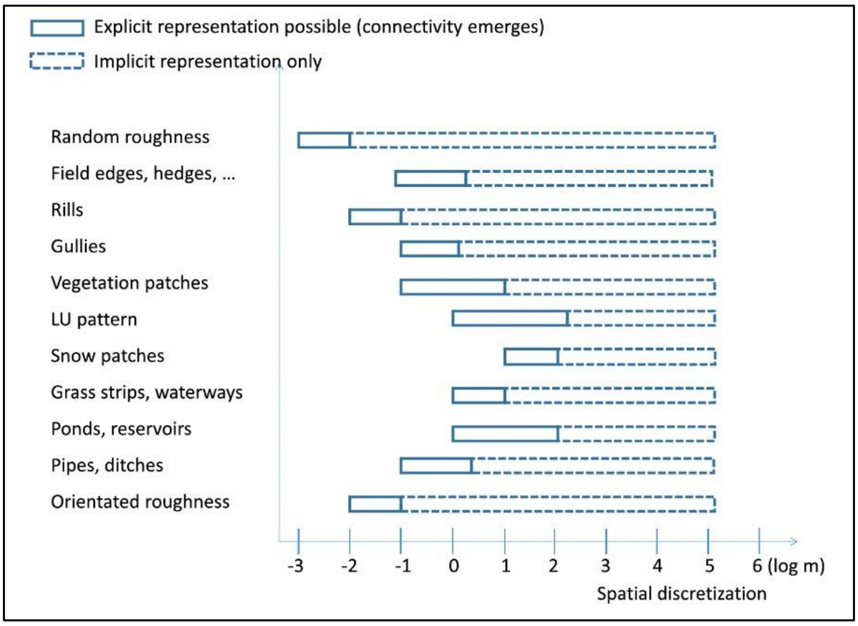


*Figure 35. Schematic representation of scales at which certain landscape features that are influential in terms of water or sediment connectivity are resolved explicitly or implicitly in environmental models (From Nunes et al., 2018).*

## 4.1 Empirical Models

### 4.1.1 Input data parametrization

The final summary from the case studies from Finland, Flanders and Italy on the optimal parametrization methods for DEM to calculate LS, R, K, C and P input factors adopted within the two RUSLE options, and WaTEM/SEDEM modelling, is presented as schematic view in Table 24.

*Table 24. Summary table of the input data sources, parametrization and processing methodologies and tools adopted in the case studies, only for spatially distributed approach at catchment level.*

| Model | Input parameter and source | Parametrization | Processing notes |
|---|---|---|---|
| **RUSLE-IC-SRD** | DEM 2x2 (Lidar-Finland) | 7 scenarios:<br>Set threshold for filling sinks at 0.05, 0.10, 0.15, 0.20 m of depth, according created DEM (5), (10), (15), (20) filled from Lidar<br>Set ditches wide at 2 and 3 pixels (4 and 6 m) with other DITCH4 and DITCH6 two scenarios | Filling tools (Lindsay, 2019) |
| | LS topographic factor | By 2x2 DEM: Methodology from Desmet & Govers (1996) | SAGA-GIS LS Module (Rill and interrill erosivity ratio = 1; stability = stable) (Conrad, 2003) |
| | R Factor | Annual average values on 1x1km ESDAC grid (Panagos, 2015d) | Ref. for calculation: Renard et al. (1997) and Rainfall Intensity Summarization Tool (RIST) software (USDA, 2014) |
| | K Factor | Regosols = 0.0570 (avg)<br>Stagnosols 0.0400 (avg) | From Finnish Soil database on major WRB soil type (Renard, 1997) |

This project has received funding from the European Union's Horizon 2020 research and innovation programme under grant agreement N° 862695

| | | | |
|---|---|---|---|
| | C Factor | Calibrated locally against erosion measurements from seven field sites | Least squares method |
| | P factor | Value = 0.6 | Ref. Renard et al. (1997) and Lilja et al., (2017a). |
| **RUSLE+USPED** | DEM 2.5x2.5<br>DEM 2x2 (Lidar RT)<br>DEM 10x10 (RT) | DEM (2.5) Resampled from 25x25 Sentinel DEM (EU DEM 1.1)<br>Setting Dams/Ponds surface at same DEM value, simulating a sink along the slope; filling DEM with Flowacc = 0 on water surface | DEM 10 and Lidar from Regione Toscana (RT) |
| | R factor | One value R (Average/years) from Agri4cast EU grid (25km)<br>Avg. value from six different functions (Ref.)<br>Annual avg. (6 functions) = 2510<br>min = 1348; max = 4057 | Ref. Arnoldus, 1977, 1980<br>Renard and Freimund, 1994<br>Lo et al., 1985<br>Yu and Rosewelt, 1996 |
| | K factor | Vertic Cambisols<br>Vertic Regosols<br>Haplic and Calcic Regosols<br>Avg. 0.035 | Ref. Torri et al. 1997 |
| | C factor | Avg arable lands = 0.244<br>min = 0,005; max = 0.400<br>Avg woodlands = 0.127<br>min = 0.000; max = 0.800<br>Other artificial (roads, buildings, mines, etc.) = 0 | Italian look-up Table from Bazzoffi (2007) |
| | P factor | = 0.9519 (only for arable lands) | Ref. Panagos et al., 2015b |
| **WaTEM/SEDEM** | DEM 2x2 (Lidar Flanders)<br>DEM 5x5<br>DEM 20x20 | DEM (5) and DEM (20) resampled from Lidar | |
| | LS topographic factor | By 2x2 DEM: methodology from Desmet & Govers (1996) | Roads, parcel borders and land use are considered (see connectivity elements) |
| | R factor | One value R (Average/years) - Royal Meteorological Institute (Ukkel, Brussels) | Ref. Verstraeten et al., 2006a |
| | K factor | *No data* | |
| | C factor | *No data* | Flanders C look-up table |
| | P factor | Not influent in the CN-WS new version | |

It is clear that the diversity of approaches in processing the various input parameters, as summarized in Table 24, does not guarantee the necessary methodological standardization. Such standardization is needed across erosion models and post-processing techniques to obtain comparable spatially distributed predictive results that can be used as a common baseline, avoiding introducing very different uncertainties by source and amplitude. This would allow for the adoption of uniform solutions to increase sediment transport disconnection. Having a common baseline is crucial for achieving comparable outcomes since soil erosion (and sediment transport) is a significant parameter within European Common Agricultural Policies (CAP) for related measures to mitigate the phenomenon.

It's evident that even the adoption of minimum standards in configuring input data does not fully resolve the different uncertainties arising from site-specific characteristics (variable soils, climatic patterns, types of crop management), which often require parameter adjustments at the local scale.

More in detail:

a) about DEM implementation, the considered case studies have reported various types of processing, starting from detailed Lidar DEM (2x2m). However, using (also by resampling)

DEMs at different resolution scales introduces, depending on the adopted methodologies, uncertainties that are often incomparable. The transformation into hydrologically corrected DEMs, achieved through sink-filling (small/large depressions), is also a factor contributing to error generation;

b) DEM derived parameters: the LS factor is the key controlling factor that effectively regulates connectivity along hillslopes and consequently water flow. As explained in the case study of Finland (paragraph 3.1.6), considering hydrologically isolated land parcels by appropriately modifying the LS factor can lead to significant differences in results, both applying RUSLE+IC+SDR and applying WaTEM/SEDEM. The presence of ditches, watercourses, sewer systems, or even areas covered by forest vegetation should be considered as breaking elements for the connectivity of hydrological flows. Nevertheless, the possibility of considering forested areas as elements of hydrological discontinuity should be verified, especially in environments with significant slopes, such as hilly and sub-mountainous areas;

c) R factor: there are various climatic reference databases at different scales, both European, such as the 25 km grid Agri4CAST - with data from 1979 to the present – and national, such as the 1x1 km grid produced by ESDAC (Panagos et al., 2015d), along with analyses based on national meteorological networks (Royal Institute - Flanders). The reference ranges of climatic data, the methods used both in calculating the R factor and those used for spatializations at different grid resolutions undoubtedly introduce various errors/uncertainties (technical and methodological). Furthermore, using a temporal average value rather than annual, monthly or hourly data introduces a conceptual uncertainty (epistemological) regarding the actual distribution of the parameter over time, which is often not considered as a modeling input option;

d) K factor: despite the generally low sensitivity of this parameter within the RUSLE formula, errors of varying amount can be introduced depending on whether the average value from digital soil maps/databases is taken. For example, the estimations made in the Finnish case study computed with Renard (1997) method, for the two reference soils mentioned (Regosols and Stagnosols, WRB 2014) derived from the Finland Soil Database were as follows: Regosols 0.0570 avg, range 0.046–0.055; Stagnosols 0.0400 avg, range 0.022–0.037 (Lilja et al., 2017a). In the Italian case study in the Tuscany Region soil database, with a more detailed geographic database, different soil types were evaluated (Vertic Cambisols, Vertic Regosols, Haplic and Calcic Regosols, WRB 2014) using a different methodology (Torri, 1997), resulting in average K values of 0.035, with a range of 0.011–0.047. This method was chosen for its superior performance (see paragraph 3.4.2) compared to Renard (1997), which yielded different results: K Renard = 0.038 avg., range 0.014–0.047;

e) C factor: there are different methods and local elaborations at national scale based on a significant series of detailed data (Bazzoffi, 2007), with synthesis and wide-scale application on Corine Land Cover codes; the formulas proposed by Panagos (2015c) adopted for EU erosion estimation as: $C_{arable} = C_{crop} \times C_{management}$ (with $C_{management} = C_{tillage} \times C_{residues} \times C_{cover}$); in the case study of Finland this factor was calibrated locally with erosion measurements; furthermore, in the case study of Flanders, a more detailed method was adopted which involves, starting from a factor related to the Main Crop (MC), a series of reduction factors, or modifications depending on whether the introduction of cover crops (CC1, CC2), agri-environment-climate measures (AECM) like buffer strips, grassed waterways, etc., and the adoption of obligatory GAEC measures (CAP) are considered. Lastly, in the application at the field/plot level of the WEPP model, detailed C values (Bazzoffi, 2007) were instead used, both at the crop and cover levels, as well as the cropping system;

f) P factor: the same consideration can be made for obtaining reliable data on management practices in large areas (catchment or regional), which are almost always available only at the field/plot scale - thus, average data were used in the case studies. Some references at EU level are given by Panagos (2015b) that summarize for each Member State three sub-factors as Pc (contouring), Psw (stone walls), Pgm (grass margins), and the average P-factor for all the arable lands (sources: LUCAS database and GAEC practices declared by farmers inside the EU Agricultural Statistics database). Looking also at these values, there is a range from min = 0.5251 to max = 0.9995, with a mean value of 0.97. In the Italian case study we took this reference value (for Italy) with P = 0.9519, in the Finland case studies was adopted a P value = 0.6. The reference average value for Finland, to perform soil erosion assessment at EU level, however, is P = 0.9942, according to Panagos (2015b).

### 4.1.2 Parametrization of indexes and transmissivity coefficients

Summarizing the indexes and parameters considered for different models (case study or literature), the following suggestions for the different case-studies with different spatially distributed approaches and scenarios are given (Table 25).

*RUSLE+IC+SDR model*

Here the data already presented in the sensitivity analysis for $IC_0$, Kic and SDR are summarized, in relation to the scenarios described in the case study of Finland (Table 25), taking into account the aggregation as average data for each single land unit/parcel.

*Table 25. Parametrization scenarios applied for sediment delivery computations.*

| **Parametrisation** | **P1** | **P2** | **P3** | **P4** | **P5** | **P6** | **P7** |
|---|---|---|---|---|---|---|---|
| **Description** | Widely used literature value | Literature value | Literature value | Literature value | Reflects local data | Reflects local data | Reflects local data |
| $IC_0$ | 0.5 | 0.5 | 0.5 | 0.1 | -4.7 | -3.3 | -5.7 |
| $K_{IC}$ | 2.0 | 1.8 | 3.5 | 2.0 | 1.0 | 1.0 | 1.0 |
| $SDR_{max}$ | 0.8 | 0.8 | 0.8 | 0.8 | 0.8 | 0.8 | 0.8 |

*RUSLE+USPED model*

For the Italian case study (Capriggine catchment), Eq. 9 was used to evaluate the Tc, considering a hillslope catchment with a slope range from 0 to 51%, mean = 15%, and a mix of arable land and woodland, adopting a pixel size of 2.5x2.5 m. The adopted parametrization of coefficients *m* and *n* is reported in Table 26, together with the statistics for the Tc values according to land use types in Table 27.

*Table 26. Parametrization of* n *and* m *coefficients for the adopted best scenario, after calibration, to calculate Transmissivity Coefficient (Tc) and Erosion/Deposition (ED) values.*

| Coefficient for TC calculation | Parametrization | Description |
|---|---|---|
| **n** | n = 1.3 (scalable to 1) in upslope areas with convex topography | m = 1.6, n = 1.3 for prevailing rill erosion while m = n = 1 for prevailing sheet erosion |
| **m** | m = 1.2 (scalable to 1) in downslope/footslope areas with convex topography | m = 1.6, n = 1.3 for prevailing rill erosion while m = n = 1 for prevailing sheet erosion |

*Table 27. Transmissivity Coefficient (Tc) ranges as average best correlated with the land use code (CLC classes).*

| CLC_Classes | Average TC | St_Dev |
|---|---|---|
| ***Discontinuous urban fabric (112)*** | 1 | 2 |

| | | |
|---|---|---|
| ***Industrial or commercial units (121)*** | 3 | 4 |
| *Road and rail networks and associated land (122)* | 5 | 12 |
| ***Mineral extraction sites (131)*** | 0 | 0 |
| ***Construction sites (133)*** | 1 | 1 |
| ***Green urban areas (141)*** | 106 | 26 |
| ***Non-irrigated arable land (211)*** | 69 | 26 |
| ***Vineyards (221)*** | 156 | 72 |
| *Fruit trees and berry plantations (222)* | 170 | 13 |
| ***Olive groves (223)*** | 194 | 81 |
| ***Pastures (231)*** | 3 | 9 |
| *Annual crops associated with permanent crops (241)* | 132 | 54 |
| ***Complex cultivation patterns (242)*** | 108 | 80 |
| *Land principally occupied by agriculture with significant areas of natural vegetation (243)* | 93 | 44 |
| ***Broad-leaved forest (311)*** | 14 | 7 |
| ***Coniferous forest (312)*** | 31 | 0 |
| ***Mixed forest (313)*** | 4 | 2 |
| ***Transitional woodland shrub (324)*** | 33 | 14 |

### *WaTEM/SEDEM model*

In the WS model, for every grid cell the transport capacity **(TC)** is calculated with the formula:

TC = ktc*R*K*T (14)

where ktc is the transport capacity coefficient, R is the rainfall erosivity factor, K is the soil erodibility factor; T is the topographical factor.

**kTC best parametrization for case study**: on rolling topography and low hills of the Flanders case studies (Molenbeek and Maarkebeek catchments), Ktc (low and high) values were parametrized as optimal within a set of 8 combinations, all considered equally valid to perform results with the minimum uncertainties, as shown in the Table 28.

*Table 28. Combinations of kTC low and kTC high optimal settings adopted for Flanders case studies.*

| Optimal Setting | $kTC_{low}$ (m) | $kTC_{high}$ (m) |
|---|---|---|
| **1** | 1 | 9 |
| **2** | 2 | 9 |
| **3** | 3 | 9 |
| **4** | 4 | 8 |
| **5** | 4 | 9 |
| **6** | 5 | 8 |
| **7** | 6 | 8 |
| **8** | 7 | 8 |

**kTC settings from the literature:** some studies in mediterranean hillslope and mountain landscapes of Italy were carried out at national scales and inside EU trials; in some of these studies WaTEM/SEDEM model performance and results were calibrated and validated with measurements of the sediments trapped inside the dams/ponds and several reference upstream catchments or watersheds (in this approach ponds were considered in WaTEM/SEDEM as water endpoint) (Van Rompaey et al., 2005). The database of sediments trapped in Italy started from 44 reservoirs measured in small (Ponds) medium (Ponds, Reservoirs) and Big (Dams) was used as validation measures at the endpoint for the

This project has received funding from the European Union's Horizon 2020 research and innovation programme under grant agreement N° 862695

WaTEM/SEDEM simulation in the upstream catchments to assess the SDR. Some different methodologies were used to calibrate the model (stratified vs global).
The parametrization of transmissivity coefficient was: kTC_A (ktc for arable croplands) with values ranging from 12 to 16; kTC_FP (for forest/pasture land) with values ranging from 30 to 35.
After this parametrization, results (Figure 36) show that i) stratified calibration procedures are more accurate than the predictions resulting from a global calibration procedure; ii) error estimation show than the model performance for the non-mountain catchments (R = 0.51) in the dataset is better than for the mountain catchments.

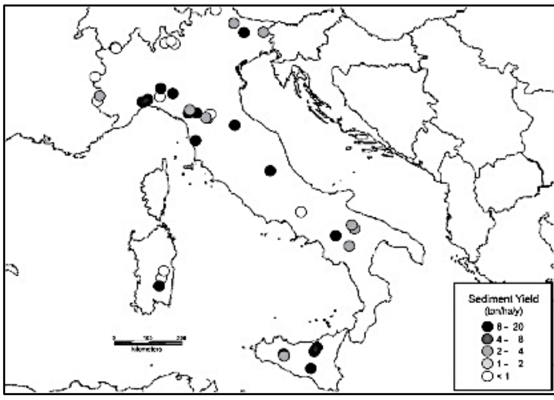

| Calibration type | Dataset | $K_{TC\_FP}$ | $K_{TC\_A}$ | ME | $R$ |
|---|---|---|---|---|---|
| Global | total dataset | 12 | 30 | −0.33 | 0.21 |
| Global | mountain catchments | 12 | 30 | −6.62 | 0.20 |
| Global | non-mountain catchments | 12 | 30 | −0.11 | 0.36 |
| Stratified | total dataset | 8/16 | 30/35 | 0.14 | 0.50 |
| Stratified | mountain catchments | 8 | 30 | 0.07 | 0.25 |
| Stratified | non-mountain catchments | 16 | 35 | 0.19 | 0.51 |

*Figure 36. Parametrization of kTC-values derived from global and stratified calibration procedures and statistical results of predicted vs measured trapped sediments (From Van Rompaey et al., 2005).*

The same approach was adopted in a previous study at EU level for Italy (Van Rompaey et al., 2003), with only 22 reservoirs used as ground truth for measures of trapped sediments in the endpoint of upstream catchment.
Parametrization used for Ktc was different, and WaTEM/SEDEM model was run with for the kTC_A parameter values ranging from 5 to 40 and for kTC_N (forest, pasture and grasslands) ranging from 20 to 100. Best kTC parameters after calibration were fixed in **kTC_A = 50** and **kTC_N = 30**.
Results indicate that, despite the Pearson's $R^2$ between observed and predicted values was 62%, and the optimal model efficiency after calibration was 0.41 (NS, model efficiency coefficient as proposed by Nash and Sutcliffe, 1970, used as a measure of likelihood), the RRMSE of the model predictions was quite high (70%). Three main sources of uncertainty were assessed to determinate these poor results, i.e. 1) error on the measured values; 2) error on the predicted SDR ratio; 3) uncertainty on the predicted soil erosion rates.

**Tillage coefficient (Ktill)**

This coefficient relates to the calculation of the amount of soil/sediment removed due to tillage translocation. The functional equations that link slope to this type of translocation imply that tillage erosion is controlled by the change in slope gradient, rather than just the slope gradient itself, leading to erosion on convex slopes and soil accumulation in concave areas. Estimating this coefficient is very challenging as it depends on a set of highly localized factors, such as the direction of tillage in relation to the maximum slope, tillage depth, and the type and speed of the mechanical tool (e.g., mouldboard plough).
References from the current version of the CN-WS model (Van Oost et al., 2000) report calibrations with values ranging between 700 and 900 kg $m^{-1}$ $yr^{-1}$, while for other experimental conditions of slope, tillage direction and different machinery Goovers et al. (1994) report values between 400 and 600 kg $m^{-1}$ $yr^{-1}$. Among the scarce literature studies, it is important to mention those by Torri and Borselli (2002) and Alba et al. (2006), concerning measurements conducted in Central Italy (Hillslope landscapes of Tuscany) with 19 experimental plots and different tillage directions relative to the maximum slope. They developed a regression model (SeTI) based on an extensive bibliography of case

studies. More recently, with new approaches proposed by Quine and Zhang (2004), measured values range between 112 (up-down along the maximum slope) and 159 (at a 45° angle with the maximum slope), citing 11 other studies with coefficients varying from 85 to 335.
**PCF:** the amount of upstream area that is transferred to a specific land use and regulate the connection inside the upstream/downstream pixel flow calculation.
**PTEF:** percentage contribution of one pixel to the downstream pixels, as a function of a specific land use of the pixel
The best parametrization come out from the analysis carried out inside the Flanders case study, considering both the two different DEM details (5 and 20 m), and is reported in Table 29.

*Table 29. PCF and PTEF optimal settings adopted for Flanders case studies*

| WS Parameters set for Flanders Catchments |
|---|
| 〖PCF〗_cropland: 90 % |
| 〖PCF〗_grasstrips: 100 % |
| 〖PCF〗_forest: 30 % |
| 〖PTEF〗_crop: 0 % |
| 〖PTEF〗_pasture: 75 % |
| 〖PTEF〗_forest: 75 % |

### *4.1.3 Parametrization of connectivity elements*

*Parcel borders and upstream land use*

The optimal parametrization methods suggested by the different case studies can be summarized:

a. in RUSLE-IC-SDR, if bordering with sewer system or ditches, buffer strips or water courses, the land use parcels are to be considered as hydrologically distinct, by configuring these elements as pixel areas/strips with distinct values (therefore ditches, watercourses and sewer system as topographic endpoints in the calculation of LS); in the IC and SDR calculation the average values (gross erosion) must be taken in account;
b. in WaTEM/SEDEM, this element connectivity is managed by the optimal setting of the PC and PTEF coefficients among parcels (paragraph 4.1.2), if hydrologically connected. If delimited by watercourses, ditches, or sewer systems, by introducing the raster singular map option (provided by WaTEM/SEDEM version used in Flanders);
c. in RUSLE+USPED approach, the presence of hydrologically influential elements on the border is missing (a representative case of most of the hilly landscapes and south-European mountains), so all the parcels are considered as hydrologically connected at the borders in the slope calculations. In case of modeling in the plain o sub-plain landscapes (with ditches and permanent watercourses and/or sewer system) parametrization will follow the RUSLE-IC-SDR approach.

*Tillage direction*

With RUSLE-IC-SDR model only the effect on gross erosion can be considered, if tillage direction is exactly according to contours. Off-grade contouring cannot be possibly considered.
With WaTEM/SEDEM model the element “tillage direction” could be managed by introducing a tillage direction raster map option and an oriented roughness map; in this case this option alters the routing on agricultural fields. When this option is enabled, the routing will follow the given tillage direction on these fields. However, it is difficult to recover this kind of information about the whole catchment, so in the case study was not assessed due to the lack of data.

This project has received funding from the European Union’s Horizon 2020 research and innovation programme under grant agreement N° 862695

For the RUSLE+USPED model it is not possible to manage directly this element; a possible solution is to consider it as implicit (lumped approach) by modifying the P factor adequately, also if actually there is a lack of knowledge about how to estimate the effects on this input parameter.

*Roads*

Both in the RUSLE-IC-SDR and RUSLE+USPED presented models it's actually not possible to manage roads elements explicitly, but could be considered a) equal to small narrow "parcels" if the working detail allow to represent them as a pixel string, with a C factor value = 0 (maximum runoff with no infiltration); b) as implicit (lumped) effect, by considering in some way the percentage of area inside the parcel as modifier of the C and P factor; or c) modifying DEM considering the slope breaks up and down the road strip (depending on its pathway with respect to the maximum slope direction).
In the WaTEM/SEDEM model the roads are set with a C Factor = -2 (Infrastructure), therefore excluded from the evaluation of the sediment dynamics (No Sedimentation), as long as it is possible to represent them to adequate detail in a raster map. If this is not possible, the use of a lumped implicit approach by modifying the value of the PCF and PTEF coefficients could be considered. This hypothesis was not yet verified and not currently implemented (introducing an epistemological uncertainty).
In the case studies none of these hypotheses has been tested, so it is not possible to evaluate the effect on uncertainty that can be introduced with the various proposed solutions.

*Ditches, underground pipe, and sewer systems*

Inside WaTEM/SEDEM model, the sewer system can be managed with a raster map option, inside which the sewers are considered as endpoint. All the pixels in the sewer map should contain values between 0 and 1. Such values represent the fraction of the outgoing sediment in that pixel that is entering the sewer system. A pixel with value 0 can be interpreted as a pixel where no sewer is present. It is very difficult to estimate this fraction, as reported in the case study (inlets not known, only strings). Modelling transport of sediment in ditches with current approach is to considered them as sediment endpoint. However, in the case study there was a lack of data, with ditches only partially known, and underground pipes not known.

*Seasonal (temporary) ditches*

Temporary ditches are a common soil management practice during fall and winter in hillslope environments of arable lands, implemented up to now under the second pillar of CAP, among the agri-environmental measures aimed to soil conservation, to be adopted on voluntary basis by farmer. The environmental efficacy of this reference standard, that is the efficacy of the temporary ditches, must be assessed by looking at the double aspect of the efficacy both in intercepting all the runoff water at the peak discharge and in reducing soil erosion to the tolerance limits.
Inside the WaTEM/SEDEM model, the use of ditches will alter the routing simulated by the model. When included, sediment and water will follow the course of the ditches instead of the steepest slope in the ditch locations. When this option is enabled, a *Ditch map* (a raster with information about the direction) should be given as model input. The model sets the C-factor at every ditch pixel tot 0.01, assuming that the ditch is covered with grass. This is a limitation that could not allow to use this option for parametrization of temporary ditches on the slopes (epistemic lack).
**From literature**: Effectiveness of this practice was tested at Italian National level by Bazzoffi et al. (2011) inside a monitoring project MONACO, for assessing the effectiveness of provided GAEC Standard "*1.1: Creation of temporary ditches for the prevention of soil erosion*" inside CAP policy.
From this study several experimental measures related to runoff peak events (643) were monitored at Plot level (CREA, S. Elisabetta and Fagna experimental farms), useful to find the best solution for optimize the distance, depth and angle vs maximum slope for planning temporary ditches network.

This project has received funding from the European Union's Horizon 2020 research and innovation programme under grant agreement N° 862695

The best for the standard was estimated for an angle of 30 degree with respect to the maximum slope direction, and parallel network at a distance of 80 m.
Many other experimental measures were gathered from some CNR and Universities experimental farms, from northern areas (Torino, Modena), to southern ones (Palermo, Regio Calabria, Sparacia) After the collected data had been processed, the following equation, valid for the Italian territory, was obtained for the estimation of the maximum runoff peak in relation to the catchment basin's area and to the gradient:

$$P=e^{a+b\cdot \ln x+c\cdot y^3} \tag{15}$$

Where P = $m^3\ s^{-1}\ ha^{-1}$, x is the area (ha), y is the mean hillslope gradient (%).
By comparing the maximum runoff peak values generated by agricultural surfaces was possible to determine the minimum values for the ditch size required to control runoff according to site-specific conditions, as shown in Table 30.

*Table 30. Maximum runoff peak values ($m^3\ s^{-1}$) calculated using equation 14 for the draining surface between two neighboring drainage ditches in relation to ditch length, slope gradient and distance between ditches.*

| Inclined distance between ditches | Length of the ditch m | Mean hillslope gradient and discharge capacity 10% $m^3\ s^{-1}$ | 15% $m^3\ s^{-1}$ | 20% $m^3\ s^{-1}$ | 25% $m^3\ s^{-1}$ |
|---|---|---|---|---|---|
| 80 m | 50 | 0.013 | 0.014 | 0.018 | 0.025 |
| | 100 | 0.021 | 0.024 | 0.030 | 0.043 |
| | 150 | 0.029 | 0.032 | 0.040 | 0.058 |
| | 200 | 0.036 | 0.040 | 0.050 | 0.072 |
| | 250 | 0.042 | 0.047 | 0.059 | 0.085 |
| 60 m | 50 | 0.010 | 0.011 | 0.014 | 0.020 |
| | 100 | 0.017 | 0.019 | 0.024 | 0.034 |
| | 150 | 0.023 | 0.026 | 0.032 | 0.047 |
| | 200 | 0.029 | 0.032 | 0.040 | 0.058 |
| | 250 | 0.034 | 0.038 | 0.047 | 0.068 |

According to the best rules to plan a temporary ditches network, a simulation was conducted applying RUSLE model in 60 trials areas in many different landscapes with arable crops all over Italy, by modifying DEM temporary ditches as a new connected stream flow network and accordingly modifying the DEM for the ditches lines with a new value of -0.5 m (as average) with respect to the original DEM (Figure 37).

This project has received funding from the European Union's Horizon 2020 research and innovation programme under grant agreement N° 862695

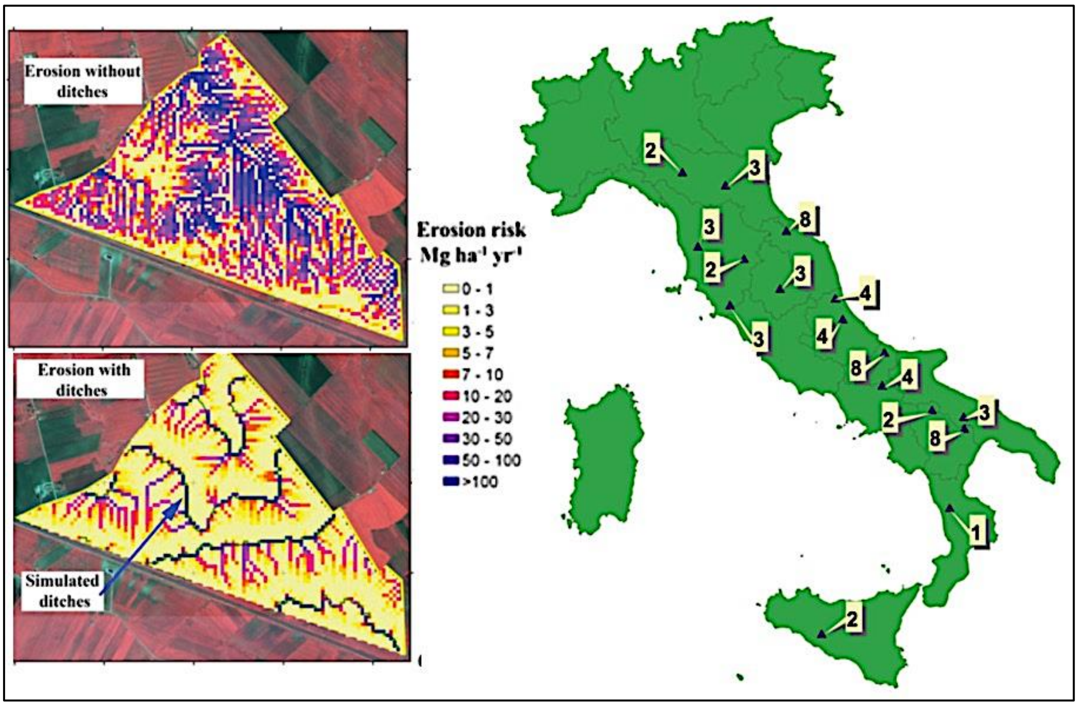


*Figure 37. On the left: comparison of the erosion risk in one of the sampled areas of the 2009 CAP measures control, obtained through the RUSLE model by simulating the absence or presence of drainage ditches at a distance of 80 m from each other. On the right: location of the 60 trial areas. The numbers indicate how many study areas are present at the sites identified by the triangles (From Bazzoffi et al., 2011).*

Results from this study point out a decrease of overall average soil erosion from the simulations without (33.0 Mg $ha^{-1}$ $yr^{-1}$) or with the temporary ditches (10.3 Mg $ha^{-1}$ $yr^{-1}$), with a significative mean decrease of 67.6%.

*Terraces*

Inside the RUSLE-based models RUSLE-IC-SDR, RUSLE+USPED and WaTEM/SEDEM terraces are not considered, except of as possible change in factor C and/or P. These elements can be considered as they own only if terraces are hydrologically isolated, and potentially if the flow pathways between terraces can be described in DEM/LS factor, and there is no partial reduction of connectivity in the flow pathways. If the geographic detail used does not allow to represent a single terrace as distinct parcel/land unit, an implicit approach could be used by considering the whole “terraced area” by modifying the slope average values, but in this last case an overestimation of erosion and sediment transport could occur. In most of the cases, there is however a lack of data on the effects on water flux and sediment transport depending on terraces morphometry and degree of conservation.

**From Literature**: Some studies on how to model soil erosion with RUSLE were applied in terraced areas of Italy (mostly vineyards and/or olive groves), with different slope and degree of terraces, the most significant of which (Bazzoffi and Gardin, 2011) was carried out to evaluate the effectiveness of the GAEC standard “retain terraces”. The study clearly shows that the degradation process of a terrace is something very complex and highly variable, depending on several factors. To simulate this process some assumptions were made in order to make possible to apply the calculation under GIS, as follows: i) the local slope length increases along the slope due to the increasing interconnection of contiguous terraces, according to increasing percentages of degradation (progressive obliteration of the isolating effect, with respect to runoff, exerted by stone walls); ii) degradation increases the gradient of terraces, due to soil erosion and landslides, which draw back the slope to its natural morphology; iii) the maximum degree of degradation (100%) corresponds to the total obliteration of one every two terraces.

This project has received funding from the European Union’s Horizon 2020 research and innovation programme under grant agreement N° 862695

A sample of results from this study (Costaviola – Calabria pilot area) is shown in the following Table 31. The range of soil erosion values predicted from conserved to removed terraces, assuming different LS values, in the two oriented - across or along the slope – case studies, could be very large from 7.8 - 136 (Mg ha$^{-1}$ yr$^{-1}$) and 10.4 - 171 (Mg ha$^{-1}$ yr$^{-1}$), respectively.

*Table 31. Scenario analysis of soil erosion (Mg ha$^{-1}$ yr$^{-1}$) in the study areas, Costaviola. Erosion risk values above the limit considered as "tolerable" (11.2 Mg ha$^{-1}$ yr$^{-1}$) are shown in italics (From Bazzoffi & Gardin, 2011).*

| Study area | Soil use | Mean slope (%) | Mean R | C | Mean soil erosion riskweighed over polygon area | | | | |
|---|---|---|---|---|---|---|---|---|---|
| | | | | | Conserved | Partially damaged | Very damaged | Partially removed | Removed |
| Costaviola# | | | | | | | | | |
| | Deciduous forest | 82.1 | 5058 | 0.003 | 0.1 | 0.2 | 0.5 | 1.2 | 3.7 |
| | Abandoned, natural veg. in evolution | 71.8 | 4745 | 0.020 | 0.6 | 1.0 | 2.9 | 6.0 | *18.7* |
| | Area with sparse vegetation | 87.8 | 4247 | 0.020 | 0.5 | 1.0 | 3.3 | 7.2 | *22.9* |
| | Arable land | 19.6 | 5083 | 0.250 | 8.8 | 11.1 | *17.7* | 27.8 | *65.7* |
| | Vineyard oriented across the slope | 54.8 | 5164 | 0.250 | 7.8 | 11.0 | *27.9* | 49.5 | *136* |
| | Vineyard oriented along the slope | 38.3 | 5398 | 0.200 | 10.4 | *14.8* | *28.9* | 56.5 | *171* |
| | Olive grove (no geometric pattern) | 45.7 | 5079 | 0.100 | 3.9 | 5.3 | *12.1* | 22.6 | *65.4* |
| | Arable land with vineyard | 41.8 | 5187 | 0.200 | 10.4 | *12.2* | *18.0* | 24.6 | *49.9* |
| | Set aside | 63.8 | 4695 | 0.020 | 0.6 | 1.0 | 2.8 | 5.6 | *17.4* |
| | Arable land with olive grove and vineyard | 41.8 | 5129 | 0.150 | 6.1 | 8.5 | *17.5* | 31.9 | *90.1* |

### *Ponds*

Inside the RUSLE-IC-SDR model case study ponds were not considered, so it's not possible to give any strategy to adequately parametrize them. Inside the RUSLE+USPED model a modification of original DEM as flat area for ponds was introduced, considering this element like a topographic sink in the process of creation of new DEM (paragraph 3.4.2).

In WaTEM/SEDEM, ponds are included in the model as if they were dams. The model sets the C-factor for every dam pixel to 0, assuming that no erosion takes place inside the dams. To include the ponds into the model, a dam map (a raster with information about the flow direction of the modelled element) as model input is included, locating the ponds. The use of dams, then, alters the routing in a similar way as ditches, and the sediment and water will follow the course of a dam instead of the steepest slope on dam locations. As the model does not distinguish between pond and sediment dams, this can be perceived as a knowledge gap in considering the ponds as a sediment trapping system, and could be considered as a methodological source of uncertainty.

### *Land Levelling*

In Italy and other countries of southern Europe (Spain, Portugal, Greece), in hilly areas, the plantation of new specialized crops (mainly orchards and vineyards) is almost always preceded by levelling of hill slopes. The purpose of these operations, which agronomists consider essential, is to achieve economic optimization: with large areas and regular slopes, the execution times of agricultural operations are reduced, and the performance of machinery is improved. The extension of levelled areas has made the morphological discontinuity of hill slopes more evident; the presence of wide uniform inclined plains on hill slopes is common to see in Italian hilly areas, in contrast with the surrounding natural morphology, which have given rise to a radical change in the landscape.

Consequently, these landscape deep modifications can lead also to a worsening of the physical and hydrological characteristics of soils, sometimes up to high depths. Land unit affected by land Levelling could be subjected to an increase of soil erosion (Bazzoffi and Tesi, 2011) due to an acceleration of water erosion, and it is easy to observe incisions on the reshaped surfaces, with an increase in rills, tunnel erosion and gullies.

Indeed, new parametrizations are to be made for this land units/parcels, by two steps, both for RUSLE and WaTEM/SEDEM modelling: i) modify DEM elevation values with the new ones (if possible, with a ground survey with GPS precision tools), and consequently new calculations for slope and LS factors; ii) introducing different values for K factor. In WaTEM/SEDEM it is necessary to modify also the Ktc and the PC and PTEF factors adequately. In case of application of physically based models, it could be necessary to measure or estimate new soil physical and hydrological parameters, as hydraulic surface roughness, soil infiltrability, permeability, and soil cohesion.

## 4.2 Physically based models

For physically based model assessment, uncertainties and sensitivity were performed only inside the Italian case study at field level. For the application, calibration, and parametrization of the WEPP model, please refer to the detailed analysis provided in the section 3.5.
In these models, generally applied at small catchment or mostly at field/plot very detailed scales, many more detailed parameters about soil physical, hydrological, geotechnical, climatic and hydraulic behavior are requested. Some suggestions about strategies to modify connectivity/disconnectivity effects of some elements that are not considered in these models - like fascine, shrub hedges, silt fences, wheel tracks (epistemic lacks) - or their arrangement along the slope and inside the different land use parcels - distributed in such a way to be not possible to consider them explicitly – are given to consider them implicitly (lumped) through proxies related to the induced changes, documented with a quick overview as summarized in the following Table 32. Using these proxies by setting values as percentage of area affected inside the land use parcels could allow to modify requested input parametrization in such a way to increase connectivity effects inside the water flow and sediment transport.

*Table 32. Overview of the connectivity elements list considered inside physically based models. Sensitivity was not determined (for WEPP model see the Italian case study at field/plot scale). Y = provided (explicit); P = indirect (lumped, by other proxies); N = not provided.*

| MODEL | | | | | | | Proxies and uncertainty source type |
|---|---|---|---|---|---|---|---|
| **Physically-Based Model** | **WEPP** | **OPEN LISEM** | **IBER** | **EROSION 3D** | **SHETRAN** | **MHYDAS-erosion** | |
| ***Connectivity features*** | | | | | | | *(T = Technical; M = Methodological)* |
| **Roughness** | P | P | P | P | P | P | Hydraulic roughness (friction) (T/M) |
| **Fascine** | P | P | P | P | P | P | Hydraulic roughness (friction) (T/M) |
| **Grass strip** | Y | Y | P | P | P | Y | Soil infiltrability, soil cohesion (T/M) |
| **Grass hedges** | P | P | P | P | P | Y | Hydraulic roughness, soil cohesion – setting correlated values (T/M) |
| **Grassed waterways** | P | P | P | P | P | P | Hydraulic roughness, soil infiltrability, soil cohesion (T/M) |
| **Shrub hedges** | P | P | P | P | P | Y | Hydraulic roughness, soil infiltrability (T/M) |
| **Silt fences** | Y | P | P | P | P | P | Hydraulic roughness (T/M) |
| **Wheel tracks** | P | Y | P | P | P | P | Hydraulic roughness, soil infiltrability, soil cohesion (T/M) |
| **Tillage direction** | P | N | N | N | N | N | Hydraulic roughness, soil infiltrability, soil cohesion (T/M) |

This project has received funding from the European Union's Horizon 2020 research and innovation programme under grant agreement N° 862695

| | | | | | | | |
|---|---|---|---|---|---|---|---|
| **Roads** | P | P | P | P | P | P | Hydraulic roughness, soil infiltrability (T/M) |
| **Ditches** | P | P | P | P | P | P | Topography, hydraulic roughness, soil infiltrability (T/M) |
| **Sewer system** | Y | N | N | N | N | N | Soil infiltrability (T/M) |
| **Watercourses** | | | | | | | Topography, hydraulic roughness, soil infiltrability (T/M) |
| **Terraces** | P | P | P | P | P | P | Topography modified slope values by DEM editing (T/M) |
| **Temporary ditches** | N | N | N | N | N | N | Topography, hydraulic roughness, soil infiltrability and/or modified slope values by DEM editing (T/M) |
| **Ponds** | P | P | P | P | P | P | Topography, hydraulic roughness, soil infiltrability, and/or modified values by DEM and hydraulic fluxes editing (T/M) |

# 5. Conclusions

Uncertainty analysis in soil erosion modelling is crucial to decide whether the predicted soil erosion and deposition map is reliable to be used for agricultural production systems or decision making. It also involves acknowledging the limitations of the models, making it a vital step towards model interpretability.

Technical and methodological uncertainties could arise from different sources, essentially linked to different scale details and different data sources for input models parameters and settings, as discussed in section 4.

This report highlights several sources of epistemological uncertainty, primarily due to a general lack of knowledge about specific processes involved in sediment transport by soil erosion. This knowledge gap is largely attributed to the scarcity of experimental research with field tests.

Looking at the presented case studies, however, other types of uncertainties emerged. Specifically, it is important to consider aleatoric uncertainty, which refers to the errors arising from different and sometimes unknown sources linked to the measurements used to calibrate and validate model predictions. Is it possible to estimate errors due to the use of independent datasets of soil erosion measures? Which methodologies are applied to these measurements, and at what scale? These are not easy questions to address, especially if we consider plot, catchment or large watershed scales. At the watershed scale it is not possible to repeat the same soil sediment measurement several times to estimate errors, due to the limitations of the measuring techniques used at the watershed outlet.

Furthermore, the last uncertainty is related to the statistical methodologies used to assess the uncertainty itself. Many methods are currently available to obtain confidence intervals of the prediction, but they are not always readily comparable. These methods include Bayesian analysis, other Likelihood approaches, Morris's Elementary Elements Screening, Monte-Carlo simulations, Quantile regression methods, among others.

Future studies are needed to advance, not only in acquiring new knowledge through additional case studies on soil erosion and sediment connectivity, but also in attempting to converge on a comparative work aiming at minimizing uncertainties and making them more comparable through some technical agreements regarding model parametrization.

This project has received funding from the European Union's Horizon 2020 research and innovation programme under grant agreement N° 862695

# References


Äijö, H., Nurminen, J., Myllys, M., Sikkilä, M., Salo, H., Paasonen-Kivekäs, M., Turunen, M., Koivusalo, H., Alakukku, L., Puustinen, M., 2018. Toimivat salaojitusmenetelmät kasvintuotannossa. (Feasible subsurface drainage methods in crop production), The Field Drainage Research Association, Helsinki (2018).

Alba, S., Borselli, L., Torri, D., Pellegrini, S., Bazzoffi, P., 2006. Assessment of tillage erosion by mouldboard plough in Tuscany (Italy). Soil Till Res. 85(1), 123–142. https://doi.org/https://doi.org/10.1016/j.still.2004.12.002

Albaradeyia, I., Hani, A., Shahrour, I., 2011. WEPP and ANN models for simulating soil loss and runoff in a semi-arid Mediterranean region. Environ. Monit. Assess. 180 (1- 4), 537–556.

Alewell, C., Borrelli, P., Meusburger, K., Panagos, P., 2019. Using the USLE: Chances, challenges and limitations of soil erosion modelling. International Soil and Water Conservation Research 7, 203–225. https://doi.org/10.1016/j.iswcr.2019.05.004

Amore, E., Modica, C., Nearing, M.A., Santoro V.C., 2004. Scale effect in USLE and WEPP application for soil erosion computation from three Sicilian basins. J. Hydrol. 293 (1–4), 100–114.

Aneseyee, A.B., Elias, E., Soromessa, T., Feyisa, G.L., 2020. Land use/land cover change effect on soil erosion and sediment delivery in the Winike watershed, Omo Gibe Basin, Ethiopia. Sci. Total Environ. 728, 138776. https://doi.org/10.1016/j.scitotenv.2020.138776

Arnoldus, H.M.J. 1977. Methodology used to determine the maximum potential average annual soil loss due to sheet and rill erosion in Morocco. FAO Soils Bull. 34, 39-51.

Arnoldus, H.M.J., 1980. An approximation of the rainfall factor in the Universal Soil Loss Equation. In: De Boodt M. & Gabriels D. (eds), Assessment of Erosion, John Wiley & Sons, Chichester, pp. 127-132.

Batista, P.V.G., Davies, J., Silva, M.L.N., Quinton, J.N., 2019. On the evaluation of soil erosion models: Are we doing enough? Earth-Sci. Rev. 197, 102898. https://doi.org/10.1016/j.earscirev.2019.102898

Batista, P., Fiener, P., Scheper, S., Alewell, C., 2021. A conceptual model-based sediment connectivity assessment for patchy agricultural catchments (preprint). Catchment hydrology/Modelling approaches. https://doi.org/10.5194/hess-2021-231

Baudrit, C., Dubois, D., 2006. Practical representations of incomplete probabilistic knowledge. Comput. Stat. Data Anal. 51, 86–108. https://doi.org/10.1016/j.csda.2006.02.009.

Bazzoffi P., 1994. The enhanced Fagna-type hydrological unit for measurement and sampling of runoff waters. International Workshop on Soil Erosion in Semi-Arid Mediterranean Areas. ESSC-CSEI, Taormina 28-30th Oct. 1993. CNR (ed.). pp.195-204.

Bazzoffi P., 2007. Erosione del suolo e sviluppo rurale. Fondamenti e manualistica per la valutazione agroambientale. Edagricole, Bologna, Italy.

Bazzoffi, P., Gardin, L., 2011. Effectiveness of the GAEC standard of cross compliance retain terraces on soil erosion control. Ital. J. Agron. 6(s1), e6. https://doi.org/10.4081/ija.2011.6.s1.e6

Bazzoffi, P., Pellegrini, S., 1992a. Erosione sui versanti e sedimentazione in un serbatoio artificiale della Valdera. Validazione della procedura E.A.R.M. per la previsione della distribuzione spaziale dei sedimenti. Costruzioni Idrauliche, IDROTECNICA, Vol.4, 1992, 217-228.

Bazzoffi, P., Pellegrini, S., 1992b. Caratteristiche delle piogge influenti sui processi erosivi nel periodo 1964-1990 in un ambiente della valle dell'Era (Toscana). Evoluzione climatica e modelli previsionali. Annali Istituto Sperimentale per lo Studio e la Difesa del Suolo, Vol. XX, 161-182.

Bazzoffi, P., Tesi, P.C., 2011. Effectiveness of the GAEC standard of cross compliance Prohibition of performing unauthorized land levelling on soil erosion control. Ital. J. Agron. 6(s1), e4. https://doi.org/10.4081/ija.2011.6.s1.e4

Bazzoffi, P., Ciancaglini, A., Laruccia, N., 2011. Effectiveness of the GAEC cross-compliance standard Short-term measures for runoff water control on sloping land (temporary ditches and grass strips) in controlling soil erosion. Ital. J. Agron. 6(s1), e3. https://doi.org/10.4081/ija.2011.6.s1.e3

Beck, M.B., 1987. Water quality modeling: A review of the analysis of uncertainty, Water Resour. Manag. 23, 1393-1442.

Behera, M., Sena, D.R., Mandal, U., Kashyap, P.S., Dash, S.S., 2020. Integrated GIS-based RUSLE approach for quantification of potential soil erosion under future climate change scenarios. Environ. Monit. Assess. 192, 733.

Bengtsson, R.L., Carter, C.E., Morris, H.F., Bartkiewicz, S.A., 1988. The Influence of Subsurface Drainage Practices on Nitrogen and Phosphorus Losses in a Warm, Humid Climate. Trans. ASAE 31, 0729–0733. https://doi.org/10.13031/2013.30775

Bengtsson, R.L., Carter, C.E., Morris, H.F., Kowalczuk, J.G., 1984. Reducing Water Pollution with Subsurface Drainage. Trans. ASAE 27, 0080–0083. https://doi.org/10.13031/2013.32739

Bengtsson, R.L., Sabbagh, G., 1990. USLE P factors for subsurface drainage on low slopes in a hot, humid climate. J Soil Water Conserv 45, 480–482.

Bengtsson, L., Seuna, P., Lepistö, A., Saxena, R. K., 1992. Particle movement of melt water in a subdrained agricultural basin. J. Hydrol. 135(1), 383–398. https://doi.org/https://doi.org/10.1016/0022-1694(92)90097-F

Beven, K., Binley A., 1992. The future of distributed models: model calibration and uncertainty prediction, Hydrol. Process 6, 279-298.

Bhuyan, S.J., Kalita, P.K., Janssen, K.A., Barnesa, P.L., 2002. Soil loss predictions with three erosion simulation models. Environ. Model. Software 17 (2), 135-144.

Borrelli, P., Alewell, C., Alvarez, P., Anache, J.A.A., Baartman, J., Ballabio, C., Bezak, N., Biddoccu, M., Cerdà, A., Chalise, D., Chen, S., Chen, W., De Girolamo, A.M., Gessesse, G.D., Deumlich, D., Diodato, N., Efthimiou, N., Erpul, G., Fiener, P., Freppaz, M., Gentile, F., Gericke, A., Haregeweyn, N., Hu, B., Jeanneau, A., Kaffas, K., Kiani-Harchegani, M., Villuendas, I.L., Li, C., Lombardo, L., López-Vicente, M., Lucas-Borja, M.E., Märker, M., Matthews, F., Miao, C., Mikoš, M., Modugno, S., Möller, M., Naipal, V., Nearing, M., Owusu, S., Panday, D., Patault, E., Patriche, C.V., Poggio, L., Portes, R., Quijano, L., Rahdari, M.R., Renima, M., Ricci, G.F., Rodrigo-Comino, J., Saia, S., Samani, A.N., Schillaci, C., Syrris, V., Kim, H.S., Spinola, D.N., Oliveira, P.T., Teng, H., Thapa, R., Vantas, K., Vieira, D., Yang, J.E., Yin, S., Zema, D.A., Zhao, G., Panagos, P., 2021. Soil erosion modelling: A global review and statistical analysis. Sci. Total Environ. 780, 146494. https://doi.org/10.1016/j.scitotenv.2021.146494

Borrelli, P., Van Oost, K., Meusburger, K., Alewell, C., Lugato, E., Panagos, P., 2018. A step towards a holistic assessment of soil degradation in Europe: Coupling on-site erosion with sediment transfer and carbon fluxes. Environ. Res. 161, 291-298. ISSN 0013-9351. https://doi.org/10.1016/j.envres.2017.11.009.

Borselli, L., Cassi, P., Torri, D., 2008. Prolegomena to sediment and flow connectivity in the landscape: A GIS and field numerical assessment. Catena 75, 268–277. https://doi.org/10.1016/j.catena.2008.07.006

Bottcher, A.B., Monke, E.J., Huggins, L.F., 1981. Nutrient and Sediment Loadings from a Subsurface Drainage System. J. ASABE 24, 1221–1226. https://doi.org/10.13031/2013.34423

Bracken, L.J., Turnbull, L., Wainwright, J., Bogaart, P., 2015. Sediment connectivity: a framework for understanding sediment transfer at multiple scales. Earth Surf. Process Landf. 40, 177–188. https://doi.org/10.1002/esp.3635

Brazier, R.E., Beven, K.J., Freer, J., Rowan, J.S., 2000. Equifinality and uncertainty in physically based soil erosion models: Application of the glue methodology to WEPP-the water erosion prediction project-for sites in the UK and USA. Earth Surf. Process Landf., 10.1002/1096-9837

Brunner, A.C., Park, S.J., Ruecker, G.R., Dikau, R., Vlek, P.L.G., 2004. Catenary soil development influencing erosion susceptibility along a hillslope in Uganda. Catena 58(1), 1e22. https://doi.org/10.1016/j.catena.2004.02.001

Cantreul, V., Bielders, C., Calsamiglia, A., Degré, A., 2017. How pixel size affects a sediment connectivity index in central Belgium. Earth Surf. Process Landf. 43, 884–893. https://doi.org/10.1002/esp.4295

Chaves, H.M.L., Nearing, M.A., 1991. Uncertainty analysis of the WEPP soil erosion model. Trans. ASAE 34(6): 2437-2444.

Chung, S.W., Gassman, P.W., Kramer, L.A., Williams, J.R., Gu, R., 1999. Validation of EPIC for two watersheds in Southwest Iowa, J. Environ. Qual. 28, 971–979.

Cochrane, T.A., Flanagan, D.C., 2005. Effect of DEM resolutions in the runoff and soil loss predictions of the WEPP watershed model, Trans. ASAE 48, 109-120.

Conrad, O., 2003. SAGA-GIS module library documentation (v2.2.0). System of Automated Geoscientific Analyses (SAGA). Available online: http://www.saga-gis.org/saga_tool_doc/2.2.0/ta_hydrology_22.html

Conrad, O., Bechtel, B., Bock, M., Dietrich, H., Fischer, E., Gerlitz, L., Wehberg, J., Wichmann, V., Böhner, J., 2015. System for Automated Geoscientific Analyses (SAGA) v. 2.1.4, Geosci. Model Dev., 8, 1991-2007, doi:10.5194/gmd-8-1991-2015.

Delogu, F., Lulli, L., 1982. Nota pedologica su cinque piccoli bacini sperimentali della Valdera (Pisa). Annali Istituto Sperimentale per lo Studio e la Difesa del Suolo. Firenze, pp. 141-145.

Deproost, P., Renders, D., Van de Wauw, J., Van Ransbeeck, N., Verstraeten, G., 2018a. Herkalibratie van WaTEM/SEDEM met het DHMV-II als hoogtemodel: eindrapport. Brussel.

Deproost, P., Renders, D., Van de Wauw, J., Van Ransbeeck, N., Verstraeten, G., 2018b. Addendum: Herkalibratie van WaTEM/SEDEM met het DHMV-II als hoogtemodel: eindrapport. Brussel.

Desmet, P.J.J., Govers, G., 1995. GIS-based simulation of erosion and deposition patterns in an agricultural landscape: a comparison of model results with soil map information. Catena 25(1–4), 389-401, ISSN 0341-8162. https://doi.org/10.1016/0341-8162(95)00019-O.

Desmet, P.J.J., Govers, G., 1996. A GIS procedure for automatically calculating the USLE LS factor on topographically complex landscape units. J Soil Water Conserv 51, 427–433.

De Vente, J., Poesen, J., 2005. Predicting soil erosion and sediment yield at the basin scale: scale issues and semi-quantitative models. Earth- Sci. Rev. 71, 95–125. https://doi.org/10.1016/j.earscirev.2005.02.002.

De Vente, J., Poesen, J., Bazzoffi, P., Van Rompaey, A., Verstraeten, G., 2006. Predicting catchment sediment yield in Mediterranean environments: the importance of sediment sources and connectivity in Italian drainage basins. Earth Surf. Process. Landf. 31, 1017–1034. DOI: 10.1002/esp.1305.

Finnish Environment Institute (SYKE), 2019. Sediment and nutrient loading to surface waters in 3 different scales. https://metasiirto.ymparisto.fi:8443/geoportal/catalog/search/resource/details.page?uuid=%7B1589 3DD0-0193-40AD-9E21-452D271DB791%7D (accessed 1.25.21).

Flanagan, D.C., Livingston, S.J. (Eds.), 1995. USDA Water Erosion Prediction Project: User Summary, National Soil Erosion Research Laboratory (NSERL) Report No. 11. West Lafayette, Indiana: USDA Agricultural Research Service NSERL.

Flanagan DC, Renschler CS, Cochrane TA (2000). Application of the WEPP model with digital topographic information, In: Parks BO, Clarke KM, Crane MP, eds. Proceedings of the 4th International Conference on Integrating Geographic Information Systems and Environmental Modeling: Problems, Prospectus, and Needs for Research, Banff, September,2000.

Flanagan, D.C., Ascough II, J.C., Nearing, M.A., Laflen, J.M., 2001. The Water Erosion Prediction Project (WEPP) Model. In: Harmon, R.S.; Doe, W.W. (2001). Landscape Erosion and Evolution Modeling || The Water Erosion Prediction Project (WEPP) Model. (Chapter 7), 145–199. doi:10.1007/978-1-4615-0575-4_7

Flanagan, D.C., Frankenberger, J.R., Ascough II, J.C., 2012. WEPP: model use, calibration and validation. Trans. ASABE 55, 1463–1477.

Foerster, S., Wilczok, C., Brosinsky, A., Segl, K., 2014. Assessment of sediment connectivity from vegetation cover and topography using remotely sensed data in a dryland catchment in the Spanish Pyrenees. J Soils Sediments 14, 1982–2000. https://doi.org/10.1007/s11368-014-0992-3

Formanek, G.E., Ross, E., Istok, J., 1987. Subsurface drainage for erosion reduction on croplands in northwestern Oregon. In: Irrigation Systems for the 21st Century. Proceedings of the Irrigation and Drainage Division Special Conference. American Society of Civil Engineers, New York, New York, pp. 25–31.

Foster, G. R., McCool, D. K., Renard, K. G., & Moldenhauer W. C. (1981). Conversion of the universal soil loss equation to SI metric units. Journal of Soil and Water Conservation, 36(6), 355–359

Foster, I.D.L., Chapman, A.S., Hodgkinson, R.M., Jones, A.R., Lees, J.A., Turner, S.E., Scott, M., 2003. Changing suspended sediment and particulate phosphorus loads and pathways in underdrained lowland agricultural catchments; Herefordshire and Worcestershire, U.K. The Interactions between Sediments and Water 119–126. https://doi.org/10.1007/978-94-017-3366-3_17

Gashaw, T., Bantider, A., Zeleke, G., Alamirew, T., Jemberu, W., Worqlul, A.W., Dile, Y.T., Bewket, W., Meshesha, D.T., Adem, A.A., Addisu, S., 2021. Evaluating InVEST model for estimating soil loss and sediment export in data scarce regions of the Abbay (Upper Blue Nile) Basin: Implications for land managers. Environ. Chall. 5, 100381. https://doi.org/10.1016/j.envc.2021.100381

Gay, A., Cerdan, O., Mardhel, V., Desmet, M., 2016. Application of an index of sediment connectivity in a lowland area. J Soils Sediments 16, 280–293. https://doi.org/10.1007/s11368-015-1235-y

Ghosal, K., Das Bhattacharya, S., 2020. A Review of RUSLE Model. J Indian Soc Remote Sens 48, 689–707. https://doi.org/10.1007/s12524-019-01097-0

Gobeyn, S., Renders, D., Callewaert, S., Deproost, P. (in preparation). Optimalisatie en actualisatie van de erosie- en sedimenttransportmodellering met het CN-WS model. Departement Omgeving, Brussel.

Gong, Y.W., Shen, Z.Y., Hong, Q., Liu, R.M., Liao, Q., 2011. Parameter uncertainty analysis in watershed total phosphorus modeling using the GLUE methodology. Agr. Ecosyst. Environ. 142, 246-255.

This project has received funding from the European Union's Horizon 2020 research and innovation programme under grant agreement N° 862695

Govers, G., Vandaele K., Desmet P., Poesen J. and Bunte K. (1994), The role of tillage in soil redistribution on hillslopes. European Journal of Soil Science, 45: 469-478. https://doi.org/10.1111/j.1365-2389.1994.tb00532.x

Govers, G., 2011. Misapplications and misconceptions of erosion models. In: Morgan, R.P.C., Nearing, M.A. (Eds.), Handbook of Erosion Modelling. Blackwell Publishing Ltd, Chichester.

Grazhdani, S., Jacquin, F., Sulçe, S., 1996. Effect of subsurface drainage on nutrient pollution of surface waters in south eastern Albania. Sci. Total Environ. 191, 15–21. https://doi.org/10.1016/0048-9697(96)05168-6

Gronsten, H.A., Lundekvam, H., 2006. Prediction of surface runoff and soil loss in southeastern Norway using the WEPP Hillslope Model. Soil Till. Res. 85 (1-2), 186–199.

Guinot, V., Gourbesville, P., 2003. Calibration of physically based models: back to basics? J Hydroinform 05.4, 233-244.

Hamel, P., Chaplin-Kramer, R., Sim, S., Mueller, C., 2015. A new approach to modeling the sediment retention service (InVEST 3.0): Case study of the Cape Fear catchment, North Carolina, USA. Sci. Total Environ. 524–525, 166–177. https://doi.org/10.1016/j.scitotenv.2015.04.027

Hamel, P., Falinski, K., Sharp, R., Auerbach, D.A., Sánchez-Canales, M., Dennedy-Frank, P.J., 2017. Sediment delivery modeling in practice: Comparing the effects of watershed characteristics and data resolution across hydroclimatic regions. Sci. Total Environ. 580, 1381–1388. https://doi.org/10.1016/j.scitotenv.2016.12.103

Heckmann, T., Cavalli, M., Cerdan, O., Foerster, S., Javaux, M., Lode, E., Smetanová, A., Vericat, D., Brardinoni, F., 2018. Indices of sediment connectivity: opportunities, challenges and limitations. Earth-Sci. Rev. 187, 77–108. https://doi.org/10.1016/j.earscirev.2018.08.004

Hrabalíková, M., Janeček, M., 2017. Comparison of different approaches to LS factor calculations based on a measured soil loss under simulated rainfall. Soil Water Res 12 (2017), 69–77. https://doi.org/10.17221/222/2015-SWR

Huang, C.H., Bradford, J.M., Laflen, J.M., 1996. Evaluation of the detachment transport coupling concept in the WEPP rill erosion equation. Soil Sci. Soc. Am. J. 60, 734-739.

Istok, J.D., Kling, G.F., 1983. Effect of subsurface drainage on runoff and sediment yield from an agricultural watershed in western Oregon, U.S.A. J. Hydrol. 65, 279–291. https://doi.org/10.1016/0022-1694(83)90082-3

Jamieson, P.D., Porter, J.R., Wilson, D.R., 1991. A test of the computer simulation model ARC-WHEAT1 on wheat crops grown in New Zealand. Field Crops Res. 27, 337-50.

Jarvis, N.J., Villholth, K.G., Ulén, B., 1999. Modelling particle mobilization and leaching in macroporous soil. Eur. J. Soil Sci. 50, 621–632. https://doi.org/10.1046/j.1365-2389.1999.00269.x

Johannsen, L., Schmaltz, E., Aust, G., 2022. Report on parameterisation of connectivity and mitigation strategies in the frequently-used soil erosion models. State-of-the-art: Connectivity in soil erosion modelling and policy, EJP SOIL SCALE project, report WP1-D1.

Joint Research Centre, 2024. Gridded Agro-Meteorological Data in Europe -AGRI4CAST. Food Security Unit of the Joint Research Center (JRC.D.5). https://agri4cast.jrc.ec.europa.eu/DataPortal/Index.aspx.

IUSS Working Group WRB, World reference base for soil resources 2014. Update 2015. International soil classification sys-tem for naming soils and creating legends for soil maps. In: World Soil Resources Report No. 106. Food and Ag-riculture Organization of the United Nations, Rome, 2015. Available online: URL https://www.fao.org/3/i3794en/I3794en.pdf (accessed 15/09/2023).

Kebede, Y.S., Endalamaw, N.T., Sinshaw, B.G., Atinkut, H.B., 2021. Modeling soil erosion using RUSLE and GIS at watershed level in the upper beles, Ethiopia. Environ. Chall. 2, 100009. https://doi.org/10.1016/j.envc.2020.100009

Kingston, D.G., Taylor, R.G., 2010. Sources of uncertainty in climate change impacts on river discharge and groundwater in a headwater catchment of the Upper Nile Basin, Uganda. Hydrol. Earth Syst. Sc. 14, 1297-1308.

Kinnell, P.I.A., 2010. Event soil loss, runoff and the Universal Soil Loss Equation family of models: A review. J. Hydrol. 385, 384–397. https://doi.org/10.1016/j.jhydrol.2010.01.024

Kukkonen, M., Niinioja, R., & Puustinen, M., 2004. Viljelykäytäntöjen vaikutus ravinnehuuhtoutumiin Liperin koekentällä Pohjois-Karjalassa.

Kwang, J.S., Parker, G., 2017. Landscape evolution models using the stream power incision model show unrealistic behavior when m / n equals 0.5. Earth Surf. Dyn. 5, 807-820. https://doi.org/10.5194/esurf-5-807-2017.

Laflen, J.M., Flanagan, D.C., Engel, B.A., 2004. Soil erosion and sediment yield prediction accuracy using WEPP. Am. Water Res. Assoc., 40, 289-297.
Legates, D.R., McCabe Jr., G.J., 1999. Evaluating the use of “goodness-of-fit” measures in hydrologic and hydroclimatic model validation, Water Resour. Res. 35, 1, 233-241.
Lilja, H., Hyväluoma, J., Puustinen, M., Uusi-Kämppä, J., Turtola, E., 2017a. Evaluation of RUSLE2015 erosion model for boreal conditions. Geoderma Reg. 10, 77–84. https://doi.org/10.1016/j.geodrs.2017.05.003
Lilja, H., Puustinen, M., Turtola, E., Hyväluoma, J., 2017b. Suomen peltojen karttapohjainen eroosioluokitus (Map-based classificication of erosion in agricultural lands of Finland. Natural Resources Institute Finland (Luke) 36.
Lindenschmidt, K.E., Fleischbein, K., Baborowski, M., 2007. Structural uncertainty in a river water quality modelling system. Ecol. model. 204, 289-300.
Lindsay, J., 2019. FillDepression algorithm of Whitebox geospatial analysis tools. WhiteboxTools User Manual. Htpps//www.whiteboxgeo.com/manual/wbt_book/
Lo, A., El-Swaify, S.A., Dangler, E.W. Shinsiro, L., 1985. Effectiveness of EI 30 as an Erosivity Index in Hawaii. Soil Erosion and Conservation. In: El-Swaify, S.A., Moldenhauer, W.C., Lo, A. (Eds.), Soil Erosion and Conservation, Soil Conservation Society of America, Ankeny, 384-392.
Loosvelt, L., 2014. Assessment of uncertainty in land surface characterization and implications for spatially distributed hydrological mod.pdf. Ghent University, Gent, Belgium.
Lu, H., Moran, C., Prosser, I.P., 2006. Modelling sediment delivery ratio over the Murray Darling Basin. Environ. Model. Softw. 21, 1297–1308.
Lulli, L., Ronchetti, G., 1973. Prime osservazioni sulla crepacciatura dei suoli delle argille plioceniche marine della valle dell'Era (Pisa). Annali Istituto Sperimentale per lo Studio e la Difesa del Suolo. Firenze, pp. 143-149.
Martini, L., Cavalli, M., Picco, L., 2022. Predicting sediment connectivity in a mountain basin: A quantitative analysis of the index of connectivity. Earth Surf. Process Landf. 47, 1500–1513. https://doi.org/10.1002/esp.5331
Mathier, L., Roy, A.G., Paré, J.P., 1989. The effect of slope gradient and length on the parameters of a sediment transport equation for sheetwash. Catena 16, 545-558. https://doi.org/10.1016/0341-8162(89)90041-6
Mbagwu, J.S.C., Bazzoffi, P., 1987. Estimating the consistency limits, moisture retention and availability of some Italian soils from physical properties. Annali Istituto Sperimentale per lo Studio e la Difesa del Suolo. Firenze, pp. 111-120.
Merritt, W.S., Letcher, R.A., Jakeman, A.J., 2003. A review of erosion and sediment transport models. Environ. Model. Software 18(8), 761–799. https://doi.org/https://doi.org/10.1016/S1364-8152(03)00078-1
Meusburger, K., Konz, N., Schaub, M., Alewell, C., 2010. Soil erosion modelled with USLE and PESERA using QuickBird derived vegetation parameters in an alpine catchment. Int. J. Appl. Earth Obs. Geoinf. 12, 208–215. https://doi.org/10.1016/j.jag.2010.02.004
Miller, S.A., Landisn, A.E., 2006. The Use of Monte Carlo analysis to characterize nitrogen fluxes in agroecosystems, Environ. Sci. Technol. 40, 2324-2332.
Mitas, L., Mitasova, H., 1998 Distributed soil erosion simulation for effective erosion prevention. Water Resour. Res. 34(3): 505-516.
Mitasova H., Hofierka J., Zlocha M., Iverson, L. R., 1996. Modelling topographic potential for erosion and deposition using GIS. Int. J. Geogr. Inf. Syst. 10(5), 629–641. https://doi.org/10.1080/02693799608902101
Moore, I.D., Burch, G.J., 1986. Physical Basis of the Length-slope Factor in the Universal Soil Loss Equation. Soil Sci. Soc. Am. J. 50, 1294-1298. https://doi.org/10.2136/sssaj1986.03615995005000050042x
Moore, I.D., Wilson, J.P., 1992. Length-slope factors for the Revised Universal Soil Loss Equation: Simplified method of estimation. J Soil Water Conserv 47 (5) 423-428.
Morgan, R.P.C., Nearing, M.A., 2011. Handbook of erosion modelling, Handbook of Erosion Modelling. https://doi.org/10.1002/9781444328455.
Moriasi, D.N., Arnold, J.G., Van Liew, M.W., Bingner, R.L., Harmel, R.D., Veith, T.L., 2007. Model evaluation guidelines for systematic quantification of accuracy in watershed simulations. Trans. ASABE 50(3):885–900. https://doi.org/10.13031/2013.23153
Najafi, S., Dragovich, D., Heckmann, T., Sadeghi, S.H., 2021. Sediment connectivity concepts and approaches. Catena 196, 104880. https://doi.org/10.1016/j.catena.2020.104880

This project has received funding from the European Union’s Horizon 2020 research and innovation programme under grant agreement N° 862695

Nandakumar, N., Mein, R.G., 1997. Uncertainty in rainfall-runoff model simulations and the implications for predicting the hydrologic effects of land-use change, J Hydrol. 192, 211-232.

Nash, J.E., Sutcliffe, J.V., 1970. River flow forecasting through conceptual models – Part 1 – A discussion of principles, J. Hydrol. 10, 282-290, doi:10.1016/0022-1694(70)90255-6

National Land Survey of Finland, 2020. Elevation model 2 m. https://www.maanmittauslaitos.fi/en/maps-and-spatial-data/expert-users/product-descriptions/elevation-model-2-m [Dataset] (accessed 5.29.20).

Nearing, M.A., 2013. Soil erosion and conservation, in: Environmental Modelling: Finding Simplicity in Complexity: Second Edition. pp. 365–378. https://doi.org/10.1002/9781118351475.ch22.

NLS, 2017. Kansallisen maastotietokannan laatumalli – Korkeusmallit (Quality model of the National Topographic Database – Digital Elevation Models National Land Survey of Finland (NLS). https://www.maanmittauslaitos.fi/sites/maanmittauslaitos.fi/files/attachments/2017/05/KMTK_korkeusmallit_laatukasikirja_2017-01-02.pdf (accessed 9.23.22).

Nopens, I., Torfs, E., Cierkens, K., 2010. Modelleren en simuleren van biosystemen. Cursus 3de Bachelor Bio-ingenieur. Met assistentie van Elena Torfs. Universiteit Gent.

NRCS (2009). Part 630 Hydrology National Engineering Handbook, Chapter 7: Hydrologic Soil Groups.

Nunes, J.P., Wainwright, J., Bielders, C.L., Darboux, F., Fiener, P., Finger, D., Turnbull, L., 2018. Better models are more effectively connected models. Earth Surf. Process. Landf. 43: 1355–1360. doi: 10.1002/esp.4323.

Oksanen, J., 2013. Can binning be the key to understanding the uncertainty of DEMs. Proceedings of the GISRUK 2013 3–5.

Onsamrarn, W., Chittamart, N., Tawornpruek, S., 2020. Performances of the WEPP and WaNuLCAS models on soil erosion simulation in a tropical hillslope, Thailand. PLoS ONE 15(11), e0241689. https://doi.org/10.1371/journal. pone.0241689

Oropeza-Mota, J.L., Larose, M., Norton, L.D., 2004. Testing the applicability of the WEPP model for predicting soil loss in tropical hillside lands in the Tuxtlas, Veracruz, Mexico. ASACSSA-SSSA Proceedings, Seattle, WA.

Ortíz-Rodríguez, A.J., Borselli, L., Sarocchi, D., 2017. Flow connectivity in active volcanic areas: Use of index of connectivity in the assessment of lateral flow contribution to main streams. Catena 157, 90–111. https://doi.org/10.1016/j.catena.2017.05.009

Othman, A.A., Ali, S.S., Salar, S.G., Obaid, A.K., Al-Kakey, O., Liesenberg, V., 2023. Insights for Estimating and Predicting Reservoir Sedimentation Using the RUSLE-SDR Approach: A Case of Darbandikhan Lake Basin, Iraq–Iran. Remote Sens. 15, 697. https://doi.org/10.3390/rs15030697

Othman, A.A., Obaid, A.K., Al-Manmi, D.A.M.A., Al-Maamar, A.F., Hasan, S.E., Liesenberg, V., Shihab, A.T., Al-Saady, Y.I., 2021. New Insight on Soil Loss Estimation in the Northwestern Region of the Zagros Fold and Thrust Belt. ISPRS Int. J. Geo-Inf. 10, 59.

Ouyang, D., Bartholic, J. 1997. Predicting Sediment Delivery Ratio in Saginaw Bay Watershed. Proceedings of the 22nd National Association of Environmental Professionals Conference Orlando, Orlando, FL, USA, 19–23 May 1997.

Ozsoy, G., Aksoy, E., 2015. Prediction of soil loss differences and sediment accumulation at the Nilufer creek watershed, Turkey, using multiyear satellite data in a GIS. Geocarto Int. 30, 843–857.

Ozsoy, G., Aksoy, E., Dirim, M.S., Tumsavas, Z., 2012. Determination of Soil Erosion Risk in the Mustafakemalpasa River Basin, Turkey, Using the Revised Universal Soil Loss Equation, Geographic Information System, and Remote Sensing. Environ. Manag. 50, 679–694.

Øygarden, L., Kværner, J., Jenssen, P.D., 1997. Soil erosion via preferential flow to drainage systems in clay soils. Geoderma 76, 65–86. https://doi.org/10.1016/S0016-7061(96)00099-7

Panagos, P., Ballabio, C., Borrelli, P., Meusburger, K., Klik, A., Rousseva, S., Tadić, M.P., Michaelides, S., Hrabalíková, M., Olsen, P., Aalto, J., Lakatos, M., Rymszewicz, A., Dumitrescu, A., Beguería, S., Alewell, C., 2015a. Rainfall erosivity in Europe. Sci. Total Environ. 511, 801–814. https://doi.org/10.1016/j.scitotenv.2015.01.008

Panagos, P., Borrelli, P., Meusburger, K., van der Zanden, E. H., Poesen, J., Alewell, C., 2015b. Modelling the effect of support practices (P-factor) on the reduction of soil erosion by water at European scale. Environ Sci. Pol. 51, 23–34. https://doi.org/https://doi.org/10.1016/j.envsci.2015.03.012

Panagos, P., Borrelli, P., Poesen, J., Ballabio, C., Lugato, E., Meusburger, K., Montanarella, L., Alewell, C., 2015c. The new assessment of soil loss by water erosion in Europe. Environ. Sci. Pol. 54 (2015), 438–447. http://dx.doi.org/10.1016/j.envsci.2015.08.012.

This project has received funding from the European Union's Horizon 2020 research and innovation programme under grant agreement N° 862695

Panagos, P., Ballabio, C., Borrelli, P., Meusburger, K., Klik, A., Rousseva, S., Tadić, M.P., Michaelides, S., Hrabalíková, M., Olsen, P., Aalto, J., Lakatos, M., Rymszewicz, A., Dumitrescu, A., Beguería, S., Alewell, C., 2015d. Rainfall erosivity in Europe Sci. Total Environ. 511, 801-814, 10.1016/j.scitotenv.2015.01.008
Pandey, A., Chowdary, V.M., Mal, B.C., Billib, M., 2009. Application of the WEPP model for prioritization and evaluation of best management practices in an Indian watershed. Hydrol. Process 23, 2997-3005.
Peckham, S.D., 2003. Fluvial landscape models and catchment-scale sediment transport. Glob. Planet. Change 39, 31-51. https://doi.org/10.1016/S0921-8181(03)00014-6
Phinzi, K., Ngetar, N.S., 2019. The assessment of water-borne erosion at catchment level using GIS-based RUSLE and remote sensing: A review. Int. Soil Water Conserv. Res. 7, 27–46. https://doi.org/10.1016/j.iswcr.2018.12.002
Pieri, L., Bittelli, M., Wu, J.Q., Dun, S., Flanagan, D.C., Rossi Pisa, P., et al., 2007. Using the Water Erosion Prediction Project (WEPP) model to simulate field-observed runoff and erosion in the Apennines mountain range, Italy. J. Hydrol. 10.1016/j.jhydrol.2006.12.014
Pimentel, D., Harvey, C., Resosudarmo, P., Sinclair, K., Kurz, D., McNair, M., Crist, S., Shpritz, L., Fitton, L., Saffouri, R., Blair, R., 1995. Environmental and Economic Costs of Soil Erosion and Conservation Benefits. Science 267, 1117–1123. https://doi.org/10.1126/science.267.5201.1117
Pinna, M., 1977. Climatologia. UTET, Torino.
Puustinen, M., Koskiaho, J., Peltonen, K., 2005. Influence of cultivation methods on suspended solids and phosphorus concentrations in surface runoff on clayey sloped fields in boreal climate. Agr Ecosyst Environ 105(4), 565–579. https://doi.org/https://doi.org/10.1016/j.agee.2004.08.005
Puustinen, M., Turtola, E., Kukkonen, M., Koskiaho, J., Linjama, J., Niinioja, R., Tattari, S., 2010. VIHMA—A tool for allocation of measures to control erosion and nutrient loading from Finnish agricultural catchments. Agr Ecosyst Environ 138(3), 306–317. https://doi.org/https://doi.org/10.1016/j.agee.2010.06.003
Quine, T.A., Zhang, Y., 2004. Re-defining tillage erosion: quantifying intensity–direction relationships for complex terrain : 1. Derivation of an adirectional soil transport coefficient. Soil Use Manage 20(2), 114–123. doi:10.1111/j.1475-2743.2004.tb00346.x
Raat, K.J., Vrugt, J.A., Bouten, W., Tietema, A., 2004. Towards reduced uncertainty in catchment nitrogen modelling: quantifying the effect of field observation uncertainty on model calibration, Hydrol. Earth Syst. Sci. 8, 751-763.
Raclot, D., Albergel, J., 2006. Runoff and water erosion modelling using WEPP on a Mediterranean cultivated catchment. Phys Chem Earth 31, 1038-1047.
Rapp, J.F., 1994. Error assessment of the revised universal soil loss equation using natural runoff plot data (Master Thesis). The University of Arizona, Arizona.
Räsänen, T.A., 2021. The erosion susceptibility of Finnish agricultural lands [Data set]. Natural Resources Insitute Finland (LUKE).
Räsänen, T.A., Tähtikarhu, M., Uusi-Kämppä, J., Piirainen, S., Turtola, E., 2023. Evaluation of RUSLE and spatial assessment of agricultural soil erosion in Finland. Geoderma Reg. 32, e00610.
Renard, K.G., Freimund J.R., 1994. Using monthly precipitation data to estimate the R factor in the revised USLE. J. Hydrol. 157, 287-306.
Renard, K.G., Foster, G.R., Weesies, G.A., McCool, D.K., Yoder, D.C., 1997. Predicting Soil Erosion by Water: A Guide to Conservation Planning with the Revised Universal Soil Loss Equation (RUSLE). Agricultural Handbook 703. US Department of Agriculture, Washington, DC, pp. 404.
Risse, L.M., Nearing, M.A., Laflen, J.M., Nicks, A.D., 1993. Error Assessment in the Universal Soil Loss Equation. Soil Sci. Soc. Am. J. 57, 825–833. https://doi.org/10.2136/sssaj1993.03615995005700030032x
Rosas, M.A., Gutierrez, R.R., 2020. Assessing soil erosion risk at national scale in developing countries: The technical challenges, a proposed methodology, and a case history. Sci. Total. Environ. 703, 135474.
Rosewell, C.J., 2001. Evaluation of WEPP for runoff and soil loss prediction in Gunnedah, NSW, Australia. Austr. J. Soil Res. 9, 230-243.
Rosso, R., 1994. An introduction to spatially distributed modelling of basin response. In: Advances in Distributed Hydrology, Rosso, R., Peano, A., Becchi, I., Bemporad, G.A. (Eds). Water Resources Publications: Fort Collins, 3-30.
Savabi, M.R., 1993. Modeling subsurface drainage and surface runoff with WEPP. J. Irrig. Drain. Eng. 119, 801-813.
Savabi, M., Flanagan, D.C., Hebel, B., Engel, B.A., 1995. Application of WEPP and GIS-GRASS to a small watershed in Indiana. J. Soil Water Conserv. 50(5):477–483.

Schwab, G.O., Fausey, N.R., Kopcak, D.G., 1980. Sediment and Chemical Content of Agricultural Drainage Water. Trans. ASAE 6, 1446–1449. https://doi.org/10.13031/2013.34796
Schwab, G.O., Nolte, B.H., Brehm, R.D., 1977. Sediment from Drainage Systems for Clay Soils. Trans. ASAE 5, 0866–0868. https://doi.org/10.13031/2013.35665
Sharda, V.N., Ojasvi, P.R., 2016. A revised soil erosion budget for India: Role of reservoir sedimentation and land-use protection measures. Earth Surf. Process. Landf. 41, 2007–2023.
Sharp, R., Douglas, J., Wolny, S., et al., 2020. InVEST 3.12.0.post8+ug.g52ebadf User's Guide. T, Stanford University, The Natural Capital Project. University of Minnesota, The Nature Conservancy, and World Wildlife Fund.
Shen, Z.Y., Hong, Q., Yu, H., 2010. Parameter uncertainty analysis of non-point source pollution from different land use types, Sci. Total Environ. 408, 1971-1978.
Simonato, T., Bischetti, G.B., Crosta, G.B., 2002. Evaluating soil erosion with RUSLE and WEPP in an alpine environment (Dorena Valley – Central Alps, Italy), Sustainable Land Management - Environmental Protection 35, 481–494.
Spadaro, G., Flanagan, D.C., Cosentino, S., Mantineo, M., 2004. Estimation of soil erosion using the WEPP model for Mediterranean conditions. Eur. Soc. Agron. 2, 2-4.
Stolpe, N.B., 2005. A comparison of the RUSLE, EPIC and WEPP erosion models as calibrated to climate and soil of south-central Chile. Acta Agr Scand B-S P 55, 2–8. https://doi.org/10.1080/09064710510008568
Tähtikarhu, M., Räsänen, T., Oksanen, J., Uusi-Kämppä, J., 2022. Exploring structural sediment connectivity via surface runoff in agricultural lands of Finland. Acta Agr Scand B-S P 72, 957–970. https://doi.org/10.1080/09064710.2022.2136583
Tarquini, S., Isola, I., Favalli, M., Battistini, A., Dotta, G., 2023. TINITALY, a digital elevation model of Italy with a 10 meters cell size (Version 1.1). Istituto Nazionale di Geofisica e Vulcanologia (INGV). https://doi.org/10.13127/tinitaly/1.1
Tarquini, S., Vinci, S., Favalli, M., Doumaz, F., Fornaciai, A., Nannipieri, L., 2012. Release of a 10-m-resolution DEM for the Italian territory: Comparison with global-coverage DEMs and anaglyph-mode exploration via the web, Comput and Geosci 38, 168-170. https://doi.org/10.1016/j.cageo.2011.04.018
Tiwari, A.K., Risse, L.M., Nearing, M.A., 2000. Evaluation of WEPP and its comaprison with USLE and RUSLE. Trans. ASAE 43, 1129–1135.
Torri, D., Borselli, L., 2002. Clod movement and tillage tool characteristics for modeling tillage Erosion. J Soil Water Conserv 57(1), 24 LP – 28.
Torri, D., Sfalanga, M., Chisci, G., 1987. Threshold conditions for incipient rilling. In: Rill Erosion, Bryan, R.B. (Ed.). Catena Supplement 8, 97-105.
Torri, D., Poesen, J., Borselli, L., 1997. Predictability and uncertainty of the soil erodibility factor using a global dataset. Catena 31(1), 1–22. https://doi.org/https://doi.org/10.1016/S0341-8162(97)00036-2
Turtola, E., Kemppainen, E., 1998. Nitrogen and phosphorus losses in surface runoff and drainage water after application of slurry and mineral fertilizer to perennial grass ley. Agr Food Sci 7(5-6), 569–581. https://doi.org/10.23986/afsci.5614
Turtola, E., Alakukku, L., Uusitalo, R., 2007. Surface runoff, subsurface drainflow and soil erosion as affected by tillage in a clayey Finnish soil. Agr Food Sci 16, 332–351. https://doi.org/10.2137/145960607784125429
Turunen, M., Warsta, L., Paasonen-Kivekäs, M., Koivusalo, H., 2017. Computational assessment of sediment balance and suspended sediment transport pathways in subsurface drained clayey soils. Soil Till Res. 174, 58–69. https://doi.org/10.1016/j.still.2017.06.002
Ulén, B., Bechmann, M., Øygarden, L., Kyllmar, K., 2012. Soil erosion in Nordic countries – future challenges and research needs. Acta Agr Scand B-S P 62, 176–184. https://doi.org/10.1080/09064710.2012.712862
USDA - United States Department of Agriculture, 2014. Rainfall Intensity Summarization Tool (RIST). Available at http://www.ars.usda.gov/News/docs.htm?docid=3251
Usher, W., Herman, J., Iwanaga, T., Teixeira, L., Cellier, N., Whealton, C., Hadka, D., Xantares, B., Rios, F., Mutel, C., Cederstrand, E., Andersen, T.K. Van Engelen, J., Lord, A.N.T., Kranas, H., Foramitti, J., Menegon, S., Dixit, V.K., Steubing, B., 2021. SALib/SALib: v1.3.13. Zenodo. https://doi.org/10.5281/zenodo.4707524
Uusi-Kämppä, J., Braskerud, B., Jansson, H., Syversen, N., Uusitalo, R., 2000. Buffer Zones and Constructed Wetlands as Filters for Agricultural Phosphorus. J. Environ. Qual. 29, 151–158. https://doi.org/10.2134/jeq2000.00472425002900010019x
Uusi-Kämppä, J., Jauhiainen, L., 2010. Long-term monitoring of buffer zone efficiency under different cultivation techniques in boreal conditions. Agr Ecosyst Environ, Special section Harvested perennial grasslands:

Ecological models for farming's perennial future 137, 75–85. https://doi.org/10.1016/j.agee.2010.01.002

Uusitalo, R., Lemola, R., Turtola, E., 2018. Surface and Subsurface Phosphorus Discharge from a Clay Soil in a Nine-Year Study Comparing No-Till and Plowing. J. Environ. Qual. 47, 1478–1486. https://doi.org/10.2134/jeq2018.06.0242

Uusitalo, R., Turtola, E., Kauppila, T., Lilja, T., 2001. Particulate Phosphorus and Sediment in Surface Runoff and Drainflow from Clayey Soils. J. Environ. Qual. 30, 589–595. https://doi.org/10.2134/jeq2001.302589x

Van Hoey, S., 2016. Development and application of a framework for model structure evaluation in environmental modelling (Doctoraat). Ghent University, Ghent, Belgium.

Vanoni, V.A., 1975. Sedimentation Engineering, Manual and Reports on Engineering; Books; Am. Soc. Civil Eng., New York, NY, USA.

Van Oost, K., Govers, G., Desmet, P., 2000. Evaluating the effects of changes in landscape structure on soil erosion by water and tillage. Landsc. Ecol. 15, 577–589. https://doi.org/10.1023/A:1008198215674

Vanrolleghem, P.A., Mannina, G., Cosenza, A., Neumann, M.B., 2015. Global sensitivity analysis for urban water quality modelling: Terminology, convergence and comparison of different methods. J. Hydrol. 522, 339–352. https://doi.org/10.1016/j.jhydrol.2014.12.056

Van Rompaey, A.J.J., Verstraeten, G., Van Oost, K., Govers, G. and Poesen, J. (2001), Modelling mean annual sediment yield using a distributed approach. Earth Surf. Process. Landforms, 26: 1221-1236. https://doi.org/10.1002/esp.275

Van Rompaey, A., Vieillefont, V., Jones, R.J.A., Montanarella, L., Verstraeten, G, Bazzoffi P., Dostal, T, Krasa, J, de Vente, J., Poesen, J., 2003. Validation of soil erosion estimates at European scale. European Soil Bureau Research Report No.13, EUR 20827 EN, (2003), 26pp. Office for Official Publications of the European Communities, Luxembourg.

Van Rompaey, A., Bazzoffi, P., Jones, R.J.A., Montanarella, L., 2005. Modeling sediment yields in Italian catchments. Geomorphology 65 (2005) 157–169. doi: 10.1016/j.geomorph.2004.08.006.

Verstraeten, G., Poesen, J., Demarée, G., Salles, C., 2006a. Long-term (105 years) variability in rain erosivity as derived from 10-min rainfall depth data for Ukkel (Brussels, Belgium): Implications for assessing soil erosion rates, J. Geophys. Res. 111, D22109, doi:10.1029/2006JD007169

Verstraeten, G., Poesen, J., Gillijns, K., Govers, G., 2006b. The use of riparian vegetated filter strips to reduce river sediment loads: an overestimated control measure? Hydrol. Process. 20, 4259–4267. https://doi.org/10.1002/hyp.6155

Verstraeten, G., Prosser, I.P., Fogarty, P., 2007. Predicting the spatial patterns of hillslope sediment delivery to river channels in the Murrumbidgee catchment, Australia. J. Hydrol. 334, 440–454. https://doi.org/10.1016/j.jhydrol.2006.10.025

Vigiak, O., Borselli, L., Newham, L.T.H., McInnes, J., Roberts, A.M., 2012. Comparison of conceptual landscape metrics to define hillslope-scale sediment delivery ratio. Geomorphology 138, 74–88. https://doi.org/10.1016/j.geomorph.2011.08.026

Wainwright, J., Parsons, A.J., Cooper, J.R., Gao, P., Gillies, J.A., Mao, L., Orford, J.D., Knight, P.G., 2015. The concept of transport capacity in geomorphology: TRANSPORT CAPACITY IN GEOMORPHOLOGY. Rev. Geophys. 53, 1155–1202. https://doi.org/10.1002/2014RG000474

Wainwright, J., Turnbull, L., Ibrahim, T.G., Lexartza-Artza, I., Thornton, S.F., Brazier, R.E., 2011. Linking environmental régimes, space and time: Interpretations of structural and functional connectivity. Geomorphology, Geomorphology on Multiscale Feedbacks in Ecogeomorphology 126, 387–404. https://doi.org/10.1016/j.geomorph.2010.07.027

Warren S. D., Mitasova H., Johnson M.R., Brown W.M., Johnson B.E., Johnston D.M., Julien P.Y., Mitas L., Molnar D.K., and Watson C.C. 2000. Digital terrain modeling and distributed soil erosion simulation/measurement for minimizing environmental impacts of military training. Center for Ecological Management of Military Lands Technical Publication Series TPS 00-14. Colorado State University,Ft. Collins.

Warsta, L., Taskinen, A., Koivusalo, H., Paasonen-Kivekäs, M., Karvonen, T., 2013. Modelling soil erosion in a clayey, subsurface-drained agricultural field with a three-dimensional FLUSH model. J. Hydrol. 498, 132–143. https://doi.org/10.1016/j.jhydrol.2013.06.020

Williams, J., Jones, C., Dyke, P., 1984. A modeling approach to determining the relationship between erosion and soil productivity. Trans. ASAE 27, 129-144.

Willmott, C., 1981. On the validation of models. Physical geograph. 2(2), 184-194.

Wischmeier, W., Smith, D., 1978. Predicting rainfall erosion losses: a guide to conservation planning. Agricultural Handbook No. 537. Washington DC, USA: U.S. Department of Agriculture.
Xu, H., Taylor, R.G., Xu, Y., 2011. Quantifying uncertainty in the impacts of climate change on river discharge in sub-catchments of the Yangtze and Yellow River Basins, China. Hydrol. Earth Syst. Sci. 15, 333-344.
Yu, B., Rosewell, C.J., 1996. A robust estimator of the R-factor for the universal soil loss equation. Trans. ASAE 39(2), 559-561.
Yu, B., Rosewell, C.J., 2001. Evaluation of WEPP for runoff and soil loss prediction at Gunnedah, NSW, Australia. Aust. J. Soil. Res. DOI 10.1071/SR00091
Yue, Y., Ni, J., Ciais, P., Piao, S., Wang, T., Huang, M., Borthwick, A.G.L., Li, T., Wang, Y., Chappell, A., Van Oost, K., 2016. Lateral transport of soil carbon and land−atmosphere CO2 flux induced by water erosion in China. Proceedings of the National Academy of Sciences 113, 6617–6622. https://doi.org/10.1073/pnas.1523358113
Zhang, X.C., Nearing, M.A., Risse, L.M., McGregor, K.C., 1996. Evaluation of runoff and soil loss predictions using natural runoff plot data. Trans. ASAE 39, 855–863.
Zhao, G., Gao, P., Tian, P., Sun, W., Hu, J., Mu, X., 2020. Assessing sediment connectivity and soil erosion by water in a representative catchment on the Loess Plateau, China. Catena 185, 104284. https://doi.org/10.1016/j.catena.2019.104284
Zheng, F., Zhang, X.C., Wang, J., Flanagan, D.C., 2020. Assessing applicability of the WEPP hillslope model to steep landscapes in the northern Loess Plateau of China. Soil Till Res. 197, 104492. https://doi.org/10.1016/ j.still.2019.104492

This project has received funding from the European Union's Horizon 2020 research and innovation programme under grant agreement N° 862695